
**Hypoxia Inducible Factor-independent functions for
the von Hippel-Lindau tumor suppressor gene**

Martijn Paul Jung Kyu Lolkema

Hypoxia Inducible Factor-independent functions for the von Hippel-Lindau tumor suppressor gene

Thesis University Utrecht
ISBN: 90-393-41508

Printed by: Febo druk B.V.

The publication of this thesis was financially supported by Astellas Pharma B.V., J.E. Jurriaanse Stichting Nederland, Bayer B.V., Ortho Biotech B.V., Amgen B.V., Merck Nederland B.V., Roche B.V., Novartis Oncology B.V., Novo Nordisk B.V., Sanofi-Aventis B.V., MSD Nederland B.V., Pfizer B.V., Astra-Zeneca B.V., Tebu-Bio B.V., Schering Plough B.V.

Hypoxia Inducible Factor-independent functions for the von Hippel-Lindau tumor suppressor gene

De functies van het von Hippel-Lindau tumor suppressor gen
onafhankelijk van de Hypoxie-geïnduceerde factor

(Met een samenvatting in het Nederlands)

Proefschrift

ter verkrijging van de graad van doctor aan de Universiteit voor Utrecht
op gezag van de Rector Magnificus, Prof. Dr. W.H. Gispen,
ingevolge het besluit van het College voor Promoties
in het openbaar te verdedigen
op dinsdag 7 februari 2006 des middags te 4.15 uur

door

Martijn Paul Jung Kyu Lolkema
geboren op 11 juni 1974 te Woolju, Korea

Promotor: Prof. Dr. E.E. Voest
co-Promotor: Dr. R.H. Giles

University Medical Center Utrecht
Faculty of Medicine
Department of Medical Oncology
The Netherlands

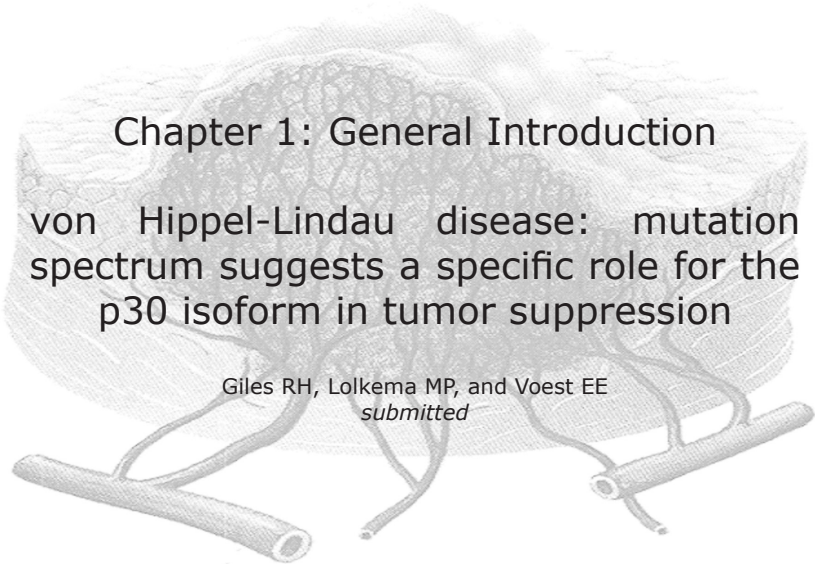
The writer of this thesis was a recipient of an AGIKO grant from the Dutch Society for Scientific Research (NWO) (920-03-179)



Voor Nicole

Contents

Chapter 1:	General Introduction von Hippel-Lindau disease: mutation spectrum suggests a specific role for the p30 isoform in tumor suppression <i>submitted</i>	8-18
Chapter 2:	Fibronectin is a hypoxia-independent target of the tumor suppressor VHL <i>FEBS Lett. 2004 Jan 2;556(1-3):137-42.</i>	20-26
Chapter 3:	Tumor suppression by the von Hippel-Lindau protein requires phosphorylation of the acidic domain. <i>J Biol Chem. 2005 Jun 10;280(23):22205-11.</i>	28-39
Chapter 4:	The von Hippel-Lindau tumor suppressor protein influences microtubule dynamics at the cell periphery. <i>Exp Cell Res. 2004 Dec 10;301(2):139-46.</i>	42-49
Chapter 5:	The von Hippel-Lindau tumor suppressor binds kinesin-2 and regulates primary cilia function. <i>Manuscript in preparation</i>	52-65
Chapter 6:	Interplay between VHL/ HIF1 α and Wnt/ β -catenin pathways during colorectal tumorigenesis <i>Oncogene in press</i>	68-77
Chapter 7:	Summary and General Discussion	80-85
Nederlandse Samenvatting		88-90
Dankwoord		92-93
Curriculum Vitae		94
List of publications		95



Chapter 1: General Introduction

von Hippel-Lindau disease: mutation spectrum suggests a specific role for the p30 isoform in tumor suppression

Giles RH, Lolkema MP, and Voest EE
submitted

von Hippel-Lindau disease: mutation spectrum suggests a specific role for the p30 isoform in tumor suppression

Giles RH, Lolkema MP, and Voest EE

submitted

Inactivating mutations of the von Hippel-Lindau gene (VHL) on chromosome 3p have been associated with the autosomal dominant VHL disease, characterized by extensively vascularized tumors and cysts in different organs, as well as the vast majority of conventional kidney cancers. The VHL gene product regulates the ubiquitination and subsequent degradation of hypoxia inducible factor (HIF), an important transcriptional activator of the genetic program triggered by hypoxia. The absence of functional VHL, thus, artificially stabilizes HIF and induces a cellular response to perceived low-oxygen tension. This illegitimate HIF signalling under normoxic conditions is likely to contribute to the extensive vascularization observed in VHL-related lesions. Here, we examine the evidence supporting the role of HIF as an oncogene, but also examine data suggesting the presence of alternative functions of VHL. For example, a subset of disease VHL alleles retains the ability to regulate HIF. We closely examine the VHL mutation spectrum in familial and sporadic tumors, which provides unique insights into several new functions ascribed to this tumor suppressor protein.

VHL disease

The von Hippel-Lindau (VHL) disease (MIM #193300) is an autosomal dominant disorder in which affected individuals have a propensity for developing both benign and malignant tumors in many organ systems. VHL patients develop vascular neoplasia, hemangioblastomas of the central nervous system and/or retina, clear cell renal cell carcinomas (ccRCCs), endocrine neoplasia of the adrenal gland (pheochromocytomas) and low-grade adenocarcinomas of the temporal bone, known as endolymphatic sac tumors. Less commonly, epididymal or broad ligament cystadenomas and pancreatic tumors are observed in VHL patients. In addition to the inherited risk for developing cancer, VHL patients develop cystic disease in various organs including the kidney, pancreas, and liver. VHL disease affects 1 in 36,000 individuals worldwide, with similar prevalence in both genders and across all ethnic backgrounds (1). Age at diagnosis for VHL varies from infancy to the seventh decade of life, with an average age at diagnosis of 26 years.

The morbidity of VHL varies, depending on the particular organ system involved. The malignant degeneration of renal cysts is commonly believed to be the most serious VHL manifestation. Approximately 75% of patients demonstrate multiple renal cysts. Renal cysts are common in the general population and are seldom clinically significant; however, in VHL patients they have a significant predilection to degenerate to

clear cell (cc) RCC (lipid-containing clear cells arranged in nests and tubules) (2). It is currently unknown whether all ccRCCs in VHL patients originate from cysts. ccRCC is the leading cause of death in patients with VHL disease, with 35-75% prevalence in one autopsy series (<http://www.emedicine.com/ped/topic2417.htm#section~bibliography>). RCC develops in VHL patients at an average age of 44 years, which is significantly younger than the average age of 62 years at which sporadic RCC develops in the general population. In addition to simple cysts and RCC, a number of other renal lesions are seen, such as angiomas and benign adenomas. To prevent the development of ccRCC in VHL patients, close surveillance using ultrasound, MRI, or CT-scan is indicated. For lesions larger than 2 cm minimal invasive and nephron-sparing surgery has been suggested to be the treatment modality of choice, although new technologies such as ultrasound guided radiofrequency ablation could become the new standard for the VHL patients (3,4). This approach potentially delays the necessity for kidney-function replacement therapy such as dialysis or transplantation for VHL patients.

The most common –and often earliest– manifestations of VHL disease in 83% of patients (5,6) comprises the second most common cause of morbidity and mortality: retinal or CNS hemangioblastomas. CNS hemangioblastomas are typically located in the cerebellum but can also occur at the brainstem, spinal cord and very rarely at the

lumbosacral nerve roots and supratentorial. These lesions are rarely malignant, however enlargement or bleeding within the CNS can result in neurological damage and death. Retinal hemangioblastomas can likewise result in considerable morbidity through retinal detachment or visual loss often leading to blindness. Typically, hemangioblastomas are cystic tumors containing a mural nodule formed by noninvasive, vacuolated stromal cells that are embedded in a network of capillaries. Ocular hemangioblastomas can be treated using laser coagulation, cryotherapy, and vitrectomy. Recently anti-VEGF (vascular endothelial growth factor) therapy has been shown to be beneficial in the treatment of these lesions, offering a new therapeutic option for therapy-resistant cases (7). CNS hemangioblastomas pose a significant challenge for neurosurgeons and new treatment modalities such as cryotherapy and local coagulation are being tested. The main goal of therapy for CNS hemangioblastomas is to minimize the local pressure effects of the lesions and to minimize destruction of normal brain tissue incurred by the treatment (8,9).

Neoplastic lesions in the adrenal glands (pheochromocytoma) appear histologically as an expansion of large chromaffin positive cells. Development of pheochromocytoma is extremely rare in the general population, but occurs in 19% of all VHL patients. Without treatment, hypertension resulting from pheochromocytomas can lead to acute heart disease, brain edema and stroke. The risk of VHL patients developing pheochromocytomas (usually benign) appears to hinge on the precise nature of the mutation responsible for VHL disease in a specific family (discussed in more detail below).

The recognition and screening of other less frequently occurring tumors associated with the VHL disease remain a clinical dilemma. However, as the life expectancy of VHL patients improves through timely recognition and treatment of the most common VHL-associated neoplasms, the less frequent tumors gain in clinical importance. Future clinical trials will elucidate the optimal management of this disease.

Diagnostic criteria

Since VHL disease is a multi-organ disease with great variability in clinical presentation, a combination of manifestations may lead

to diagnosis. Accepted criteria for diagnosis are (1) more than one angioblastoma in the CNS or retina, (2) a single angioma of the CNS or retina plus a visceral complication (multiple renal, pancreatic, or hepatic cysts; pheochromocytoma; renal cancer), or (3) a family history plus any one of the above manifestations. *VHL* gene mutation analysis is recommended when one of the following criteria are met: a patient with classic VHL disease and/or first-degree family members; a person from a family in which a germline *VHL* gene mutation has been identified (pre-symptomatic test); a VHL-suspected patient, i.e., one with multicentric tumors in one organ, bilateral tumors, two affected organ systems, one VHL-associated tumor at a young age (<50 years for hemangioblastoma and pheochromocytoma or <30 years for ccRCC); or a patient with family history of hemangioblastoma, renal cell carcinoma, or pheochromocytoma (10). Regular surveillance is strongly suggested for at-risk individuals starting from age four, or until genetic testing excludes the presence of the familial mutant allele in an individual.

VHL is a tumor suppressor

VHL patients are highly susceptible to tumor development because they already carry one mutated VHL allele in all of their cells. The chance inactivation of the second allele in a single cell is capable of initiating neoplastic growth. However, while VHL disease is rare, biallelic loss of *VHL* in certain tumor types is quite common. Not surprisingly, the tumor types most likely to harbor two independent inactivating VHL mutations, are also the same tumor types most frequently observed in VHL patients. For example, about 50% sporadic CNS and retinal hemangiomas also show biallelic loss of *VHL* (11,12). Most strikingly, it is estimated that 80% of sporadic ccRCCs –the 7th most common cancer of any type- have acquired biallelic VHL mutations, implying that the function of VHL is especially important for curtailing neoplasia of the kidney (reviewed in: (13,14)). Mouse xenograft studies have demonstrated that reintroduction of wild-type VHL into patient-derived ccRCC cells inhibits the ability of these cells to form tumors (15). Tumor suppressor genes form an arbitrary group of proteins whose biallelic inactivating mutation ultimately results in neoplastic transformation (16). Thus *VHL* is consid-

ered to belong to the family of classic tumor suppressor proteins, and is often dubbed the “gatekeeper” of the kidney.

The molecular mechanism of VHL function: its role in oxygen sensing

The best-known function for VHL is its role in the oxygen-sensing pathway. A wide variety of symptoms associated with the VHL disease and ccRCC such as increased angiogenesis and polycythemia suggested a correlation between the function of VHL and the adaptive response to oxygen deprivation (17). However, insight into the molecular mechanism came from a landmark study in *C. elegans*, in which substantial phenotypic overlap was observed between genetic mutants for the orthologs of *VHL* and prolyl hydroxylases (*PHDs*), suggesting a common pathway (18). This genetic insight linked several pieces of loose data into a simple but elegant mechanism for the biological oxygen sensor. Multiple lines of evidence had indicated that the hypoxia-inducible factor α (HIF α) was subject to PHD-mediated hydroxylation under normoxic conditions, requiring the presence of iron, 2-oxoglutarate, PHDs, and most importantly, oxygen. Once modified by the -OH group, HIF α can be captured by VHL, which then delivers HIF α to an E3-ubiquitin ligase complex, thereby targeting HIF α for degradation by the proteasome (19-25). The interplay of these proteins, centered around the presence of an -OH group, results in a direct molecular oxygen sensor. The absence of oxygen, and thus -OH modification of HIF α , simply abrogates the ability of VHL to recognize HIF α . HIF α levels are thus transiently stabilized, causing accumulation in the cytoplasm and ultimately translocate to the nucleus where it functions as a transcription factor. *VHL* mutations, by allowing inappropriate stabilization of HIF α , result in illegitimate hypoxic signaling in the presence of oxygen. The activation of HIF-mediated transcription accounts for a large number of phenotypes ascribed to VHL: e.g. the presence of elevated angiogenesis, altered extracellular matrix interactions, and the sporadic presence of polycythemia (2).

HIF- and VHL-related target gene expression has been studied extensively and has led to the recognition of a large set of hypoxia-responsive genes (26-29). The genes that

are upregulated in the absence of VHL or the presence of HIF are indeed involved in the promotion of the adaptive response to hypoxia and can be classified into a few functional classes of genes: oxygen transport genes (e.g. EPO), promoters of angiogenesis (e.g. VEGF, PAI-1), and anaerobic energy metabolism (e.g. GLUT-1, LDH-A) (30). The affected genes are by large thought to promote tumor growth, with some notable exceptions. Pro-apoptotic proteins and growth inhibitory proteins Bnip3, cyclin G2, and DEC1 are upregulated by HIF transcription but their function would predict them to be less favorable for tumor growth. Thus there seems to be a subtle balance between the growth promoting and apoptotic effects of HIF target genes in oxygen homeostasis. However, in tumorigenesis, HIF seems to tip towards growth stimulatory functions (31). Furthermore, it has been reported that paralogs HIF1 α and HIF2 α have different functions, favoring a role for HIF2 α in the development of ccRCC (32).

VHL gene.

The human *VHL* gene spans 3 exons residing on the short arm of chromosome 3 (3p25) and encodes a ubiquitously expressed 4.7-kilobase messenger RNA. The first exon encodes the N-terminal half of the VHL protein which contains the sequences that are reported to be crucial for the recognition of hydroxylated HIF by VHL (Ser111 and His115), and the second exon encodes the α -domain important for the binding between VHL and Elongin C. This interaction occurs at residues 157-171 and forms the connection of VHL to the E3-ubiquitin ligase complex involved in the poly-ubiquitination of HIF α subunits (33). The third exon contributes to the structural beta domain complementing the region important for HIF binding. Two protein products are encoded by VHL, a 30kD full-length protein (p30, 213 amino acids), and a 19 kD protein (p19, 160 amino acids) generated by alternative translation initiation of an internal methionine at position 54 (34,35) (Fig. 1). Both the p30 and p19 isoforms were shown to suppress tumor formation in nude mice and both are fully capable of targeting HIF α subunits to the proteasome (34,36,37). The first 53 residues of p30 contain eight repetitions of a five-residue acidic repeat, which collectively form an N-terminal acidic domain of unknown

function. The remaining functions of residues 54-213 appear to be identical between p30 and p19 (34). p30 is found primarily in cytoplasm, whereas p19 is also present in the nucleus (35,38). However, this difference in localization has not yet led to differences in known VHL functionality, raising the issue of the biological relevance of the acidic domain.

Germline inactivating mutations of a single *VHL* allele co-segregate with VHL disease (39). Mechanisms of *VHL* inactivation have been described to include intragenic mutations, mitotic recombination events, and hypermethylation of the promoter region. Mutations in virtually every of the 213 residues have been reported in three excellent databases (see *VHL* mutation databases). Global mutation analysis of 823 patient records identifies 36% as frameshifts, (28.5% deletions, and 7.5% insertions), 60% point mutations (48% missense, 12% nonsense), with the remaining mutations categorized as complex (Fig. 2). Nonsense mutations are far less likely to occur in exon 2 than exon 3.

Most clinical genetic facilities screen VHL mutations by direct sequencing of the three exons. Single exon or larger deletions of VHL can best be detected by rapid quantitative RT-PCR assay (40). Somatic inactivation of the wild type *VHL* allele is believed to be the initial transforming event in all VHL disease-associated neoplasms, although additional mutations are probably necessary for progression in carcinogenesis.

The *VHL* gene - the p19 isoform in particular - has been conserved throughout evolution and can be found in all multicellular organisms examined to date. Sequence analysis shows a striking conservation of amino acids that are crucial for HIF α binding (Fig. 3a) and the association with elongin C as part of the E3 ligase complex (Fig. 3b). These data suggest that the role for VHL in regulating HIF levels seems to be conserved through evolution. However there appears one or more hypoxia-independent functions for VHL as well; analysis of VHL in *C. elegans* has produced the strongest evidence to date that a group of genes is regulated by VHL in a manner independent of oxygen levels (41). Furthermore, multiple groups have reported microarray analyses in mammalian cell lines that indicate a role for VHL in transcriptional regulation, independent of its interaction with HIF (26-28,42,43). Thus,

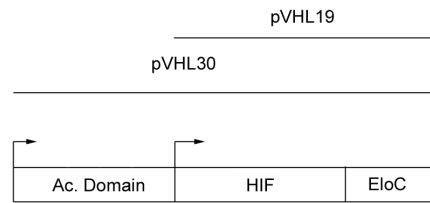


Fig. 1. Cartoon of VHL protein domains.

VHL contains two functional translational initiation sites resulting in 2 VHL isoforms; a full-length protein (VHLp30) with an N-terminal acidic domain of unknown function, and a downstream reading frame (VHL p19) starting at methionine 54. Both isoforms contain sequences responsible for binding to HIF- α and Elongin C (EloC). Although the vast majority of VHL mutations are downstream of the second initiation site, thereby altering both isoforms, 8% of unique mutations have been described that are not predicted to affect the structure or function of the smaller p19 isoform.

while the role of VHL in the regulation of the cellular response to oxygen remains the best characterized and is likely to contribute to its tumor suppressor function, one or more additional functions may exist.

Genotype-phenotype correlation: a strong case for a HIF-independent function for VHL

Different genetic mutations in *VHL* give rise to consistent disease manifestations, suggesting that some genotype-phenotype correlations exist. For example, missense mutations in residues 74-90 confer 75% genetic susceptibility for RCC (44). Likewise, VHL kindreds with a deletion or protein truncation mutation of the *VHL* gene have less than 10% risk for developing pheochromocytoma, while the risk is 50% in kindreds with a missense mutation (Fig. 2). From the mutation in the *VHL* gene, one can make informed predictions as to which tumors will develop in a particular family. Accordingly, patients are clinically categorized based on their predisposition to pheochromocytoma: type 1 patients have low incidence of pheochromocytomas, whereas type 2 families are defined by the presence of pheochromocytoma (45). Type 2 VHL disease can be further subclassified into type 2A, type 2B and type 2C ((46) and Table 1). While type 2A patients have only a small chance of developing ccRCC, they may develop any of the other visceral complications associated with

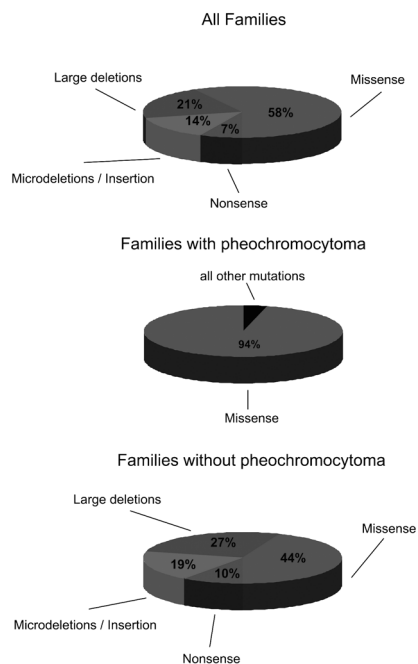


Fig. 2. Distribution of mutation types in VHL families.

VHL families can be grouped by their propensity to develop pheochromocytomas. Top panel, all families taken together give a fairly even distribution of mutation events. Middle panel, almost all families with pheochromocytomas (type 2 disease) are characterized by missense mutations. Bottom panel, families with pheochromocytomas. Modified from the National Cancer Institute.

the disease. One large family originally from the Black Forest region of Germany carrying a missense mutation (Y98H) comprises a significant portion of patients with this subtype, and it has been suggested that the mortality rate for those carrying this mutation was much lower than in unselected *VHL* mutations (47). Type 2B families are susceptible to all VHL-related tumors, but are always characterized by the presence of angiomas and ccRCC in addition to pheochromocytoma. Zbar et al. confirmed previous observations that germline *VHL* mutations at codon 167 (R167Q, R167W) convey a much higher risk for the development of pheochromocytoma (64%) and RCC than families without a mutation at codon 167 (7%) (48). The reported reduced risk for RCC in individuals with a complete deletion of *VHL* (49) possibly defines a new VHL

phenotype, characterized by a low risk for both RCC and pheochromocytoma.

The only disease manifestation families with type 2C disease develop is pheochromocytoma (13,14). The best characterized type 2C allele cosegregating with the syndrome contains both P81S as well as L188V mutations (50). Other typical type 2C mutations include R64P, V84L, and F119S. Of great interest is the fact that type 2C mutant alleles retain their ability to regulate HIF- α levels (51,52). Whether the regulation of HIF by type 2C-*VHL* alleles is empirically comparable to wild-type *VHL in vivo* remains yet to be validated in target tissue (e.g., in a type 2C patient's pheochromocytoma). Some very recent evidence regarding pheochromocytoma development places VHL together with all other known familial pheochromocytoma genes in a common pathway involving succinate dehydrogenase components (enzymes of the energy and respiratory system in mitochondria). By suppressing transcription factor JunB, VHL promotes apoptosis in sympathetic neuronal precursor cells (53). *VHL* mutant alleles, including type 2C variants, abolished this function of VHL, suggesting a HIF-independent role for this pathway in at least pheochromocytoma generation, if not

Table 1. VHL disease subtypes

Type	Pheochromocytoma	Angioma	RCC	HIF regulation
1	No	Yes	Yes	Defective
2A	Yes	Yes	No	Diminished (MT stability defect)
2B	Yes	Yes	Yes	Defective
2C	Yes	No	No	Normal

RCC, Renal cell carcinoma; MT, microtubule

all VHL-related tumorigenesis. Alternatively, another recent paper details how loss of either succinate dehydrogenase subunits B or D, respectively associated with two distinct pheochromocytoma syndromes, triggers a HIF1 α response, just like *VHL*-loss. The researchers further establish that high HIF1 α levels can suppress the B subunit in a regulatory loop (54). These apparently conflicting data make it difficult to completely exclude a role for HIF activation in pheochromocytoma development.

A few years ago, recessive "mild" mutations of *VHL* were discovered in polycythemia patients in the Chuvash Republic, formerly of the Soviet Union. This distinct congenital syndrome

was characterized by a constitutively homozygous *VHL* missense R200W mutation (55). Since then, four other missense *VHL* mutations have been identified in congenital polycythemia: D126Y, V130L, H191D, and P192S (56,57). Pastore et al. (2003) conclude that homozygous or compound heterozygous *VHL* mutations are the most frequent cause of congenital polycythemia (56). *VHL* polycythemia patients manifest thrombosis and vascular abnormalities, due to elevated normoxic levels of HIF α commensurate with their elevated serum erythropoietin and VEGF concentrations. However, despite upregulated HIF α levels, Chuvash polycythemia patients are not predisposed to cancer (57). The existence of this syndrome suggests that upregulation of HIF α alone does not appear to be oncogenic in humans. However,

the elevated HIF levels in polycythemia patients are possibly below a threshold necessary to initiate tumor growth. Alternatively, comparing polycythemia patients to *VHL* patients might suggest that tumors in *VHL* patients might arise through an alternate, HIF-independent tumor suppressor function of *VHL*.

Elucidating the crystal structure of *VHL* allowed significant insight into the correlation existing between genotype and phenotype in *VHL*. It began with the identification of two very well conserved residues, H115 and S111, that are essential in the binding of *VHL* to HIF by forming hydrogen bonds with a hydroxylated proline (58-60). These critical *VHL* residues are encoded by the second exon and contribute to a β -sheet structure. The third exon of *VHL* encodes an α -helical structure important for the binding of Elongin

Table 2. N-terminal *VHL* mutations

AA ¹	DNA mutation	Protein mutation	p19 altered?	CNS or retinal angioma?	Other Phenotype	reference
1	3G>A	M1I	No	No	RCC	(77)
10	28G>T	E10X	No	N/A	Sp. RCC	(78)
	28G>T	E10X	No	N/A	Sp. RCC	(78)
14	42insA	Frameshift res14	No	Unknown	RCC	(79)
18	52G>A	A18T	No	No	RCC	(80)
25 ²	73C>T	P25L	No	Unknown	RCC	(81)
	73C>T	P25L	No	N/A	Sp. Pheochrom	(82)
	73C>T	P25L	No	Yes	Unknown	(83)
	73C>T	P25L	No	Yes	Kidney/pancreatic cysts	(84)
38	112T>C	S38P	No	No	RCC, Pheochrom	(85)
40	119_118dup	Frameshift res40	No	Unknown	Type 1	(86)
46	136G>T	E46X	No	No	Type 1	(87)
52	154G>A	E52K	No	Late-onset	Type 1	(87)
53	159-168del	Frameshift res53	Yes	Yes	N/A	(81)
	160-175del	Frameshift res53	Yes	N/A	Sp. RCC	(88)
54	162-166del	Frameshift res54	Yes	N/A	RCC	(89)
	162insT	Frameshift res54	Yes	N/A	Pheochrom	(87)
	162delG	Frameshift res54	Yes	N/A	RCC	(77)
	162G>C	M54I	Yes	Yes	Pheochrom	Personal Communication ³
55	163-164del	Frameshift res55	Yes	N/A	RCC	(78)
	165dup	Frameshift res55	Yes	Yes	Unknown	(86)
	163delG	Frameshift res55	Yes	Yes	Unknown	(90)
	163delG	Frameshift res55	Yes	Yes	Unknown	(91)
	163delG	Frameshift res55	Yes	N/A	Pheochrom	(92)
56	167insA	Frameshift res56	Yes	Yes	Unknown	(86)
	166-178del	Frameshift res56	Yes	Yes	RCC	(93)
59	175-183del	In-frame Δ 59-61	Yes	N/A	Sp.RCC	(88)
	176-177del	Frameshift res59	Yes	N/A	RCC	(77)
	175delC	Frameshift res59	Yes	Yes	Type 1	(86)

¹ Abbreviations: AA, amino acid; RCC, renal cell carcinoma; Pheochrom, pheochromocytoma; Sp., sporadic; N/A, not applicable; Type 1, *VHL* subtype without pheochromocytoma.

² The P25L mutation is of questionable pathogenicity; it has been found in 2/500 (0.4%) alleles in the non-affected population.

³ Personal Communication, RB van der Luijt, UMC Utrecht, the Netherlands

C (residues 157-171) (33) and is frequently altered in naturally occurring VHL mutations (48,61-63). The crystal structure predicts that VHL L158 and C162 directly contact elongin C, whereas Q164 and R167 stabilize the VHL interface without direct contact. Mutations affecting L158 and C162 completely abrogate elongin binding, whereas mutations affecting Q164, V166, and R167 alter VHL conformation sufficiently to lead to a partial loss of elongin-binding activity. Alleles Y98H and W117R do not compromise binding to the elongins and Cul2, but do allow HIF accumulation through an unknown mechanism. By contrast, type 2C mutant L188V retains the ability to bind to elongins and Cul2 and HIF is regulated apparently normally (33).

Is HIF an oncogene?

Multiple studies have shown increased HIF expression among various tumors such as breast, colon, head and neck and cervix (64,65). Moreover, in breast cancer the patient prognosis seems to correlate with the expression of HIF (66,67). Therefore it seems plausible that HIF plays a prominent role in the development of renal cell carcinoma. Several research groups have addressed this role; collectively, these articles suggest that HIF2 α (and not HIF1 α) is the main effector of tumorigenesis upon VHL loss. Using a xenograft model of 786-O VHL-deficient ccRCC cells genetically engineered to re-express VHL, the first of these studies examined whether overexpressed stabilized HIF can counteract tumor suppression by VHL. When subsequently engineered to express HIF2 α with a point mutation in the amino acid crucial for the oxygen dependent prolyl-hydroxylation (68), these cells were able to override the VHL-mediated tumor suppression. However, similar experiments using HIF1 α did not result in a similar abolition of VHL mediated tumor suppression (69). Although these studies suggest a role for HIF2 α in tumorigenesis, they do not address the more physiologically relevant question of whether the suppression of endogenous HIF2 α would be sufficient to abrogate tumor development in these patient-derived renal cell carcinoma cells. By knocking down HIF2 α by RNAi, data supporting a putative oncogenic role for HIF2 α was generated (70,71). These experimental data do not, however, exclude additional

tumor suppressor functions for VHL. The *in vivo* experiments described in these papers were terminated after 8-10 weeks, whereas recent experiments demonstrate that beyond this time point 786-O cells engineered to express a mutant VHL that is still capable of controlling HIF levels fails to suppress tumor formation (72). We conclude that, although HIF regulation certainly seems to be an attractive candidate, additional VHL-functions are likely to participate in VHL-mediated tumor suppression.

Candidate HIF-independent functions for VHL

Ohh et al. described the first E3 ligase-independent function for VHL: binding to fibronectin (73). To date, all tested *VHL* point mutants have shown reduced binding to intracellular fibronectin which is presumably responsible for the observation that cells lacking VHL are defective in proper deposition of the extracellular fibronectin. Post-translational neddylation of VHL seems to regulate the binding of fibronectin to VHL and subsequent deposition (74). Furthermore, fibronectin expression at the mRNA level is regulated by VHL in a hypoxia-independent fashion (42). These observations, however, are largely correlative; the exact molecular mechanisms by which VHL stimulates fibronectin deposition have yet to be elucidated.

Recently, residues 95-123 of VHL have been described to be important in the stabilization of the microtubule cytoskeleton (38). This novel VHL function is independent of its participation in E3 ligase complexes. Because microtubule dynamics are potentially important in regulating cancer-related processes including chromosomal stability, migration, and polarity, this VHL function might contribute to its ability to suppress tumor formation. Interestingly, type 2A VHL mutations Y98H and Y112H (as well as one type 2C allele) abrogate the protein's ability to stabilize microtubules (38). Yet these alleles are associated with a low risk of RCC, a conundrum that has been difficult to resolve.

The 5' prime acidic domain of VHL: a region important in HIF-independent function?

The 5' acidic domain of *VHL* is relatively new

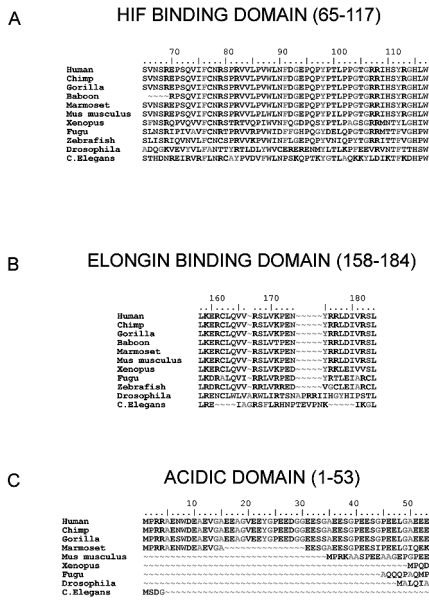


Fig. 3. Conservation of VHL functional domains.

Sequence alignment of four primates (Human, chimpanzee, gorilla and marmoset), mouse, frog (Xenopus), puffer fish (Fugu), fruit fly (Drosophila), and C. elegans (worm). (A) The HIF- α binding domain; (B) the Elongin C binding domain; (C) the acidic domain is only present in mammals. Position numbers refer to the human residue number.

in evolution, and may be unique to mammals. Composed of tandem copies of the pentameric repeat GXEEX, mice have only a single copy while the marmoset (New World Monkey) bears three. In baboons, chimpanzees, gorillas, and humans, the *VHL* gene contains 8 acidic repeats (75) (Fig. 3c). The amplification of the number of acidic repeats might reflect increasing functionality of the acidic domain of *VHL* in higher mammals. The fact that the p19 isoform of VHL is still expressed in mammals in addition to the longer isoform containing acidic repeats, suggests that the two isoforms may have separate, non-overlapping functions. We performed literature and database searches for *VHL* mutations in familial and sporadic tumors (*VHL* mutation databases) and found 32 familial and sporadic mutations reported in the first 59 residues of p30 (Table 2), comprising 8% of unique mutations. Strikingly, 12 mutations are predicted to only affect the p30 isoform, i.e. translation

of p19 should not be affected as a result of the mutation. Five missense mutations disrupting negatively charged or hydrophobic residues in the acidic domain might interfere with as yet unidentified protein binding partners or alter p30 conformation. It should be noted, however, that it is unclear whether the P25L mutation is a rare naturally occurring polymorphism (that happens to segregate with the disease in four families) or a true disease-associated allele. Three nonsense mutations and two frameshifts are predicted to produce a truncated N-terminal fragment in addition to unaffected p19 from the same allele, raising the possibility of a dominant negative function for the N-terminal sequences. Additional nonsense mutations in the first 53 residues exist but have not yet been reported (personal communication, S. Richard). One additional mutation replaces methionine 1 with an isoleucine, abrogating all translation of p30 specifically. None of the studies reporting these mutations mentions the relevance of these mutations with regard to p19. It is possible that mutations lying 5' to the p19 coding region could alter mRNA stability or translation efficiency; no study has examined expression level of the two isoforms as a result of these mutations. Theoretically, however, p19 expression will not be affected by acidic domain mutations; consequently, mutations in the first 159 nucleotides of the open reading frame of *VHL* should not be considered null alleles. Since wild-type expression of p19 is equivalent to p30, (35) mutations affecting p30 only - even if the other allele carries an inactivating mutation affecting both p19 and p30 - can be predicted to retain at least 25% of HIF regulation due to the single remaining allele encoding p19 (76). Moreover, because these tumors will not harbor biallelic inactivating mutations of p19, the p19 isoform of VHL fails to conform to the classic definition of a tumor suppressor protein (16).

Recently, we have found that phosphorylation of VHL seems to be dependent on the presence of the acidic domain (72). Our data demonstrate that acidic domain phosphorylation does not affect HIF α regulation, but is important for proper binding with fibronectin. Moreover, a phospho-defective mutant fails to suppress tumor formation in nude mice indicating the need for a fully functional acidic domain in VHL mediated tumor suppression. This finding connects one of the candidate HIF independent functions

for VHL to the function of the acidic domain and strengthens the notion that the acidic domain is important for the role VHL has in humans.

Hypothesis

Examination of the *VHL* mutation spectrum in familial and sporadic tumors suggests that mutations specifically occurring in the p30 isoform of VHL do not necessarily affect HIF regulation and are sufficient for tumorigenesis. Accordingly, it is interesting to note that the most common and early neoplasm accounting for the first manifestation of the disease in 83% of VHL patients (5,6) –retinal or CNS hemangiomas– appear to be absent or occur with late-onset in patients with p30-specific mutations (Table 2). The under-representation of angiomas implies that upon somatic inactivation of the second *VHL* allele, the p19 allele produced from an allele with a 5' mutation is sufficient to suppress hemangioma development (76). Our analysis supports the notion put forth by a number of groups that VHL-mediated tumor suppression is HIF-independent, mediated by an unknown function of the N-terminal acidic domain.

Concluding remarks

Clinical hallmarks of VHL disease are development of retinal and central nervous system (CNS) hemangiomas, pheochromocytomas, multiple cysts of the pancreas and kidneys, and a high potential for malignant transformation of renal cysts into carcinoma. Given the wide age range and pleiotropic manner in which VHL disease can be manifested, diagnosis of VHL disease and treatment of patients and their at-risk relatives are challenging. Each different type of VHL-related neoplasm is associated with a different histology and different clinical course, and might respond to different forms of therapy. Understanding the genetic basis of VHL disease coupled with an understanding of the particular anatomical venue provides a unique opportunity for the development of allele-specific forms of therapy.

References

1. Maher, E. R., Iselius, L., Yates, J. R., Littler, M., Benjamin, C., Harris, R., Sampson, J., Williams, A., Ferguson-Smith, M. A., and Morton, N. (1991) *J Med Genet* 28(7), 443-447

2. Kaelin, W. G., Jr. (2004) *Clin Cancer Res* 10(18 Pt 2), 6290S-6295S
3. Hes, F. J., Slootweg, P. J., van Vroonhoven, T. J., Hene, R. J., Feldberg, M. A., Zewald, R. A., Ploos van Amstel, J. K., Hoppener, J. W., Pearson, P. L., and Lips, C. J. (1999) *Eur J Clin Invest* 29(1), 68-75
4. Veltri, A., De Fazio, G., Malfitana, V., Isolato, G., Fontana, D., Tizzani, A., and Gandini, G. (2004) *Eur Radiol*
5. Maher, E. R., Yates, J. R., Harries, R., Benjamin, C., Harris, R., Moore, A. T., and Ferguson-Smith, M. A. (1990) *Q J Med* 77(283), 1151-1163
6. Melmon, K. L., and Rosen, S. W. (1964) *Am J Med* 36, 595-617
7. Madhusudan, S., Deplanque, G., Braybrooke, J. P., Cattell, E., Taylor, M., Price, P., Tsaloumas, M. D., Moore, N., Huson, S. M., Adams, C., Frith, P., Scigalla, P., and Harris, A. L. (2004) *Jama* 291(8), 943-944
8. Weil, R. J., Lonser, R. R., DeVroom, H. L., Wanebo, J. E., and Oldfield, E. H. (2003) *J Neurosurg* 98(1), 95-105.
9. Lonser, R. R., Weil, R. J., Wanebo, J. E., DeVroom, H. L., and Oldfield, E. H. (2003) *J Neurosurg* 98(1), 106-116.
10. Hes, F. J., Lips, C. J., and van der Luijt, R. B. (2001) *Neth J Med* 59(5), 235-243.
11. Glasker, S., Bender, B. U., Apel, T. W., van Velthoven, V., Mulligan, L. M., Zentner, J., and Neumann, H. P. (2001) *J Neurol Neurosurg Psychiatry* 70(5), 644-648
12. Sprenger, S. H., Gijtenbeek, J. M., Wesseling, P., Scot, R., van Calenbergh, F., Lammens, M., and Jeuken, J. W. (2001) *J Neurooncol* 52(3), 241-247.
13. Lonser, R. R., Glenn, G. M., Walther, M., Chew, E. Y., Libutti, S. K., Linehan, W. M., and Oldfield, E. H. (2003) *Lancet* 361(9374), 2059-2067
14. Sano, T., and Horiguchi, H. (2003) *Microsc Res Tech* 60(2), 159-164
15. Iliopoulos, O., Kibel, A., Gray, S., and Kaelin, W. G., Jr. (1995) *Nat Med* 1(8), 822-826.
16. Sherr, C. J. (2004) *Cell* 116(2), 235-246
17. Golde, D. W., Hocking, W. G., Koeffler, H. P., and Adamson, J. W. (1981) *Ann Intern Med* 95(1), 71-87
18. Epstein, A. C., Gleadle, J. M., McNeill, L. A., Hewitson, K. S., O'Rourke, J., Mole, D. R., Mukherji, M., Metzen, E., Wilson, M. I., Dhanda, A., Tian, Y. M., Masson, N., Hamilton, D. L., Jaakkola, P., Barstead, R., Hodgkin, J., Maxwell, P. H., Pugh, C. W., Schofield, C. J., and Ratcliffe, P. J. (2001) *Cell* 107(1), 43-54
19. Ivan, M., Kondo, K., Yang, H., Kim, W., Valianido, J., Ohh, M., Salic, A., Asara, J. M., Lane, W. S., and Kaelin, W. G., Jr. (2001) *Science* 292(5516), 464-468.
20. Zhu, H., and Bunn, H. F. (2001) *Science* 292(5516), 449-451
21. Maxwell, P. H., Wiesener, M. S., Chang, G. W., Clifford, S. C., Vaux, E. C., Cockman, M. E., Wykoff, C. C., Pugh, C. W., Maher, E. R., and Ratcliffe, P. J. (1999) *Nature* 399(6733), 271-275.
22. Yu, F., White, S. B., Zhao, Q., and Lee, F. S. (2001) *Proc Natl Acad Sci U S A* 98(17), 9630-

9635

23. Jaakkola, P., Mole, D. R., Tian, Y. M., Wilson, M. I., Gielbert, J., Gaskell, S. J., Kriegsheim, A., Hebestreit, H. F., Mukherji, M., Schofield, C. J., Maxwell, P. H., Pugh, C. W., and Ratcliffe, P. J. (2001) *Science* 292(5516), 468-472.
24. Hon, W. C., Wilson, M. I., Harlos, K., Claridge, T. D., Schofield, C. J., Pugh, C. W., Maxwell, P. H., Ratcliffe, P. J., Stuart, D. I., and Jones, E. Y. (2002) *Nature* 417(6892), 975-978.
25. Min, J. H., Yang, H., Ivan, M., Gertler, F., Kaelin, W. G., Jr., and Pavletich, N. P. (2002) *Science* 296(5574), 1886-1889.
26. Jiang, Y., Zhang, W., Kondo, K., Klco, J. M., St Martin, T. B., Dufault, M. R., Madden, S. L., Kaelin, W. G., Jr., and Nacht, M. (2003) *Mol Cancer Res* 1(6), 453-462.
27. Zatyka, M., da Silva, N. F., Clifford, S. C., Morris, M. R., Wiesener, M. S., Eckardt, K. U., Houlston, R. S., Richards, F. M., Latif, F., and Maher, E. R. (2002) *Cancer Res* 62(13), 3803-3811.
28. Wykoff, C. C., Pugh, C. W., Maxwell, P. H., Harris, A. L., and Ratcliffe, P. J. (2000) *Oncogene* 19(54), 6297-6305.
29. Vengellur, A., Woods, B. G., Ryan, H. E., Johnson, R. S., and LaPres, J. J. (2003) *Gene Expr* 11(3-4), 181-197.
30. Wenger, R. H. (2002) *Faseb J* 16(10), 1151-1162.
31. Greijer, A. E., and van der Wall, E. (2004) *J Clin Pathol* 57(10), 1009-1014.
32. Hu, C. J., Wang, L. Y., Chodosh, L. A., Keith, B., and Simon, M. C. (2003) *Mol Cell Biol* 23(24), 9361-9374.
33. Ohh, M., Takagi, Y., Aso, T., Stebbins, C. E., Pavletich, N. P., Zbar, B., Conaway, R. C., Conaway, J. W., and Kaelin, W. G., Jr. (1999) *J Clin Invest* 104(11), 1583-1591.
34. Schoenfeld, A., Davidowitz, E. J., and Burk, R. D. (1998) *Proc Natl Acad Sci U S A* 95(15), 8817-8822.
35. Iliopoulos, O., Ohh, M., and Kaelin, W. G., Jr. (1998) *Proc Natl Acad Sci U S A* 95(20), 11661-11666.
36. Blankenship, C., Naglich, J. G., Whaley, J. M., Seizinger, B., and Kley, N. (1999) *Oncogene* 18(8), 1529-1535.
37. Iliopoulos, O., Kibel, A., Gray, S., and Kaelin, W. G., Jr. (1995) *Nat Med* 1(8), 822-826.
38. Hergovich, A., Lisztwan, J., Barry, R., Ballschmieter, P., and Krek, W. (2003) *Nat Cell Biol* 5(1), 64-70.
39. Latif, F., Tory, K., Gnarr, J., Yao, M., Duh, F. M., Orcutt, M. L., Stackhouse, T., Kuzmin, I., Modi, W., Geil, L., and et al. (1993) *Science* 260(5112), 1317-1320.
40. Hoebbeck, J., van der Luijt, R., Poppe, B., De Smet, E., Yigit, N., Claes, K., Zewald, R., de Jong, G. J., De Paepe, A., Speleman, F., and Vandensompele, J. (2005) *Lab Invest* 85(1), 24-33.
41. Bishop, T., Lau, K. W., Epstein, A. C., Kim, S. K., Jiang, M., O'Rourke, D., Pugh, C. W., Gleadle, J. M., Taylor, M. S., Hodgkin, J., and Ratcliffe, P. J. (2004) *PLoS Biol* 2(10), e289.
42. Bluysen, H. A., Lolkema, M. P., van Beest, M., Boone, M., Snijckers, C. M., Los, M., Gebbink, M. F., Braam, B., Holstege, F. C., Giles, R. H., and Voest, E. E. (2004) *FEBS Lett* 556(1-3), 137-142.
43. Wykoff, C. C., Sotiropoulos, C., Cockman, M. E., Ratcliffe, P. J., Maxwell, P., Liu, E., and Harris, A. L. (2004) *Br J Cancer* 90(6), 1235-1243.
44. Gallou, C., Chauveau, D., Richard, S., Joly, D., Giraud, S., Olschwang, S., Martin, N., Saquet, C., Chretien, Y., Mejean, A., Correas, J. M., Benoit, G., Colombeau, P., Grunfeld, J. P., Junien, C., and Beroud, C. (2004) *Hum Mutat* 24(3), 215-224.
45. Neumann, H. P., and Wiestler, O. D. (1991) *Lancet* 338(8761), 258.
46. Brauch, H., Bohm, J., and Hofler, H. (1995) *Pathologie* 16(5), 321-327.
47. Bender, B. U., Eng, C., Olschewski, M., Berger, D. P., Laubenberg, J., Althofer, C., Kirste, G., Orszagh, M., van Velthoven, V., Miosczka, H., Schmidt, D., and Neumann, H. P. (2001) *J Med Genet* 38(8), 508-514.
48. Zbar, B., Kishida, T., Chen, F., Schmidt, L., Maher, E. R., Richards, F. M., Crossey, P. A., Webster, A. R., Affara, N. A., Ferguson-Smith, M. A., Brauch, H., Glavac, D., Neumann, H. P., Tisherman, S., Mulvihill, J. J., Gross, D. J., Shuin, T., Whaley, J., Seizinger, B., Kley, N., Olschwang, S., Boisson, C., Richard, S., Lips, C. H., Lerman, M., and et al. (1996) *Hum Mutat* 8(4), 348-357.
49. Cybulski, C., Krzystolik, K., Murgia, A., Gorski, B., Debniak, T., Jakubowska, A., Martella, M., Kurzawski, G., Prost, M., Kojder, I., Limon, J., Nowacki, P., Sagan, L., Bialas, B., Kaluza, J., Zdunek, M., Omulecka, A., Jaskolski, D., Kostyk, E., Koraszewska-Matuszewska, B., Haus, O., Janiszewska, H., Pecold, K., Starzycka, M., Slomski, R., Cwirko, M., Sikorski, A., Gliniewicz, B., Cyrylowski, L., Fiszler-Maliszewska, L., Gronwald, J., Toloczko-Grabarek, A., Zajaczek, S., and Lubinski, J. (2002) *J Med Genet* 39(7), E38.
50. Weirich, G., Klein, B., Wohl, T., Engelhardt, D., and Brauch, H. (2002) *J Clin Endocrinol Metab* 87(11), 5241-5246.
51. Clifford, S. C., Cockman, M. E., Smallwood, A. C., Mole, D. R., Woodward, E. R., Maxwell, P. H., Ratcliffe, P. J., and Maher, E. R. (2001) *Hum Mol Genet* 10(10), 1029-1038.
52. Hoffman, M. A., Ohh, M., Yang, H., Klco, J. M., Ivan, M., and Kaelin, W. G., Jr. (2001) *Hum Mol Genet* 10(10), 1019-1027.
53. Lee, S., Nakamura, E., Yang, H., Wei, W., Linggi, M. S., Sajan, M. P., Farese, R. V., Freeman, R. S., Carter, B. D., Kaelin, W. G., Jr., and Schlisio, S. (2005) *Cancer Cell* 8(2), 155-167.
54. Dahia, P. L., Ross, K. N., Wright, M. E., Hayashida, C. Y., Santagata, S., Barontini, M., Kung, A. L., Sanso, G., Powers, J. F., Tischler, A. S., Hodin, R., Heitritter, S., Moore, F., Dluhy, R., Sosa, J. A., Ocal, I. T., Benn, D. E., Marsh, D. J., Robinson, B. G., Schneider, K., Garber, J., Arum, S. M., Korbonits, M., Grossman, A., Pigny, P., Toledo, S. P., Nose, V., Li, C., and Stiles, C. D. (2005) *PLoS Genet* 1(1), e8.
55. Ang, S. O., Chen, H., Hirota, K., Gordeuk, V. R., Jelinek, J., Guan, Y., Liu, E., Sergueeva, A. I., Miasnikova, G. Y., Mole, D., Maxwell, P. H., Stockton, D. W., Semenza, G. L., and Prchal, J. T. (2002) *Nat Genet* 32(4), 614-621.

56. Pastore, Y. D., Jelinek, J., Ang, S., Guan, Y., Liu, E., Jedlickova, K., Krishnamurti, L., and Prchal, J. T. (2003) *Blood* 101(4), 1591-1595
57. Gordeuk, V. R., Sergueeva, A. I., Miasnikova, G. Y., Okhotin, D., Voloshin, Y., Choyke, P. L., Butman, J. A., Jedlickova, K., Prchal, J. T., and Polyakova, L. A. (2004) *Blood* 103(10), 3924-3932
58. Stebbins, C. E., Kaelin, W. G., Jr., and Pavletich, N. P. (1999) *Science* 284(5413), 455-461
59. Min, J. H., Yang, H., Ivan, M., Gertler, F., Kaelin, W. G., Jr., and Pavletich, N. P. (2002) *Science* 296(5574), 1886-1889
60. Hon, W. C., Wilson, M. I., Harlos, K., Claridge, T. D., Schofield, C. J., Pugh, C. W., Maxwell, P. H., Ratcliffe, P. J., Stuart, D. I., and Jones, E. Y. (2002) *Nature* 417(6892), 975-978
61. Lonergan, K. M., Iliopoulos, O., Ohh, M., Kamura, T., Conaway, R. C., Conaway, J. W., and Kaelin, W. G., Jr. (1998) *Mol Cell Biol* 18(2), 732-741.
62. Kibel, A., Iliopoulos, O., DeCaprio, J. A., and Kaelin, W. G., Jr. (1995) *Science* 269(5229), 1444-1446.
63. Kishida, T., Stackhouse, T. M., Chen, F., Lerman, M. I., and Zbar, B. (1995) *Cancer Res* 55(20), 4544-4548.
64. Jubb, A. M., Pham, T. Q., Hanby, A. M., Frantz, G. D., Peale, F. V., Wu, T. D., Koeppen, H. W., and Hillan, K. J. (2004) *J Clin Pathol* 57(5), 504-512
65. Talks, K. L., Turley, H., Gatter, K. C., Maxwell, P. H., Pugh, C. W., Ratcliffe, P. J., and Harris, A. L. (2000) *Am J Pathol* 157(2), 411-421
66. Bos, R., van der Groep, P., Greijer, A. E., Shvarts, A., Meijer, S., Pinedo, H. M., Semenza, G. L., van Diest, P. J., and van der Wall, E. (2003) *Cancer* 97(6), 1573-1581
67. Vleugel, M. M., Greijer, A. E., Shvarts, A., van der Groep, P., van Berkel, M., Aarbodem, Y., van Tinteren, H., Harris, A. L., van Diest, P. J., and van der Wall, E. (2005) *J Clin Pathol* 58(2), 172-177
68. Kondo, K., Klcó, J., Nakamura, E., Lechpammer, M., and Kaelin, W. G., Jr. (2002) *Cancer Cell* 1(3), 237-246
69. Maranchie, J. K., Vasselli, J. R., Riss, J., Bonifacio, J. S., Linehan, W. M., and Klausner, R. D. (2002) *Cancer Cell* 1(3), 247-255
70. Kondo, K., Kim, W. Y., Lechpammer, M., and Kaelin, W. G., Jr. (2003) *PLoS Biol* 1(3), E83
71. Zimmer, M., Doucette, D., Siddiqui, N., and Iliopoulos, O. (2004) *Mol Cancer Res* 2(2), 89-95
72. Lolkema, M. P., Gervais, M. L., Snijckers, C. M., Hill, R. P., Giles, R. H., Voest, E. E., and Ohh, M. (2005) *J Biol Chem* 280(23), 22205-22211
73. Ohh, M., Yauch, R. L., Lonergan, K. M., Whaley, J. M., Stemmer-Rachamimov, A. O., Louis, D. N., Gavin, B. J., Kley, N., Kaelin, W. G., Jr., and Iliopoulos, O. (1998) *Mol Cell* 1(7), 959-968.
74. Stickle, N. H., Chung, J., Klcó, J. M., Hill, R. P., Kaelin, W. G., Jr., and Ohh, M. (2004) *Mol Cell Biol* 24(8), 3251-3261
75. Woodward, E. R., Buchberger, A., Clifford, S. C., Hurst, L. D., Affara, N. A., and Maher, E. R. (2000) *Genomics* 65(3), 253-265.
76. Giles, R. H., and Voest, E. E. (2005) Tumor suppressors APC and VHL: Gatekeepers of the Intestine and Kidney. In: Macieira-Coelho, A. (ed). *Development Biology of Neoplastic Growth*, Springer-Verlag, Berlin Heidelberg
77. Gallou, C., Longuemaux, S., Delomenie, C., Mejean, A., Martin, N., Martinet, S., Palais, G., Bouvier, R., Droz, D., Krishnamoorthy, R., Junien, C., Beroud, C., and Dupret, J. M. (2001) *Pharmacogenetics* 11(6), 521-535
78. Gallou, C., Joly, D., Mejean, A., Staroz, F., Martin, N., Tarlet, G., Orfanelli, M. T., Bouvier, R., Droz, D., Chretien, Y., Marechal, J. M., Richard, S., Junien, C., and Beroud, C. (1999) *Hum Mutat* 13(6), 464-475
79. Suzuki, H., Ueda, T., Komiya, A., Okano, T., Isaka, S., Shimazaki, J., and Ito, H. (1997) *Oncology* 54(3), 252-257
80. Kishida, T., Chen, F., Lerman, M. I., and Zbar, B. (1995) *J Med Genet* 32(12), 938-941
81. Oberstrass, J., Reifenberger, G., Reifenberger, J., Wechsler, W., and Collins, V. P. (1996) *J Pathol* 179(2), 151-156
82. Brieger, J., Weidt, E. J., Gansen, K., and Decker, H. J. (1999) *Clin Genet* 56(3), 210-215
83. van der Harst, E., de Krijger, R. R., Dinjens, W. N., Weeks, L. E., Bonjer, H. J., Bruining, H. A., Lamberts, S. W., and Koper, J. W. (1998) *Int J Cancer* 77(3), 337-340
84. Rothberg, P. G., Bradley, J. F., Baker, D. W., and Huelsman, K. M. (2001) *Mol Diagn* 6(1), 49-54
85. Li, C., Weber, G., Ekman, P., Lagercrantz, J., Norlen, B. J., Akerstrom, G., Nordenskjold, M., and Bergerheim, U. S. (1998) *Hum Mutat Suppl* 1, S31-33
86. Crossey, P. A., Foster, K., Richards, F. M., Phipps, M. E., Latif, F., Tory, K., Jones, M. H., Bentley, E., Kumar, R., Lerman, M. I., and et al. (1994) *Hum Genet* 93(1), 53-58
87. Olschwang, S., Richard, S., Boisson, C., Giraud, S., Laurent-Puig, P., Resche, F., and Thomas, G. (1998) *Hum Mutat* 12(6), 424-430
88. Foster, K., Prowse, A., van den Berg, A., Fleming, S., Hulsbeek, M. M., Crossey, P. A., Richards, F. M., Cairns, P., Affara, N. A., Ferguson-Smith, M. A., and et al. (1994) *Hum Mol Genet* 3(12), 2169-2173
89. Shuin, T., Kondo, K., Torigoe, S., Kishida, T., Kubota, Y., Hosaka, M., Nagashima, Y., Kitamura, H., Latif, F., Zbar, B., and et al. (1994) *Cancer Res* 54(11), 2852-2855
90. Martin, R. L., Walpole, I., and Goldblatt, J. (1996) *Hum Mutat* 7(2), 185
91. Chen, F., Kishida, T., Yao, M., Hustad, T., Glavac, D., Dean, M., Gnarr, J. R., Orcutt, M. L., Duh, F. M., Glenn, G., and et al. (1995) *Hum Mutat* 5(1), 66-75
92. Koch, C. A., Huang, S. C., Zhuang, Z., Stolle, C., Azumi, N., Chrousos, G. P., Vortmeyer, A. O., and Pacak, K. (2002) *Oncogene* 21(3), 479-482
93. Whaley, J. M., Naglich, J., Gelbert, L., Hsia, Y. E., Lamiell, J. M., Green, J. S., Collins, D., Neumann, H. P., Laidlaw, J., Li, F. P., and et al. (1994) *Am J Hum Genet* 55(6), 1092-1102

Chapter 2:

Fibronectin is a hypoxia-independent target of the tumor suppressor VHL

Bluyssen HA*, Lolkema MP*, van Beest M, Boone M, Sniijckers CM, Los M, Geb-
bink MF, Braam B, Holstege FC, Giles RH, Voest EE

FEBS Lett. 2004. Jan 2;556(1-3):137-42

*Contributed equally

Fibronectin is a hypoxia-independent target of the tumor suppressor VHL

Bluyssen HA*, Lolkema MP*, van Beest M, Boone M, Snijckers CM, Los M, Gebbink MF, Braam B, Holstege FC, Giles RH, Voest EE

FEBS Lett. 2004. Jan 2;556(1-3):137-42

*Contributed equally

The von Hippel-Lindau (VHL) tumor suppressor gene regulates the extracellular matrix by controlling fibronectin deposition. To identify novel VHL-target genes, we subjected mRNA from VHL deficient RCC cells (786-0-pRC) and a transfectant re-expressing wildtype VHL (786-0-VHL) to differential expression profiling. Among the differentially expressed genes, we detected that fibronectin is upregulated in the presence of VHL, while not affected by hypoxia. Thus regulation of fibronectin deposition by VHL occurs at the transcriptional level, irrespective of oxygen levels.

Introduction

Von Hippel-Lindau disease is caused by inactivation of the von Hippel-Lindau (VHL) tumor suppressor gene, and is characterized by the formation of hypervascularized neoplasms, including virtually all sporadic and inherited renal cell carcinomas (RCCs) (1,2).

VHL functions as the substrate recognition moiety of the E3 ubiquitin ligase complex, VCB-CUL2 E3 that targets the α -subunit of the hypoxia-inducible factor (HIF) for degradation by the proteasome under normoxic conditions (3). HIF is a transcription factor regulating genes encoding proteins that function to increase O₂ delivery, allow metabolic adaptation and promote cell survival (4). RCCs lacking functional VHL exhibit high levels of stabilized nuclear HIF, resulting in excessive transcription of HIF target genes, the best documented of which being the vascular endothelial growth factor (VEGF) (5,6). HIF-independent functions of VHL have been described in recent literature. VHL binds the extracellular matrix protein fibronectin; VHL-deficient cells show impaired fibronectin deposition possibly contributing to tumorigenesis and directly influencing the behavior of tumor cells (7).

We and others have previously demonstrated that VHL appears to control extracellular matrix (ECM) degradation by regulating both metalloproteinases -2 and -9 and their inhibitors (8), as well as the urokinase-type plasminogen activator system (9,10). In addition, by promoting the assembly of actin and vinculin, VHL was found to affect

cytoskeletal organization, focal adhesion formation and cell motility (11). VHL influences effects on proliferation, cell cycle progression, as well as alterations of the extracellular matrix interactions. Furthermore, fibronectin gene (FN1) expression has been correlated with increased tumor cell growth and invasiveness of VHL-defective RCCs (12).

To identify novel VHL-target genes, we subjected VHL-deficient RCC cell line (786-0-pRC) and transfectants re-expressing wild-type VHL cDNA (786-0-VHL) to differential expression profiling and identified a group of 16 genes that were either negatively or positively regulated by VHL. Of these genes two interesting features were noticed. The first was a group of genes positively regulated by VHL. Our results confirmed and expanded on earlier reports using differential hybridization (11, 13-16). Interestingly, we identified the gene encoding fibronectin, *FN1*, as a gene positively regulated by VHL, whose transcription levels are unaltered by hypoxia. These data support the hypothesis that VHL also regulates transcription in a HIF-independent manner. Secondly, our data suggest that VHL regulates fibronectin mRNA levels. This knowledge, taken together with the fact that VHL binds fibronectin, increases our understanding of how VHL regulates fibronectin deposition.

Material and Methods

Cell lines

Stable transfectants of 786-0 cells expressing vector backbone alone (786-0-RC) or

**Table 1. VHL target genes
Upregulated**

Accession number	Gene ID		Cy3/Cy5 (Log2 ratio)	Biological function
AA099195	GDIB	GDP dissociation inhibitor B	1.2	Intracellular vesicle transport
AA136799	GADD45	Gene activated by DNA-damage	0.7	Stress response; cell cycle arrest; cell death
AA195589	FN1	Fibronectin	1.6	Cellular adhesion
H07071	VCAM1	Vascular cell adhesion molecule 1	0.8	Cellular adhesion
R81846	FRIL	Ferritin light chain	0.8	Metal transport; RNA stability
W69515	MKK2	MAP kinase kinase 2	0.8	Stress response; nuclear export; cell growth
H52752	GR75	Heat-shock 70-KD protein	0.7	Stress response; cell growth; cellular aging
AA023029	PPP5	Serine/threonine Protein phosphatase 5	0.7	Mitosis; RNA biogenesis; transcription
AA151568	TEGT	Testis enhanced gene transcript	0.7	Cell death
H02641	VHL	Von Hippel-Lindau	0.9	

Downregulated

Accession number	Gene ID		Cy3/Cy5 (Log2 ratio)	Biological function
AA037034	COXA	Cytochrome C oxidase	-1.0	Metabolic response; electron transfer
H86642	CERU	Ceruloplasmin transport	-1.0	Metabolic response; copper
N31417	IGFBP3	Insulin-like growth factor binding protein 3	-2.3	Cell growth
N40420	CGD1	Cyclin D1	-0.8	Cell growth; cell cycle regulator
N91060	VEGF	Vascular endothelial growth factor	-0.9	Angiogenesis; cell growth
N31209	NUP153	Nucleoporin 153	-0.8	Nuclear-cytoplasmic transport
R92231	TLE1	Transducin-like enhancer protein 1	-0.7	Cell differentiation; cell fate

wild type VHL (786-0-VHL) (obtained from W. Kaelin, Dana Farber Cancer Institute, USA) were grown in DMEM (Invitrogen, Carlsbad, CA, USA) supplemented with 10% fetal calf serum (FCS) (Invitrogen, Carlsbad, CA, USA), L-glutamine (2 µM), penicillin (50 IU/ml), and streptomycin sulphate (50 µg/ml) (Invitrogen, Carlsbad, CA, USA).

RNA isolation

Total RNA was isolated using RNAzol B as described by the manufacturer (Campro Scientific, Veenendaal, The Netherlands) and dissolved in DepC-treated milliQ H₂O. Poly A+ RNA was extracted and purified using the oligotex mRNA Mini kit (Qiagen, Valencia, CA, USA).

Microarray analysis

1 µg of poly A+ RNA of each sample was reverse transcribed into cDNA using a reverse transcription kit (Invitrogen, Carlsbad, CA, USA) in combination with an oligo-dT15 primer (Invitrogen, Carlsbad, CA, USA) and

amino allyl containing dUTPs (Sigma, St. Louis, MO, USA). cDNAs were fluorescently labeled with either Cy3 or Cy5 (Amersham Biotech, Buckinghamshire, UK). Chromaspin columns were used to remove unincorporated Cy-dyes (Clontech, Palo Alto, CA, USA). Labeled cDNAs (100 ng per sample in hybridization buffer) were subjected to competitive hybridization on a 1.7K human microarray (obtained from the Microarray Facility of University of Toronto; <http://www.uhnres.utoronto.ca/services/microarray>). Hybridization buffer contained 25% formamide, 2.5X SSC, 0.2% SDS, 100 µg/ml herring sperm DNA and 200 µg/ml E. coli tRNA. A coverslip (25X25 mm) was applied to the microarray after which 30 µl of hybridization mix was applied to hybridize in a hybridization chamber (Corning, New York, USA) overnight in a 42°C water bath. After hybridization, microarrays were washed at room temperature in 1XSSC with 0.2% SDS for four minutes, 0.1XSSC with 0.2% SDS for four minutes, and 0.1XSSC for four

minutes, successively. Subsequently, microarrays were dried by centrifugation (5 min. at 124g) and scanned using a confocal laser scanner (Packard Scanarray 4000XL from Perkin Elmer, Boston, MA, USA). Data were analyzed using Imagene software (Biodiscovery Inc., El Segundo, CA, USA).

RT-PCR analysis

One and a half μg of total RNA was reverse transcribed to obtain cDNA for reverse transcription polymerase chain reaction (RT-PCR) using SuperScript II Rnase H- Reverse Transcriptase (according to manufacturer; Invitrogen, Carlsbad, CA, USA). Gene-specific cDNA fragments were amplified by 25 cycles of PCR consisting of 1 min. at 95°C, 1 min. at 55°C and 2 min. at 72°C. PCR fragments were analyzed by DNA gel electrophoresis. The following primers were used for

RT-PCR: VEGF forward primer: 5'-cgaaacatgaactttctctgc, reverse primer: 5'-ccactctgtgatgattctgc (127 bp product), Glucose Transporter-1 (GLUT-1) forward primer: 5'-ttcaatgctgatgatgaacc, reverse primer: 5'-gtacacaccgatgatgaagc (114 bp product), Insulin-like Growth Factor Binding Protein-3 (IGFBP-3) forward primer: 5'-gaacttctctccgagtcc, reverse primer: 5'-ccttctgtcacagttggga (136 bp product), FN1 forward primer: 5'-caagccagatgtcagaagc, reverse primer: 5'-ggatggtgcatcaatggca (138 bp product), 18S forward primer: 5'-agttggtggagcgattgtc, reverse primer: 5'-tattgtcactctcgggtgg (142 bp product)

Western analysis

Approximately 1×10^6 cells were lysed in 400 μl lysis buffer (20 mM Tris-HCl pH 8.0; 1% Triton-X-100; 140 mM NaCl; 10% glycerol; 0.005% Bromo-Phenol-Blue; 8% β -mercaptoethanol) containing the 'complete' cocktail of protease inhibitors (Roche, Basel, Switzerland). Cell remnants were removed by centrifugation (5 min. at 16,100 g at 4°C) and cleared lysates were stored at -20°C. Approximately 20 μg of protein per lane were analyzed by SDS-PAGE followed by western blotting using a polyclonal antibody specific for IGFBP3 (1:200; kind gift from Dr. J. van Doorn, WKZ Utrecht, the Netherlands), and monoclonal antibodies for fibronectin (1:500; M010, FN30-8, TaKaRa Biomedicals, Shiga, Japan) and for VHL (1:500; IG32, BD-Pharmingen, San Diego, USA), respectively. Antibodies were diluted in PBS containing 5% non-fat dried milk and 0.1% Tween-20. Swine anti-rabbit or rabbit anti-mouse horseradish peroxidase (1:10,000; Pierce, Rockford, IL, USA) was used as a secondary antibody and enhanced chemiluminescence (Perkin Elmer Life sciences, Boston, MA, USA) was used for detection.

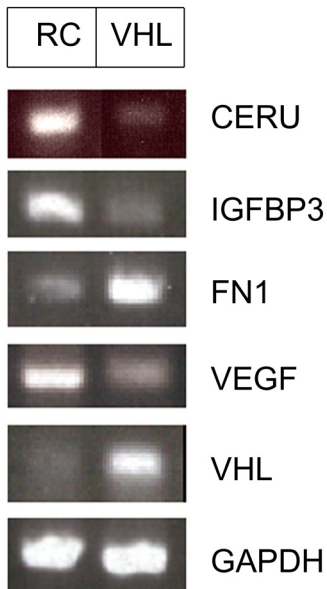


Figure 1: Fibronectin (FN1) gene expression is positively regulated by VHL.

Gene expression levels of *CERU*, *IGFBP3*, *FN1*, *VEGF*, *VHL*, and *GAPDH* were determined by RT-PCR analyses. All panels show specific products for the indicated genes. Left lanes represent VHL-mutant cell line 786-0-RC (RC); right lanes represent the same cell line stably overexpressing VHL, 786-0-VHL (VHL). The housekeeping gene *GAPDH* functions as a control for loading. Previously reported in the literature, *VEGF*, *CERU*, and *IGFBP3* are all negatively regulated by VHL. *FN1* expression, however, is regulated by VHL in the opposite manner.

IGFBP3 and fibronectin detection assays

Secretion levels of IGFBP3 in conditioned medium were determined as described previously (17). Secretion levels of fibronectin were determined by sandwich enzyme-linked immuno-sorbent assay (ELISA) (18) using a polyclonal antibody specific for fibronectin and a monoclonal antibody against fibronectin (respectively M010 and FN30-8, TaKaRa Biomedicals, Shiga, Japan). Rabbit anti-mouse peroxidase was used as a third antibody for detection and quantification.

Real-Time PCR

Real-time PCR was performed using the iCycler iQ real-time PCR detection system (Bio-Rad, Hercules, CA, USA). An optical 96 well reaction plate (Bioplastics, North Ridgeville, OH, USA) and iCycler iQ sealing tape (Bio-Rad, Hercules, CA, USA) was used for PCR amplification. The final reaction mixture of 15 μ l consisted of diluted cDNA, 1 X PCR buffer (Amersham Biotech, Buckinghamshire, UK), 0.05 mM dNTPs (Amersham Biotech,

Buckinghamshire, UK), 100 μ M forward primer, 100 μ M reverse primer and 0.375 units Taq polymerase (Amersham Biotech, Buckinghamshire, UK). For detection of the PCR product in real-time, the SYBR Green I fluorophore (Roche, Basel, Switzerland) was used in a final 10,000-fold dilution. The cDNA was further diluted 6-fold or 2,000-fold prior to PCR amplification of *GLUT-1*, *IGFBP-3* and *FN1* or *18S*, respectively. Gene-specific cDNA fragments, using the same primers as mentioned before, were amplified by 40 cycles of PCR consisting of 30 sec. at 94°C, 30 sec. at 58°C and 30 sec. at 72°C. For each assay, specific targets were amplified in triplicate with their respective standard curve. The equation of the standard curve was used to determine the starting quantity of the samples with the iCycler analysis software. All experimental samples were normalized to *18S* quantities.

Results and discussion

Identification of VHL-regulated genes by microarray analysis

In an attempt to identify novel VHL-target genes involved in tumorigenesis, we subjected mRNA from a VHL effective renal carcinoma cell line (786-0-pRC) and transfectants re-expressing a wildtype *VHL* allele (786-0-VHL) to differential expression profiling. A glass-chip based cDNA array representing about 1700 distinct human genes was spotted in duplicate (obtained from the Microarray Facility of the University of Toronto: <http://www.uhnres.utoronto.ca/services/microarray>). The cDNA made from purified mRNA from 786-0-VHL cells was labeled with Cy3 and mixed with Cy5 labeled cDNA transcribed from 786-0-pRC purified mRNA. After normalization, the Cy3/Cy5 ratio of each gene individually was determined from three independent experiments and overlapping sets of genes were selected. In this way 9 genes, with an average log₂ ratio above 0.7, were considered positively regulated by VHL, whereas 7 genes, that had an average log₂ ratio of -0.7 or below, were considered negatively regulated (Table I). The expression of the *GAPDH* gene was not regulated by VHL (not shown). In addition, the average Cy3/Cy5 log₂ ratio of the *VHL* gene (as expected above 0.7) was used as an internal control as a measure of the reliability of the observed changes.

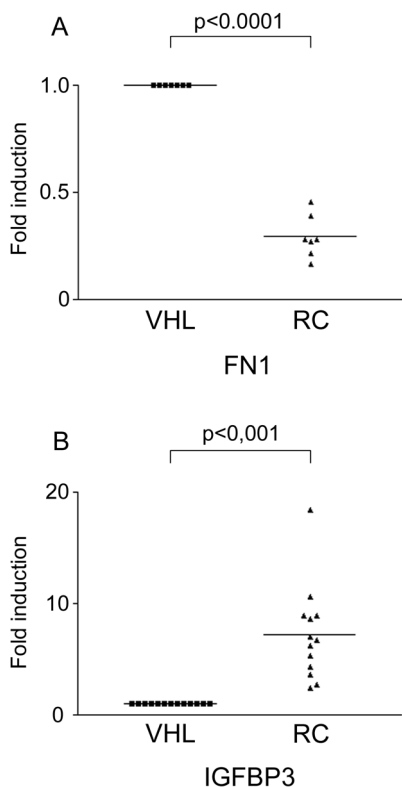


Figure 2: Quantification of IGFBP3 and fibronectin gene expression.

(A) Levels of fibronectin mRNA expression were determined by real-time PCR. The amount of mRNA measured in the 786-0-VHL cell line (VHL) was normalized to 1 and the amount of mRNA in the 786-0-RC cell line (RC) is relative to this amount. Each individual point in the plot is an independent measurement. There is a statistically significant upregulation of fibronectin in the presence of VHL. (B) Quantification of *IGFBP3* mRNA expression performed as described above shows a statistically significant decrease of mRNA levels in the presence of VHL.

RT-PCR was performed as an independent test to confirm the differential expression of some of the genes identified by DNA microarray. As shown in Figure 1, the expression of *FN1* and *VHL* was shown to be higher in 786-0-VHL cells than in 786-0-pRC cells. The opposite was true for *CERU*, *IGFBP3* and *VEGF*. The expression of *GAPDH* was taken as an internal control. In conclusion, similar expression patterns of VHL-target genes were found when measured by these two independent methods.

Using the Gene Ontology Consortium classification of biological processes, these target genes could be classified according to their biological function (Table I). In this way, VHL was shown to be a negative regulator of genes involved in cell proliferation such as *IGFBP3* and *cyclinD1*. Moreover, VHL appeared to positively regulate *GADD45*, a gene involved in cell cycle arrest, as well as *FN1* and *VCAM1* (encoding the vascular cell adhesion molecule), both of which have roles in cell adhesion. Literature searches revealed that eight of the VHL-target genes identified in our study (*VEGF*, *CERU*, *COXA*, *IGFBP3*, *cyclinD1*, *GADD45*, *VCAM1*, and *FN1*) have been previously implicated in the development of RCC (19-23). We further focused on fibronectin as this protein is reported to interact with VHL and is believed to be regulated in a post-transcriptional manner by VHL. However, the transcriptional regulation of *FN1* by VHL has not yet been reported.

Role of VHL in regulation of fibronectin

Levels of fibronectin mRNA increased 3.7-fold in the presence of VHL as measured by repeated real-time PCR analyses (Fig. 2), *IGFBP3* was used to study the behavior of genes down-regulated by VHL. Protein expression levels were determined in whole cell lysates of 786-0-VHL versus 786-0-pRC cells by western analysis. Figure 3A correlates higher fibronectin levels with VHL in 786-0-VHL cells. In contrast, increased levels of *IGFBP3* were detected in 786-0-pRC cells as compared to 786-0-VHL cells. Conditioned medium of 786-0-pRC and 786-0-VHL cells recapitulated the differential secretion of fibronectin and *IGFBP3* (Fig. 3B). 786-0-VHL cells secreted 15-fold more fibronectin than 786-0-pRC cells. Accordingly, *IGFBP3* secretion was relatively high (20-fold) in cultured medium from 786-0-pRC cells

when compared to that of 786-0-VHL cells. Together, these data imply that aberrant production and secretion of fibronectin and *IGFBP3* is directly related to VHL expression in RCC cell lines. It is worthy of noting that fibronectin mRNA levels are remarkably less sensitive to re-expression of VHL than detectable secreted protein levels (approximately 4-fold, discussion below).

Fibronectin is an extracellular glycoprotein that binds to and signals through heterodimeric cell surface receptors known as integrins (24). Loss of fibronectin matrix assembly has been recognized as a feature of cellular transformation (25). Fibronectin has the ability to decrease the metastatic behavior of malignant cells by increasing the interaction between tumor cells and their micro-

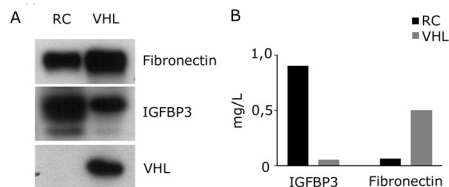


Figure 3: Secretion of *IGFBP3* and fibronectin are inversely regulated by VHL.

(A) Intracellular protein levels of *IGFBP3*, fibronectin and VHL determined by western blot analyses. Left and right lanes contain protein lysates derived from 786-0-RC cell line (RC) and 786-0-VHL (VHL) cell lines, respectively. Upper panel: fibronectin levels increase in the presence of VHL. Middle panel: less *IGFBP3* is detected in the presence of VHL. Lower panel: VHL levels. (B) Levels of secreted *IGFBP3* and fibronectin (FN) depicted left and right, respectively, in conditioned medium from 786-0-RC (RC; black bars) and 786-0-VHL (VHL; gray bars) cell lines. Detection of secreted protein by ELISA was performed in at least three independent experiments.

environment via the integrin receptor family (26). Furthermore, fibronectin can revert some aspects of the malignant phenotype of tumor cells, including proliferation and migration (27). Previous reports have described a physical interaction between VHL and intracellular fibronectin *in vivo*; this interaction affected the ability of cells to assemble an extracellular fibronectin matrix (7). We report here—using the same cell system used to determine VHL-fibronectin binding—that fibronectin mRNA levels are regulated by VHL. The difference in fibronectin secretion in our experiments could not be directly accounted for by mRNA

increase (15-fold vs. 3.7-fold). Our data thus does not exclude the notion that VHL binding to fibronectin regulates the amount of fibronectin deposition in a post-transcriptional manner (7). However, we propose an additional way that VHL regulates fibronectin: at the transcriptional level.

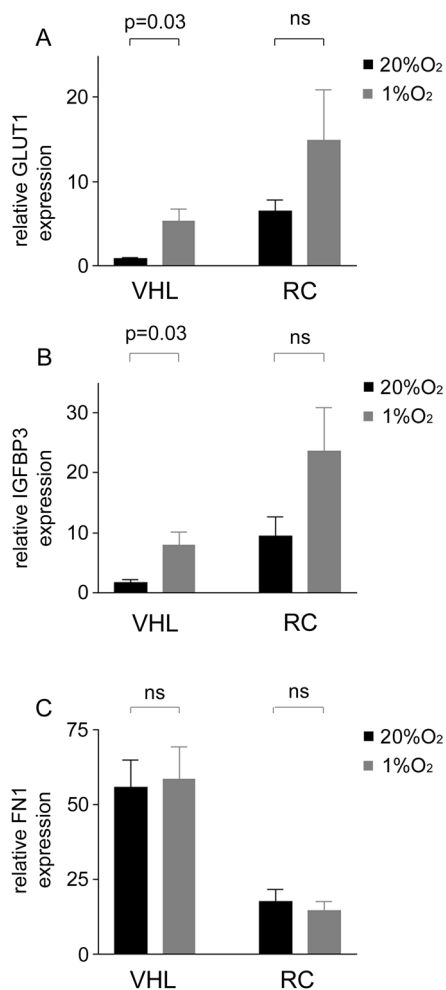


Figure 4: Fibronectin is a hypoxia-independent target of VHL transcriptional regulation.

Cells were either cultured under normoxia (20% O₂; light bars) or hypoxia (1% O₂; dark bars) for 20 hours. The left two columns represent cDNA derived from the 786-0-VHL cell line (VHL) and the right two columns represent cDNA derived from the 786-0-RC (RC) cell line. These results represent the mean of six independent experiments in triplicate \pm standard error of the mean. P-values were determined by paired, two-tailed t-test. (n.s., not significant). (A) *GLUT-1* mRNA levels were measured by real-time PCR as a positive control for hypoxia-induction. As expected, *GLUT-1* expression increases in response to hypoxia in the 786-0-VHL cell line. (B) Like *GLUT-1*, *IGFBP3* mRNA levels are significantly regulated by hypoxia. (C) *FN1* mRNA expression does not respond to hypoxia in either the 786-0-RC or in the 786-0-VHL cell lines.

Effect of hypoxia on the VHL-target genes *FN1* and *IGFBP3*

Because many of known VHL target genes (including *VEGF*) are regulated by the HIF transcription factors, we next determined the effect of hypoxia on the expression of *FN1* and *IGFBP3*. Therefore, we cultured 786-0-VHL or 786-0-pRC cells under normoxic (20% O₂) or hypoxic (1% O₂) conditions for 18 hours. Total RNA was extracted from these cells and subjected to quantitative real-time PCR to follow the expression of *GLUT-1* (which is a known hypoxia-inducible gene) (4), *IGFBP3* and *FN1*. The expression of *18S* (which is not affected by hypoxia) was taken as an internal control and used to normalize expression of *GLUT-1*, *IGFBP3* and *FN1*.

As shown in Figure 4A, hypoxia significantly induces the expression of *GLUT-1* by 6.7-fold in 786-0-VHL cells after 18 hours of hypoxic treatment ($p = 0.025$; Fig. 4A). In 786-0-pRC cells the expression of *GLUT-1* mRNA was not significantly changed. Similar results were also shown for *VEGF* expression under these conditions (data not shown). As expected, hypoxia also induced *IGFBP3* mRNA expression (approximately 5-fold; $p = 0.029$) in 786-0-VHL cells, whereas in the absence of functional VHL (i.e. 786-0-pRC), *IGFBP3* expression did not significantly differ (Fig. 4B). This implicated a role of HIF in the regulation of the *IGFBP3* gene by VHL. Although the expression of both *GLUT-1* and *IGFBP3* in 786-0-pRC was not significantly altered by hypoxia, a trend towards induction of transcription was present (Fig. 4A and B). In contrast, *FN1* expression was not affected by hypoxia in 786-0-VHL cells as well as in 786-0-pRC cells, and suggested a HIF-independent mechanism of regulation by VHL. To chemically mimic the effect of hypoxia we administered cobalt chloride to these cell lines, thereby artificially stabilizing HIF and stimulating HIF-mediated transcription (28). This method was able to reproduce hypoxia

effects on *GLUT-1*, *VEGF*, *IGFBP3* and *FN1* expression (data not shown).

Our data demonstrate positive regulation of *FN1* by VHL thereby suggesting the existence of a HIF-independent pathway of transcriptional control by VHL. Our findings support the hypothesis that VHL is positioned in both HIF-independent and HIF-dependent pathways that are involved in extracellular matrix deposition (14,29). HIF-independent VHL transcriptional targets provide a possible link with the tumor suppressor mechanism of VHL. It is tempting to speculate that the induction of genes in the presence of VHL and the downregulation of these genes in the absence of VHL both play a role in the development of the malignant properties of RCCs.

Acknowledgments

We thank Maarten Pennings for performing the fibronectin ELISA's and Germa Tooten for IGFBP3 quantifications. This study was supported in part by the Dutch Cancer Society (grant UU 1999-1879 and UU 1999-2114 to EV).

Reference List:

- (1) Kaelin, W. G., Jr. (2002) *Nat.Rev.Cancer* 2, 673-682
- (2) Ohh, M. and Kaelin, W. G., Jr. (1999) *Mol.Med.Today* 5, 257-263
- (3) Epstein, A. C., Gleadle, J. M., McNeill, L. A., Hewitson, K. S., O'Rourke, J., Mole, D. R., Mukherji, M., Metzen, E., Wilson, M. I., Dhanda, A., Tian, Y. M., Masson, N., Hamilton, D. L., Jaakkola, P., Barstead, R., Hodgkin, J., Maxwell, P. H., Pugh, C. W., Schofield, C. J. and Ratcliffe, P. J. (2001) *Cell* 107, 43-54
- (4) Semenza, G. (2002) *Biochem.Pharmacol.* 64, 993-998
- (5) George, D. J. and Kaelin, W. G., Jr. (2003) *N.Engl.J.Med.* 349, 419-421
- (6) Yang, J. C., Haworth, L., Sherry, R. M., Hwu, P., Schwartzentruber, D. J., Topalian, S. L., Steinberg, S. M., Chen, H. X. and Rosenberg, S. A. (2003) *N.Engl.J.Med.* 349, 427-434
- (7) Ohh, M., Yauch, R. L., Lonergan, K. M., Whalley, J. M., Stemmer-Rachamimov, A. O., Louis, D. N., Gavin, B. J., Kley, N., Kaelin, W. G. and Jr., Iliopoulos, O. (1998) *Mol.Cell* 1, 959-968
- (8) Koochekpour, S., Jeffers, M., Wang, P. H., Gong, C., Taylor, G. A., Roessler, L. M., Stearman, R., Vasselli, J. R., Stetler-Stevenson, W. G., Kaelin, W. G., Jr., Linehan, W. M., Klausner, R. D., Gnarr, J. R. and Vande Woude, G. F. (1999) *Mol. Cell Biol.* 19, 5902-5912
- (9) Los, M., Zeamari, S., Foekens, J. A., Gebbink, M. F. and Voest, E. E. (1999) *Cancer Res.* 59, 4440-4445
- (10) Zatyka, M., da Silva, N. F., Clifford, S. C.,

- Morris, M. R., Wiesener, M. S., Eckardt, K. U., Houlston, R. S., Richards, F. M., Latif, F. and Maher, E. R. (2002) *Cancer Res.* 62, 3803-3811
- (11) Kamada, M., Suzuki, K., Kato, Y., Okuda, H. and Shuin, T. (2001) *Cancer Res.* 61, 4184-4189
- (12) Lieubeau-Teillet B, Rak J, Jothy S, Iliopoulos O, Kaelin W, Kerbel RS (1998) *Cancer Res.* 58, 4957-62
- (13) Galban, S., Fan, J., Martindale, J. L., Cheadle, C., Hoffman, B., Woods, M. P., Temeles, G., Brieger, J., Decker, J. and Gorospe, M. (2003) *Mol. Cell Biol.* 23, 2316-2328
- (14) Wykoff, C. C., Pugh, C. W., Maxwell, P. H., Harris, A. L. and Ratcliffe, P. J. (2000) *Oncogene* 19, 6297-6305
- (15) Wykoff, C. C., Pugh, C. W., Harris, A. L., Maxwell, P. H. and Ratcliffe, P. J. (2001) *Novartis. Found.Symp.* 240, 212-225
- (16) Zatyka, M., da Silva, N. F., Clifford, S. C., Morris, M. R., Wiesener, M. S., Eckardt, K. U., Houlston, R. S., Richards, F. M., Latif, F. and Maher, E. R. (2002) *Cancer Res.* 62, 3803-3811
- (17) de Vries, B. B., Robinson, H., Stolte-Dijkstra, I., Tjon Pian Gi, C. V., Dijkstra, P. F., van Doorn, J., Halley, D. J., Oostra, B. A., Turner, G. and Niermeijer, M. F. (1995) *J.Med.Genet.* 32, 764-769
- (18) Di Girolamo, N., Underwood, A., McCluskey, P. J. and Wakefield, D. (1993) *Diabetes* 42, 1606-1613
- (19) Boer, J. M., Huber, W. K., Sultmann, H., Wilmer, F., von Heydebreck, A., Haas, S., Korn, B., Gunawan, B., Vente, A., Fuzesi, L., Vingron, M. and Poustka, A. (2001) *Genome Res.* 11, 1861-1870
- (20) Hintz, R. L., Bock, S., Thorsson, A. V., Bovens, J., Powell, D. R., Jakse, G. and Petrides, P. E. (1991) *J.Urol.* 146, 1160-1163
- (21) Stassar, M. J., Devitt, G., Brosius, M., Rinnab, L., Prang, J., Schradin, T., Simon, J., Petersen, S., Kopp-Schneider, A. and Zoller, M. (2001) *Br.J.Cancer* 85, 1372-1382
- (22) Takahashi, M., Rhodes, D. R., Furge, K. A., Kanayama, H., Kagawa, S., Haab, B. B. and Teh, B. T. (2001) *Proc.Natl.Acad.Sci.U.S.A* 98, 9754-9759
- (23) Young, A. N., Amin, M. B., Moreno, C. S., Lim, S. D., Cohen, C., Petros, J. A., Marshall, F. F. and Neish, A. S. (2001) *Am.J.Pathol.* 158, 1639-1651
- (24) Ruoslahti, E. (1999) *Adv.Cancer Res.* 76, 1-20
- (25) Plantefaber, L. C. and Hynes, R. O. (1989) *Cell* 56, 281-290
- (26) Giancotti, F. G. and Ruoslahti, E. (1990) *Cell* 60, 849-859
- (27) Pasqualini, R., Bourdoulous, S., Koivunen, E., Woods, V. L., Jr. and Ruoslahti, E. (1996) *Nat. Med.* 2, 1197-1203
- (28) Yuan Y, Hilliard G, Ferguson T, Millhorn DE. (2003) *J. Biol. Chem.* 278:15911-6
- (29) Jiang, Y., Zhang, W., Kondo, K., Klco, J. M., St Martin, T. B., Dufault, M. R., Madden, S. L., Kaelin, W. G., Jr. and Nacht, M. (2003) *Mol.Cancer Res.* 1, 453-462

A grayscale microscopic image of cells, likely showing a cluster or colony. The image is used as a background for the text. The text is centered and reads: Chapter 3: Tumor suppression by the von Hippel-Lindau protein requires phosphorylation of the acidic domain. Below this, the authors are listed: Lolkema MP*, Gervais ML*, Snijckers CM, Hill RB, Giles RH, Voest EE†, Ohh M†. The journal citation is: J Biol Chem. 2005 Jun 10;280(23):22205-11. At the bottom, it says *†Contributed equally.

Chapter 3:

Tumor suppression by the von Hippel-Lindau protein requires phosphorylation of the acidic domain.

Lolkema MP*, Gervais ML*, Snijckers CM, Hill RB, Giles RH, Voest EE†, Ohh M†.

J Biol Chem. 2005 Jun 10;280(23):22205-11

*†Contributed equally

Tumor suppression by the von Hippel-Lindau protein requires phosphorylation of the acidic domain.

Lolkema MP*, Gervais ML*, Snijckers CM, Hill RP, Giles RH, Voest EE†, Ohh M†.

J Biol Chem. 2005 Jun 10;280(23):22205-11.

*†Contributed equally

The tumor suppressor function of the von Hippel-Lindau protein has previously been linked to its role in regulating hypoxia inducible factor levels. However, VHL gene mutations suggest a hypoxia inducible factor-independent function for the N-terminal acidic domain in tumor suppression. Here we report that phosphorylation of the N-terminal acidic domain of the von Hippel-Lindau protein by casein kinase 2 is essential for its tumor suppressor function. This post-translational modification does not affect the levels of hypoxia inducible factor, however it does change the binding of the von Hippel-Lindau protein to another known binding partner: fibronectin. Cells expressing phospho-defective mutants cause improper fibronectin matrix deposition and demonstrate retarded tumor formation in mice. We propose that phosphorylation of the acidic domain plays a role in the regulation of proper fibronectin matrix deposition and that this may be relevant for the development of VHL-associated malignancies.

Introduction

In some anatomical venues neoplastic transformation occurs upon biallelic inactivation of the von Hippel-Lindau gene (*VHL*) (1). In their lifetime, patients carrying a mutated *VHL* gene are predisposed to multiple tumors in a number of organs including the retina, cerebellum, spinal cord, adrenal gland, and kidney. Despite this phenotypic heterogeneity, *VHL* patients can be segregated based on their likelihood of developing pheochromocytoma. That is, Type 1-*VHL* patients are at low risk of developing pheochromocytoma, but do develop clear-cell renal cell carcinoma (CC-RCC). Type 2 patients develop pheochromocytoma and are further subdivided; Type 2A patients have low risk for CC-RCC, and Type 2B patients have high risk for CC-RCC. Types 1, 2A and 2B patients all develop the two cardinal features of the *VHL* disease, namely retinal and central nervous system (CNS) haemangioblastoma. However, Type 2C patients exclusively develop pheochromocytoma (2,3).

pVHL forms a multiprotein complex (VEC) with elongin C, elongin B, Cul-2, and Rbx-1 (reviewed in: (4)). VEC functions as an E3 ubiquitin ligase to target the α subunit of a heterodimeric transcription factor called HIF (hypoxia-inducible factor) for polyubiquitination (5-7). The polyubiquitin-tagged HIF α is subsequently degraded by the 26S proteasome. pVHL functions as the target

recognition moiety of the VEC complex and specifically recognizes prolyl-hydroxylated HIF α subunits (8,9). This post-translational modification of HIF α requires oxoglutarate, iron and oxygen (8-10). Thus, ubiquitin-mediated destruction of HIF α occurs selectively under normoxic conditions. Accordingly, biallelic inactivation of the *VHL* gene through mutation, deletion, or promoter silencing generally leads to the stabilization of HIF α and thereby promotes the up-regulation of numerous HIF-target genes, resulting in an inappropriate triggering of the hypoxic response under normal oxygen tension (4). However, type 2C patient mutations do not affect E3 ligase function of pVHL and hence HIF regulation is normal, yet these patients nevertheless develop pheochromocytoma (3). Therefore we hypothesized that another function of pVHL is essential for its tumor suppressor activity.

The *VHL gene* produces two wild-type isoforms, the 30kD full-length pVHL30 and a shorter 19kD pVHL19 that is generated by an alternative translational initiation at methionine 54 (11-13). Both pVHL30 and pVHL19 form an active VEC complex and both proteins independently have been shown to suppress tumor formation in nude mouse xenograft assays (12-14). However, analyzing known mutations in *VHL* patients revealed a number of disease-associated mutations in the acidic domain that would not affect the transcription and function of

the pVHL19 isoform (*VHL mutation database*; <http://www.umd.be:2020/>). Hence, although the functional significance of the extra N-terminal acidic domain of pVHL30 remains unclear, this region in pVHL clearly contributes to the tumor suppressor function of pVHL.

Here, we show that pVHL30 is phosphorylated within the N-terminal acidic domain by casein kinase (CK) 2. The phosphorylation status of pVHL30 does not affect the E3 ubiquitin ligase function. Ablation of CK2-specific phosphorylation sites or inhibition of CK2 activity increased affinity to fibronectin, yet resulted in decreased deposition of extracellular fibronectin. Interestingly, cells expressing phospho-defective pVHL delay the onset of tumor formation in a SCID xenograft assay. Hence, CK2-mediated phosphorylation represents a HIF-independent tumor suppressor function of the acidic domain of pVHL.

Methods and Materials

Cell culture

Human kidney 293T cells and 786-O CC-RCC cells were cultured in RPMI 1640 or Dulbecco's modified Eagle medium (DMEM) medium containing 10% heat-inactivated fetal bovine serum (FBS) (Sigma, St. Louis, MO) supplemented with penicillin, streptomycin and glutamine and maintained at 37°C in a humidified 5% CO₂ atmosphere. 786-O subclones stably expressing HA-pVHL30(WT) (786-WT), HA-pVHL30(AAA) (786-AAA), or empty plasmid (786-MOCK) were generated as previously described (15).

Antibodies

Monoclonal anti-GAL4 (DBD; RK5C1 Santa Cruz Biotechnology, Santa Cruz, CA), anti-HA (12CA5, hybridoma supernatant) (Roche, Basel, Switzerland), anti-VSV (P4D5, hybridoma supernatant), anti-RPTP μ (3D7, hybridoma supernatant), anti-Cul2 (Zymed, San Francisco, CA), anti- α tubulin (Sigma, St. Louis, MO), polyclonal anti-GLUT1 (Alpha Diagnostics, San Antonio, TX), anti-CK2 (Santa Cruz Biotechnology, Santa Cruz, CA) and anti-fibronectin (TaKaRa Biomedicals, Shiga, Japan) were obtained from the indicated companies.

Plasmids

pVHL30 and pVHL19 isoforms were cloned into a pcDNA₃ vector (Stratagene, La Jolla,

CA) containing an N-terminal VSV-or HA-tag. Mammalian expression plasmid pRc-CMV-HA-pVHL(WT) was described previously (15) and pRc-CMV-HA-pVHL(AAA) were generated using the QuikChange Site-Directed Mutagenesis Kit (Stratagene, La Jolla, CA). S33A, S38A, and S43A substitutions were generated using the following primer sets: 5'-CGGGGAGGAGGCGGGCGCCGAGGAG-3'/5'-CTCTCGGCGCCCGCCTC CTCCCG-3', 5'-GCGCCGAGGAGGCGCCCGGAAGAG-3'/5'-CTCTTCCGG GCCGGCCTCTCGGCGC-3', and 5'-GGCCCGAAGAGGCCGCGCCG-GAGG-3'/5'-CCTCCGGGCGGCCTCTCCGGGCC-3', respectively. The authenticity of all plasmids was confirmed by direct DNA sequencing.

Immunoprecipitation and immunoblotting

For immunoprecipitations (IP), protein A/G agarose beads (Santa Cruz Biotechnology, Santa Cruz, CA) and antibody were pre-coupled for 30 min and washed twice with Triton-lysis buffer (20mM TRIS pH 8.0, 140mM NaCl, 10% glycerol, 1% Triton X-100). Samples were added to the pre-coupled beads and binding was allowed to occur for 90 min at 4°C, then washed 4 times with 800 ml of Triton-lysis buffer, submitted to SDS-PAGE gel electrophoresis and electrotransferred onto a PVDF membrane (Bio-Rad Laboratories Inc., Mississauga, ON). Specific protein bands on Western blots were visualized using the various indicated antibodies. All primary antibodies were diluted in PBS containing 5% non-fat dry milk and 0.1% Tween-20. Goat-anti-mouse-HRP or goat-anti-rabbit-HRP (Pierce, Rockford, IL) was used 1:20,000 as secondary antibody after which enhanced chemiluminescence (Perkin Elmer Life Sciences, Boston, MA) was performed for detection.

[³²P]-orthophosphate labeling

786-WT or 293T cells were seeded in 6 well plates and grown to 80% confluency. Cells were washed once with phosphate-free medium (ICN Biochemicals, Irvine, CA) followed by growth in phosphate-free medium supplemented with 200 μ Ci of [³²P]-orthophosphate and labeled for 4 hours. Cells were transferred to ice, washed with ice-cold PBS and then lysed using 500 μ l of Triton-lysis buffer containing protease inhibitor mix (Roche, Basel, Switzerland) and phosphatase inhibitor mix (0.1mg/ml Na₃VO₄, 0.1mg/ml β -glycerophosphate and 1mg/ml

Na₄P₂O₇). These lysates were then submitted for various immunoprecipitations.

In vitro kinase assay

Plasmids encoding wild-type or the indicated mutant pVHL were in vitro transcribed and translated using the TNT Quick-Coupled Transcription/Translation System (Promega, Madison, WI). 5U of recombinant casein kinase 2a (CK2a) (Promega, Madison, WI) with the recommended buffer and 1µl of in vitro translated protein were mixed in a reaction volume of 50µl with 10µCi of [³²P] g-ATP (Perkin Elmer Life sciences, Boston, MA) for 30 min at 30°C. In vitro translated products were immunoprecipitated to increase the specificity of the signal. CK2 inhibitors daidzein (Sigma, St. Louis, MO) and 4,5,6,7-tetrabromobenzotriazole (TBB, a kind gift from D. Shugar, Warsaw, Poland) were used at indicated concentrations during the incubation with [³²P] γ-ATP.

Gel filtration assay

The gel filtration assay was done using a column containing a biogel A15-m (Bio-Rad Laboratories Inc., Mississauga, ON). The column was equilibrated using PBS, pH7.4 and 200µl of crude cell lysate in Triton-lysis buffer was run at 0.5 ml/min and samples of 0.5ml each were collected. The bed volume of the column used was 25ml. Fractions were collected and subsequently submitted to TCA precipitation. The precipitated proteins were dissolved in 50µl of 1X sample buffer and used for western blotting.

In vitro ubiquitination assay

In vitro ubiquitination assay was performed as previously described (6). Briefly, [³⁵S]methionine-labeled reticulocyte lysate HA-HIF1α[ODD] translation product (4µl) was incubated in RCC 786-O S100 extracts (100-150µg) supplemented with 8 µg/µl of ubiquitin (Sigma), 100ng/µl of ubiquitin-aldehyde (BostonBiochem, Cambridge, MA), and an ATP-regenerating system (20 mM Tris [pH 7.4], 2 mM ATP, 5 mM MgCl₂, 40 mM creatine phosphate, 0.5 µg/µl of creatine kinase) in a reaction volume of 20 to 30µl for 1.5 h at 30 °C.

Metabolic labeling

Metabolic labeling was performed as previously described (16). In brief, radioisotopic labeling was performed by methionine starvation for 45 minutes, followed by growth in

5 ml of methionine-free DMEM supplemented with [³⁵S]-methionine (100µCi/ml medium) (Amersham Biotech, Buckinghamshire, UK) and 2% dialyzed-FBS for 3hr at 37 °C in a humidified 5% CO₂ atmosphere.

Fibronectin ELISA

Fibronectin ELISA was performed as previously described (2;16). In brief, cells (2 x 10³) were grown for 4 days in 96-well microtiter plates (Costar, Cambridge, MA) prior to cell removal with PBS containing 2mM EDTA. Complete removal of cells was visualized by phase microscopy. Plates were blocked with PBS containing 0.1% heat-inactivated BSA (Invitrogen, Carlsbad, CA, USA) for 1 hour at 37°C and subsequently incubated with 10 µg/ml rabbit anti-fibronectin antibody in PBS/0.1% BSA for 1 hr. Plates were washed three times with PBS and alkaline phosphatase-conjugated goat anti-rabbit IgG (0.1 µg/ml) was added for 1 hr at 37°C. Plates were washed three times with PBS and developed with 1.0 mg/ml p-Nitrophenyl Phosphate in 0.2 M Tris buffer (Sigma, St. Louis, MO). Reactions were stopped with 3 M NaOH and the OD at 405 nm was measured on a microplate reader.

SCID mouse xenograft assay

Multiple 786-O subclones expressing pVHL(WT), pVHL(AAA), or plasmid alone MOCK were grown to approximately 90% confluence in a humidified 5% CO₂ atmosphere at 37°C. Cells were harvested with 0.25% Trypsin/1 mM EDTA solution. 2x10⁶ cells in 50 µl of 1xPBS were injected intramuscularly into the left hind leg of SCID male mice (Charles River Lab). Tumor growth was assessed and measured weekly by carefully passing the tumor-bearing leg through a series of holes of decreasing diameter (0.5 mm decrements) in a plastic rod.

Results

The acidic domain of pVHL30 is phosphorylated by CK2

To determine whether the two naturally occurring pVHL isoforms are phosphorylated, 293T cells were transfected with VSV-tagged pVHL30 and pVHL19, and metabolically labeled with [³²P]-orthophosphate. Cells were then lysed, immunoprecipitated with anti-VSV antibody, resolved on SDS-PAGE, and immunoblotted with anti-VSV antibody (Fig.

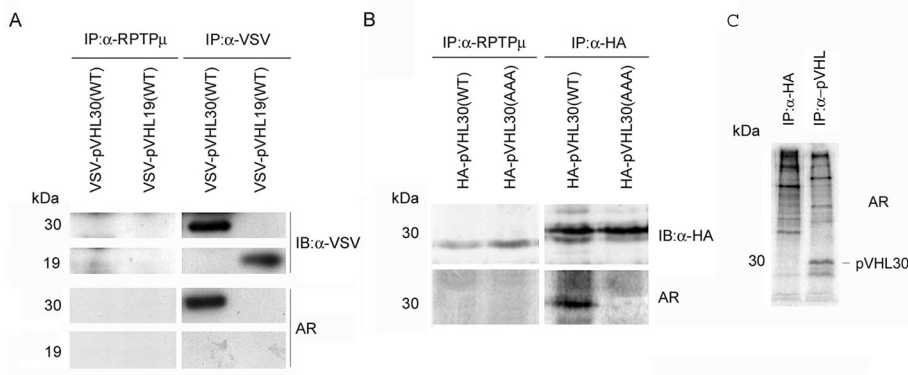


Figure 1: pVHL30, but not pVHL19, is phosphorylated.

(A) 293T cells were transfected with VSV-pVHL30 or VSV-pVHL19 and metabolically labeled with [³²P]-orthophosphate. Cells were lysed, immunoprecipitated with anti-RPTPμ mAb as a negative control (left upper panels) and anti-VSV mAb (right upper panels), and immunoblotted with anti-VSV mAb. Lower panels, autoradiography of the immunoblot showing [³²P] incorporation. (B) 293T cells were transfected with HA-pVHL30(WT) or HA-pVHL30(AAA) and metabolically labeled with [³²P]-orthophosphate. Cells were lysed, immunoprecipitated with anti-RPTPμ mAb as a negative control and anti-HA mAb (upper panels), and immunoblotted with anti-HA mAb. Autoradiography of the immunoblot showing [³²P] incorporation (bottom panels). (C) 293T cells were metabolically labeled with [³²P]-orthophosphate. Cells were lysed, immunoprecipitated with anti-pVHL mAb or anti-HA mAb as a negative control, bound proteins were separated on SDS-PAGE gel electrophoresis and submitted to autoradiography. IB, immunoblot; AR, autoradiography; IP, immunoprecipitation; kDa, kilodalton

1A). Autoradiography of the immunoblot demonstrates that while VSV-pVHL30 incorporated [³²P]-orthophosphate, VSV-pVHL19 did not (Fig. 1A). Computer-based scanning of the full-length pVHL30 indicated multiple potential phosphorylation sites over the entire open reading frame and three predicted CK2-phosphorylation sites in the acidic domain at S33, S38, and S43 (data not shown). Thus, we generated the triple mutant pVHL30(AAA) with serine (S) to alanine (A) substitutions at each of these positions and found that pVHL30(AAA) was no longer ca-

pable of incorporating [³²P]-orthophosphate (Fig. 1B). These results suggest that in an overexpression system pVHL30, but not pVHL19, is phosphorylated at one or more of the serine residue(s) within the acidic domain. To determine the physiologic relevance of this finding we metabolically labeled 293T cells with [³²P]-orthophosphate. Cells were then lysed, immunoprecipitated with anti-pVHL antibody, resolved on SDS-PAGE and blotted (Fig. 1C). Autoradiography of this blot clearly showed a specific band at about 30kD in the anti-pVHL immunoprecipitation

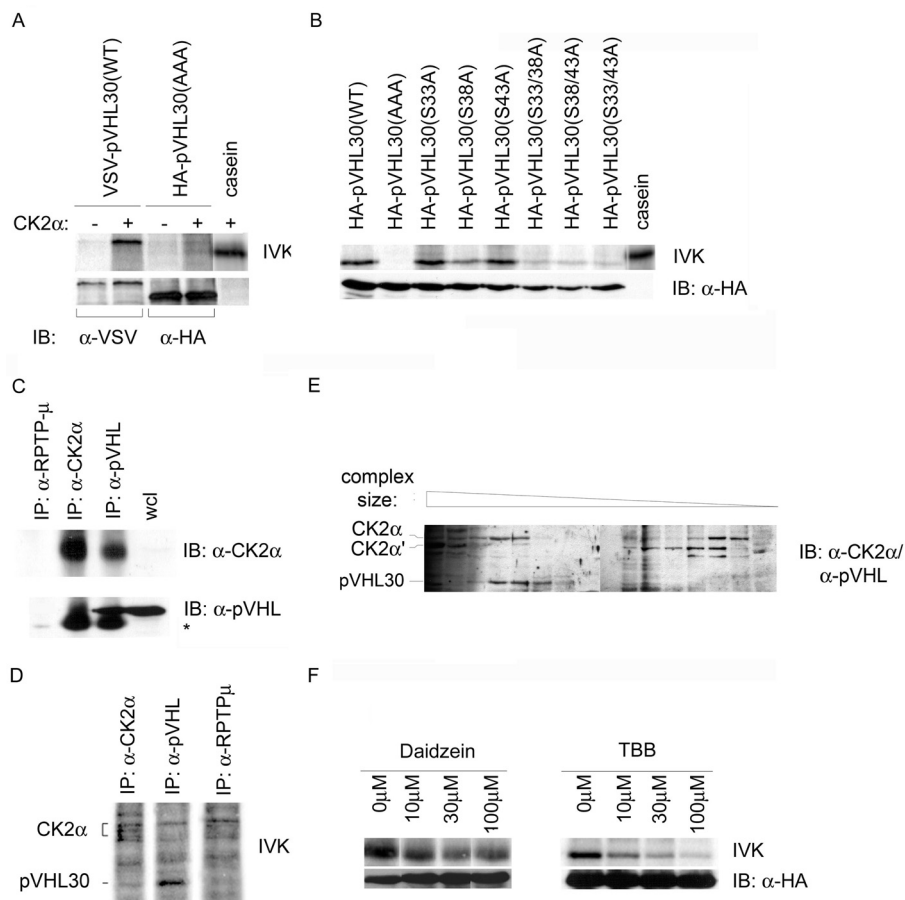


Figure 2: CK2 phosphorylates pVHL30.

(A) In vitro kinase assay (IVK) of in vitro translated VSV-pVHL30(WT) and HA-pVHL30(AAA). After translation proteins were immunoprecipitated with anti-VSV or anti-HA antibody, CK2α was added in the presence of $[^{32}\text{P}] \gamma\text{-ATP}$. Immunoblots with an anti-VSV and anti-HA antibody (lower panel) and visualized by autoradiography (upper panel). Casein was used as a positive control. (B) In vitro translated HA-pVHL30 with the indicated mutations were immunoprecipitated with anti-HA antibody and treated as described above, CK2-mediated phosphorylation (Upper panel). Anti-HA immunoblot of the in vitro translated pVHL used in IVK assay (Lower panel). (C) 786-WT cell lysates were immunoprecipitated with anti-RPTP- μ mAb as a negative control and anti-pVHL mAb, bound proteins were separated on SDS-PAGE and immunoblotted with an anti-CK2 antibody (upper panel) or anti-pVHL antibody (lower panel). (D) 293T cells were lysed and used for endogenous IP of CK2α, pVHL or RPTP μ (aspecific control). The samples were incubated with $[^{32}\text{P}] \gamma\text{-ATP}$, separated on SDS-PAGE and blotted. Bands were visualized using autoradiography. (E) 293T cells were lysed and the lysate was submitted to gel filtration. Fractions of different sizes were collected and after TCA-precipitation the proteins were submitted to western blot analysis using anti-CK2α and anti-pVHL. (F) 293T cells were transfected with HA-pVHL30(WT). IVK assay of anti-HA immunoprecipitations were performed without or with increasing concentrations of the indicated CK2-specific inhibitors (Upper panel). Anti-HA immunoblot indicates equal loading (Lower panel). IVK, in vitro kinase assay; IP, immunoprecipitation; IB, immunoblot; kDa, kilodalton; wcl, whole cell lysate; *, Antibody light chain.

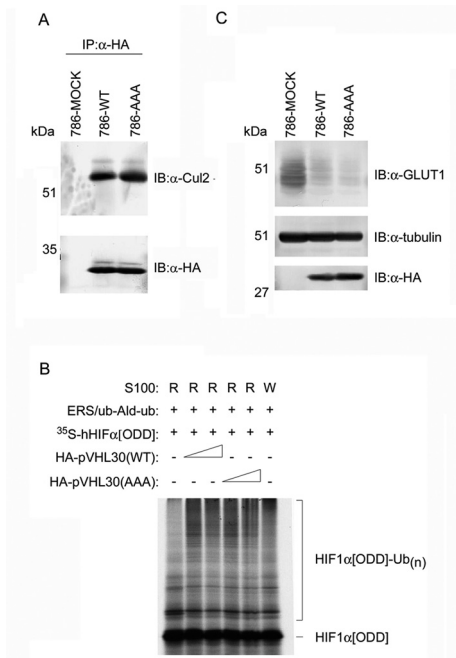


Figure 3: pVHL30(AAA) forms a functional E3 ubiquitin ligase.

(A) 786-O cells stably transfected with plasmids encoding HA-pVHL30(WT) (786-WT), HA-pVHL(AAA) (786-AAA), or empty plasmid (786-MOCK) were lysed and submitted to immunoprecipitation with anti-HA mAb. Bound proteins were separated on SDS-PAGE and immunoblotted with an anti-Cul2 antibody (upper panel) or an anti-HA antibody (lower panel). (B) In vitro ubiquitination of [³⁵S]-labeled HA-hHIF1α(ODD) was performed using S100 extracts generated from 786-MOCK (lanes 1-5), and S100 extracts derived from 786-WT (lane 6). Reaction mixtures were supplemented with increasing amounts of in vitro translated HA-pVHL30(WT) (2 and 4μL; represented by a triangle), in vitro translate HA-pVHL30(AAA) (2 and 4μL; represented by a triangle), or mock translate (2μL), in the presence of purified PHD. All reaction mixtures were immunoprecipitated with anti-Gal4 antibody. Bound proteins were then separated on SDS-PAGE and visualized by autoradiography. (C) Whole cell extracts prepared from the indicated 786-O stable subclones were separated on SDS-PAGE and immunoblotted with an anti-GLUT1 antibody (upper panel), an anti-tubulin antibody (middle panel) as a loading control, or an anti-HA antibody (lower panel). IP, immunoprecipitation; IB, immunoblot; kDa, kilodalton; R, S100 lysate derived from 786-MOCK cells; W: S100 lysate derived from 786-WT cells.

and not in the anti-HA control. From these data we concluded that the phosphorylation of pVHL30 as observed, occurs endogenously.

To directly address whether CK2 is responsible for the phosphorylation of pVHL30 at the predicted serine residues, we performed an in vitro kinase (IVK) assay using in vitro translated VSV-pVHL30(WT) and HA-pVHL30(AAA) with or without recombinant CK2α, the catalytic subunit of CK2 (Fig. 2A). Autoradiography of the IVK assay clearly demonstrates that pVHL30(WT), but not pVHL30(AAA), was phosphorylated by CK2α (Fig. 2A). Casein was used as a positive control for the CK2-mediated IVK assays (Fig. 2A). To determine the exact site or sites of pVHL30 phosphorylation, single and double S to A mutants were generated and analyzed using the IVK assay (Fig. 2B). All in vitro translated single S to A mutants were phosphorylated by recombinant CK2α. It should however be noted that pVHL30(S38A) had noticeably weaker phosphorylation signal. All double S to A mutants showed significantly weaker phosphorylation profiles compared to their wild-type counterpart (Fig. 2B). These data suggest that all three serine residues can serve as CK2-mediated phosphorylation sites, and that the phosphorylation of any one site appears to be temporally and spatially independent of the other two sites' phosphorylation status.

During the course of these IVK assays, we observed that even without adding exogenous CK2α, anti-pVHL30(WT) immunoprecipitates derived from 293T cells exhibited endogenous kinase activity capable of phosphorylating casein (data not shown). Likewise, immunoprecipitates of pVHL30(AAA), which themselves cannot be phosphorylated (Figs. 1A, 2A, 2B), were also capable of phosphorylating purified casein (data not shown). These data suggest that CK2 exists in a complex with pVHL30 irrespective of its phosphorylation status. To further verify that pVHL30-associated kinase is CK2α, 786-O RCC subclones stably expressing HA-pVHL30(WT) (786-WT) were lysed and immunoprecipitated with an anti-pVHL antibody, anti-CK2α antibody, and anti-RPTPμ antibody as a negative control (Fig. 2C). Bound proteins were resolved on SDS-PAGE and immunoblotted with an anti-CK2α antibody and anti-pVHL antibody, which showed that CK2α associates with pVHL30 (Fig. 2C). To determine whether this interaction

occurs in the absence of overexpression, we performed an IP using an anti-CK2 α antibody, an anti-pVHL antibody and anti-RPTP μ antibody as a negative control, which was followed by an IVK assay, resolved on SDS-PAGE gel and visualized by autoradiography. Kinase activity was detected in immunoprecipitates of pVHL and CK2 α , which showed phosphorylation of endogenous pVHL30 (Fig.

2D, lanes 1 and 2). We also observed phosphorylated proteins co-migrating with CK2 α , suggesting autophosphorylation of CK2 α (Fig. 2D). These results suggest that pVHL30 and CK2 α interact under a physiologic condition. Furthermore we performed a size-gel filtration assay to separate endogenous multiprotein complexes from 293T lysate according to their size. After performing the

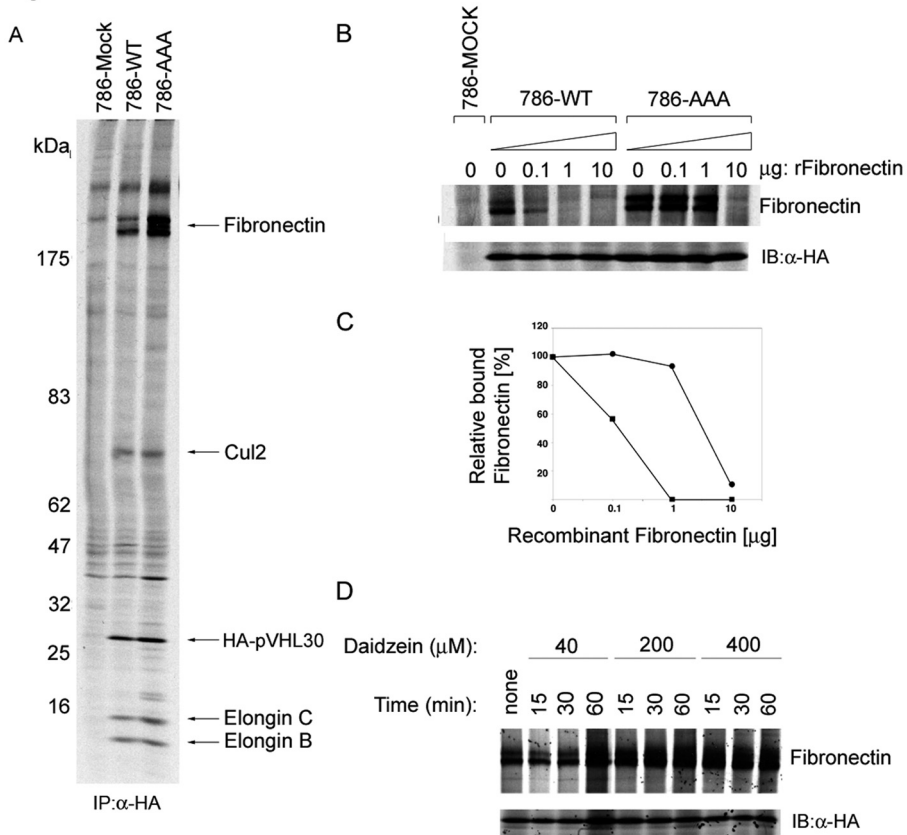


Figure 4: Inhibition of CK2-mediated phosphorylation of pVHL30 increases binding to fibronectin.

(A) The indicated 786-O subclones were radiolabeled with [35 S]-methionine. Cells were lysed and immunoprecipitated with anti-HA antibody. The bound proteins were resolved on SDS-PAGE and visualized by autoradiography. (B) The indicated radiolabeled cells were lysed in the presence of increasing amounts of purified recombinant fibronectin and immunoprecipitated with anti-HA antibody. Bound proteins were resolved on SDS-PAGE and visualized by autoradiography. (C) Densitometry of B. 100% binding represents pVHL30-bound fibronectin in the absence of competing exogenous purified fibronectin. (D) 786-O subclones ectopically expressing HA-pVHL(WT) were radiolabeled with [35 S]-methionine in the presence of increasing concentrations of specific CK2 inhibitor daidzein. Cells were lysed and immunoprecipitated with anti-HA mAb, resolved by SDS-PAGE, and visualized by autoradiography. Upper panel shows bands at the molecular weight of fibronectin, lower panel shows bands at the molecular weight of pVHL indicating equal loading. IP, immunoprecipitation; kDa, kilodalton

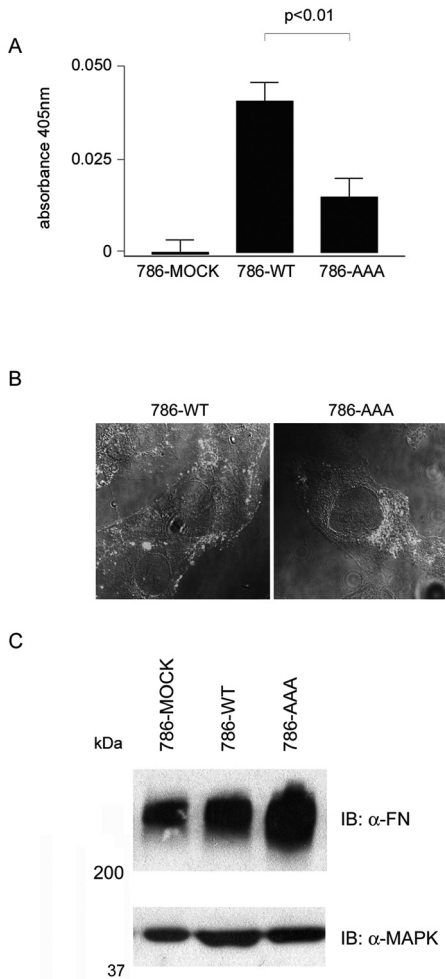


Figure 5: pVHL30(AAA)-expressing RCC cells accumulate intracellular fibronectin.

(A) Fibronectin deposited by 786-MOCK, 786-WT, and 786-AAA cells grown for 4 days in 96-well plates in octoplets were measured by fibronectin ELISA. Relative amounts of fibronectin deposited by cells were normalized against mean of readings obtained from wells containing cell culture media alone for the indicated period. (B) 786-WT and 786-AAA cells were grown on coverslips for 4 days, fixed using ice-cold methanol and stained for fibronectin. Thin slices (0,6µm) of the cells above the level of the matrix were taken using a confocal microscope. (C) 786-MOCK, 786-WT and 786-AAA cells were grown for 4 days, whole cell lysates were prepared after 30 min of trypsin/EDTA treatment at 37°C, then resolved on SDS-PAGE and immunoblotted for fibronectin (upper panel) and MAPK (lower panel) as a loading control. IB, immunoblot; kDa, kilodalton

gel filtration according to size, proteins were concentrated using TCA-precipitation and immunoblotted for pVHL and CK2α. In the fraction containing pVHL30 we do find CK2α, again supporting the notion that pVHL and CK2α are present in the same protein complex (Fig. 2E).

We next examined the effect of specific CK2 inhibitors, daidzein and 4,5,6,7-tetrabromobenzotriazole (TBB), on the phosphorylation of pVHL30. To this end, anti-HA immunoprecipitates from 293T cells transfected with HA-pVHL30 were prepared and used in an IVK assay in the presence of 0, 10, 30, and 100µM daidzein or TBB (Fig. 2F). We observed dosage-dependent inhibition of pVHL30 phosphorylation (Fig. 2F). Collectively, these results show that CK2α binds and phosphorylates pVHL30.

VEC complex formation and function are independent of pVHL30 phosphorylation

To address whether the pVHL30(AAA) mutant is capable of forming an E3 ligase complex, we tested the ability of pVHL30(AAA) to bind to Cul2, a component of the VEC complex that acts as a scaffold. 786-WT, 786-AAA, or 786-MOCK cells were lysed, immunoprecipitated with an anti-HA antibody, resolved on SDS-PAGE, and immunoblotted with an anti-Cul2 antibody and anti-HA antibody (Fig. 3A). This assay shows that pVHL30(AAA) bound Cul2 similar to pVHL30(WT). Furthermore, immunoprecipitation of HA-pVHL30(AAA) from metabolically labeled 786-AAA cells co-precipitated elongin B, elongin C, and Cul2 (Fig. 4A). These results demonstrate that pVHL30(AAA) forms a VEC complex.

We next asked whether pVHL30(AAA) can ubiquitinate HIF1α(ODD) by performing an *in vitro* ubiquitination assay. S100 extracts prepared from 786-MOCK cells lacking pVHL supplemented with *in vitro* translated empty plasmid failed to support the ubiquitination of [³⁵S]-labeled HA-HIF1α(ODD) (Fig. 3B, lane 1). However, S100 extracts supplemented with either increasing amounts of *in vitro* translated HA-pVHL30(WT) (Fig. 3B, lanes 2 and 3) or increasing amounts of *in vitro* translated HA-pVHL30(AAA) (Fig. 3B, lanes 4 and 5) ubiquitinated [³⁵S]-labeled HA-HIF1α(ODD). As expected, S100 extracts made from 786-WT cells supported the ubiquitination of [³⁵S]-labeled HA-HIF1α(ODD) (Fig. 3B, lane 6). Furthermore,

whole cell extract made from 786-AAA cells down-regulated the expression of HIF-target gene GLUT1 under normal oxygen tension similar to 786-WT cells (Fig. 3C). Whole cell extract made from 786-MOCK cells showed over-expression of GLUT1 under normal oxygen tension. These results indicate that phosphorylation of pVHL30 by CK2 is not required for participation in the VEC complex to ubiquitinate HIF α .

Phosphorylation of pVHL30 regulates binding and secretion of fibronectin into extracellular space

Interestingly, HA-pVHL30(AAA) bound strikingly more fibronectin (approximately 3-fold, as measured by densitometry) than HA-pVHL30(WT) to fibronectin (Fig. 4A). Furthermore, the addition of increasing amounts of purified recombinant fibronectin during lysis of radio-labeled cells resulted in greater reduction of fibronectin bound to HA-pVHL30(WT) compared to HA-pVHL30(AAA) (Fig. 4B and C). For example, whereas no appreciable effect was observed on HA-pVHL30(AAA) binding to fibronectin, there was 40% reduction in fibronectin binding by HA-pVHL30(WT) upon the addition of 0.1 μ g of purified fibronectin, as measured by densitometry (Fig. 4C). Addition of 1 μ g of purified fibronectin almost completely competed against the

binding of endogenous fibronectin to HA-pVHL30(WT), but negligibly affected the binding of endogenous fibronectin to non-phosphorylatable HA-VHL30(AAA). Collectively these data imply that dephosphorylation of pVHL30 enhances its ability to bind fibronectin or reduces its ability to release fibronectin.

We next asked whether the inhibition of CK2 activity would recapitulate the increased binding of pVHL30(WT) to fibronectin. During metabolic labeling, 786-WT cells were treated with increasing concentrations of CK2-specific inhibitor diadzein. Cells were then lysed, immunoprecipitated with anti-HA antibody, resolved on SDS-PAGE, and visualized by autoradiography. As predicted, the inhibition of CK2 by diadzein increased pVHL30(WT) binding to fibronectin (Fig. 4B). This effect was not simply due to increased expression of pVHL30(WT) in diadzein-treated cells, as noted by relatively equal loading of de novo translated pVHL30(WT) (Fig. 4B). Treatment with staurosporine (a general serine/threonine kinase inhibitor excluding CK2) had negligible effect on fibronectin binding (data not shown). These results suggest that a specific inhibition of CK2 enhances pVHL30 binding to fibronectin.

We next asked what effect pVHL30 binding of fibronectin had on subsequent deposition of fibronectin in the extracellular space. Relative

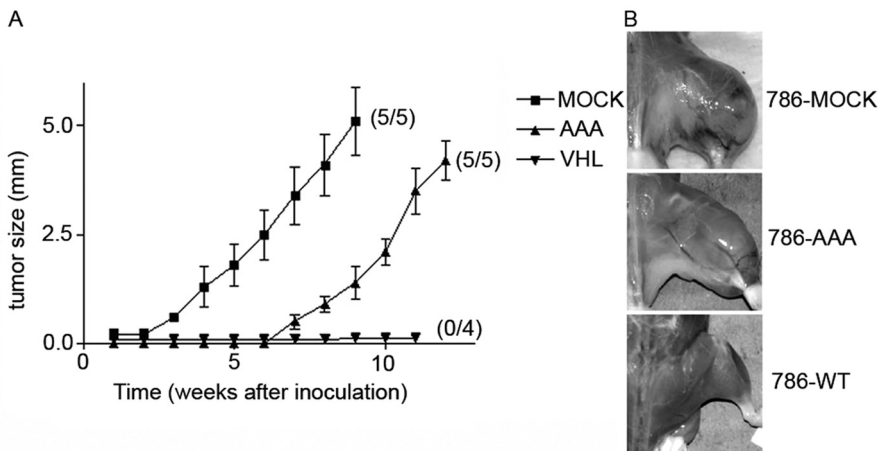


Figure 6: pVHL30(AAA) fails to suppress tumor development in SCID mice xenograft assay.

(A) A graph of tumor-growth over time in mice injected with the indicated 786-O stable subclones. The total number of mice that grew tumor is indicated on the right. This is a representative experiment of three experiments. (B) Tumor-take in representative mouse injected with either 786-O cells stably expressing MOCK, pVHL30(WT), or pVHL30(AAA).

amounts of fibronectin deposited by 786-MOCK, 786-WT and 786-AAA cells grown on 96 well plates for 4 days were measured by ELISA using anti-fibronectin antibody after the cells were removed using Trypsin-free EDTA solution to preserve any fibronectin that was deposited on plastic. As expected, 786-MOCK cells deposited significantly less fibronectin than 786-WT cells. However, the enhanced fibronectin binding by pVHL(AAA) resulted in less fibronectin deposition than 786-WT cells (Fig. 5A). Anti-fibronectin immunofluorescence using confocal microscopy demonstrated an expected fibronectin staining in the cytoplasm and along the cell periphery in 786-WT cells (Fig. 5B). However, 786-AAA cells showed excessive perinuclear fibronectin staining as well as punctate staining along the cell cortex (Fig. 5B). Concordantly, 786-AAA cells showed more intracellular fibronectin expression than in 786-WT cells (Fig. 5C). 786-WT and 786-AAA cells showed similar *de novo* translation of fibronectin as measured by [³⁵S]-metabolic labeling (data not shown). These data suggest that although 786-AAA cells are capable of producing fibronectin, they are less capable of releasing fibronectin into the extracellular space, which would account for the increased intracellular accumulation of fibronectin.

Phosphorylation of pVHL30 is required for tumor suppression in SCID mice

To determine if phosphorylation plays a role in tumor suppression, multiple 786-O subclones expressing pVHL(WT), pVHL(AAA), or plasmid alone (MOCK) were injected intramuscularly into the left hind legs of SCID mice. Tumor-take and -size were monitored and measured weekly (Fig. 6). After approximately 3-4 weeks, as expected, 786-MOCK cells began to form tumors (15/15). The mice injected with 786-AAA cells began to develop tumors (15/15) after 7-8 weeks, while mice injected with multiple 786-WT subclones were tumor-free (0/14). These results demonstrate that the phosphorylation of pVHL30 within the first 53 amino acids have a direct role in tumor suppression.

Discussion

Not all VHL disease-causing mutations result in the dysregulation of HIF activity (2;3;17). For example, Type 2C-associated mutations such as L188V or K159E have been shown

to have wild-type or 'normal' E3 ubiquitin ligase activity to target HIF α subunits for oxygen-dependent polyubiquitination. However, every VHL disease-causing mutant tested to date has shown a failure to bind fibronectin, resulting in a reduction of extracellular fibronectin matrix assembly (2;3;17). Here we show that inhibition of pVHL phosphorylation, either by serine to alanine substitutions or by treatment with CK2-specific inhibitors, results in markedly increased binding of pVHL30 to fibronectin, while maintaining wild-type E3 ligase function. This increased binding, however, led to reduced fibronectin deposition in the extracellular space. The improper deposition of fibronectin into the extracellular space or interference with its proper function has been correlated with the development of dysplasia in *Xenopus* and fibronectin has been shown to influence the malignant behavior of tumor cells in experimental mouse models (18;19). Thus, we postulate that the tumor suppressor function of the phosphorylation of pVHL30 is related to the regulation of proper fibronectin deposition.

The tumor suppressor function of pVHL we describe here requires the N-terminal acidic domain and is independent of the regulation of HIF α . Multiple papers have recently been published regarding the role of stabilized HIF in tumorigenesis, using an identical cell system as we describe here. Collectively, these articles suggest that HIF2 α is the effector of tumorigenesis upon loss of functional pVHL. In the first 2 studies, Kondo et al. (2002) and Maranchie et al. (2002) address whether overexpressed stabilized HIF can counteract tumor suppression by pVHL (20,21). Kondo et al. (22) show that the 786-O cells expressing stable HIF2 α are able to override the pVHL-mediated tumor suppression. However, these studies do not address the more physiologically relevant question of whether the suppression of endogenous HIF2 α would be sufficient to abrogate tumor development in these patient-derived renal cell carcinoma cells (786-O RCC). Kondo et al. and Zimmer et al. do address this question with HIF2 α RNAi; their data indeed support an oncogenic role for HIF2 α (22,23). These experimental data do not, however, exclude further tumor suppressor functions for pVHL. The *in vivo* experiments described in these papers were terminated after 8-10 weeks, whereas our experiments demonstrate that this time point

is only when the 786-O cells deficient for CK2-mediated phosphorylation begin forming detectable tumors (Fig. 6). Moreover, tumor growth in the absence of HIF2 α is retarded, but not completely inhibited (22). On the basis of these findings and our data, we propose that although HIF2 α is an important regulator of tumor growth, it is not the only effector of tumorigenesis in pVHL-deficient cancers. These data lead us to hypothesize that an additional tumor suppressor function is linked to the phosphorylation of the acidic domain of pVHL.

The regulation of fibronectin by pVHL is tightly linked to the development of VHL disease. It follows then that there are multiple levels of fibronectin regulation by pVHL30. First, pVHL30 positively regulates transcription of the gene encoding fibronectin, *FN1*, in a HIF-independent manner (24). Second, as shown here, phosphorylation of the N-terminal acidic domain of pVHL30 mediates the engagement and/or disengagement of fibronectin. Third, modification of pVHL30 by ubiquitin-like molecule NEDD8 is linked to fibronectin binding, where the inhibition of pVHL30 neddylation prohibited fibronectin binding (18). Thus, fibronectin deposition by pVHL seems to be a highly regulated process and is unique to the pVHL30 isoform, as pVHL19 does not bind fibronectin (11).

We show here that CK2 exists in a complex with pVHL30 and phosphorylates S33, S38, and S43 in the N-terminal acidic domain of pVHL30. CK2 is a hetero-tetrameric complex composed of two β and two α subunits (25). The two β subunits have no kinase activity, but are thought to have a regulatory role enhancing the catalytic activity of the α subunits (25). Differential gene expression profiling of chemically-induced kidney carcinoma cells of Eker rats demonstrated over-expression of CK2 β subunits, indicating that amplification of CK2 α function may be involved in renal carcinogenesis (26). In support of this notion, human kidney tumors have been shown to express elevated levels of CK2 α and CK2 β (27). Moreover, CK2 localizes and binds to microtubules and has been shown to phosphorylate various microtubule-binding proteins (28-31). Recently, pVHL has been shown to associate with microtubules (32), which raises the possibility that pVHL30 and CK2 interact on microtubules. Taken together our data present a novel tumor suppressor function for the acidic domain of pVHL, which might help to elucidate the

complex genotype-phenotype correlation in the VHL disease.

Acknowledgements

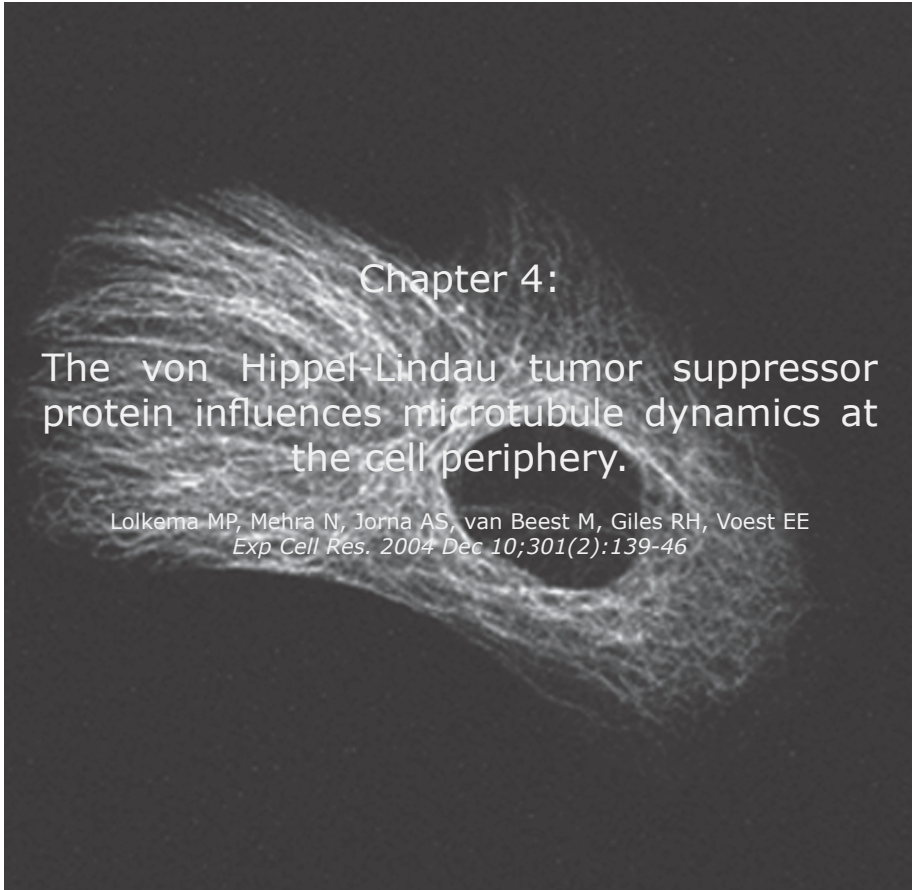
We thank the members of Ohh and Voest labs for helpful discussions and comments. We also thank Dr. Heng Qi, Bob Kuba, Dorus Mans and Natalie H. Stickle for their technical assistance.

Reference List

- (1) Lonser, R. R., Glenn, G. M., Walther, M., Chew, E. Y., Libutti, S. K., Linehan, W. M., and Oldfield, E. H. (2003) *Lancet* 361, 2059-2067
- (2) Hoffman, M. A., Ohh, M., Yang, H., Klco, J. M., Ivan, M., and Kaelin, W. G., Jr. (2001) *Hum.Mol. Genet.* 10, 1019-1027
- (3) Clifford, S. C., Cockman, M. E., Smallwood, A. C., Mole, D. R., Woodward, E. R., Maxwell, P. H., Ratcliffe, P. J., and Maher, E. R. (2001) *Hum.Mol. Genet.* 10, 1029-1038
- (4) Maynard, M. A. and Ohh, M. (2004) *Am.J.Nephrol.* 24, 1-13
- (5) Kamura, T., Sato, S., Iwai, K., Czyzyk-Krzeska, M., Conaway, R. C., and Conaway, J. W. (2000) *Proc.Natl.Acad.Sci.U.S.A* 97, 10430-10435
- (6) Ohh, M., Park, C. W., Ivan, M., Hoffman, M. A., Kim, T. Y., Huang, L. E., Pavletich, N., Chau, V., and Kaelin, W. G. (2000) *Nat.Cell Biol.* 2, 423-427
- (7) Cockman, M. E., Masson, N., Mole, D. R., Jaakkola, P., Chang, G. W., Clifford, S. C., Maher, E. R., Pugh, C. W., Ratcliffe, P. J., and Maxwell, P. H. (2000) *J.Biol.Chem.* 275, 25733-25741
- (8) Ivan, M., Kondo, K., Yang, H., Kim, W., Valiando, J., Ohh, M., Salic, A., Asara, J. M., Lane, W. S., and Kaelin, W. G., Jr. (2001) *Science* 292, 464-468
- (9) Jaakkola, P., Mole, D. R., Tian, Y. M., Wilson, M. I., Gielbert, J., Gaskell, S. J., Kriegsheim, A., Hestrestreit, H. F., Mukherji, M., Schofield, C. J., Maxwell, P. H., Pugh, C. W., and Ratcliffe, P. J. (2001) *Science* 292, 468-472
- (10) Epstein, A. C., Gleadle, J. M., McNeill, L. A., Hewitson, K. S., O'Rourke, J., Mole, D. R., Mukherji, M., Metzzen, E., Wilson, M. I., Dhanda, A., Tian, Y. M., Masson, N., Hamilton, D. L., Jaakkola, P., Barstead, R., Hodgkin, J., Maxwell, P. H., Pugh, C. W., Schofield, C. J., and Ratcliffe, P. J. (2001) *Cell* 107, 43-54
- (11) Iliopoulos, O., Ohh, M., and Kaelin, W. G., Jr. (1998) *Proc.Natl.Acad.Sci.U.S.A* 95, 11661-11666
- (12) Schoenfeld, A., Davidowitz, E. J., and Burk, R. D. (1998) *Proc.Natl.Acad.Sci.U.S.A* 95, 8817-8822
- (13) Blankenship, C., Naglich, J. G., Whaley, J. M., Seizinger, B., and Kley, N. (1999) *Oncogene* 18, 1529-1535
- (14) Iliopoulos, O., Kibel, A., Gray, S., and Kaelin, W. G., Jr. (1995) *Nat.Med.* 1, 822-826
- (15) Lonergan, K. M., Iliopoulos, O., Ohh, M., Kamura, T., Conaway, R. C., Conaway, J. W., and Kaelin, W. G., Jr. (1998) *Mol.Cell Biol.* 18, 732-741

-
- (16) Ohh, M., Yauch, R. L., Lonergan, K. M., Whaley, J. M., Stemmer-Rachamimov, A. O., Louis, D. N., Gavin, B. J., Kley, N., Kaelin, W. G., Jr, and Iliopoulos, O. (1998) *Mol.Cell* 1, 959-968
- (17) Stickle, N. H., Chung, J., Klco, J. M., Hill, R. P., Kaelin, W. G., Jr, and Ohh, M. (2004) *Mol.Cell Biol.* 24, 3251-3261
- (18) Marsden, M. and DeSimone, D. W. (2001) *Development* 128, 3635-3647
- (19) Pasqualini, R., Bourdoulous, S., Koivunen, E., Woods, V. L., Jr, and Ruoslahti, E. (1996) *Nat. Med.* 2, 1197-1203
- (20) Kondo, K., Klco, J., Nakamura, E., Lechpammer, M., and Kaelin, W. G., Jr. (2002) *Cancer Cell* 1, 237-246
- (21) Maranchie, J. K., Vasselli, J. R., Riss, J., Bonifacio, J. S., Linehan, W. M., and Klausner, R. D. (2002) *Cancer Cell* 1, 247-255
- (22) Kondo, K., Kim, W. Y., Lechpammer, M., and Kaelin, W. G., Jr. (2003) *PLoS.Biol.* 1, E83
- (23) Zimmer, M., Doucette, D., Siddiqui, N., and Iliopoulos, O. (2004) *Mol.Cancer Res.* 2, 89-95
- (24) Bluysen, H. A., Lolkema, M. P., van Beest, M., Boone, M., Snijckers, C. M., Los, M., Gebbink, M. F., Braam, B., Holstege, F. C., Giles, R. H., and Voest, E. E. (2004) *FEBS Lett.* 556, 137-142
- (25) Meggio, F. and Pinna, L. A. (2003) *FASEB J.* 17, 349-368
- (26) Patel, S. K., Ma, N., Monks, T. J., and Lau, S. S. (2003) *Mol.Carcinog.* 38, 141-154
- (27) Stalter, G., Siemer, S., Becht, E., Ziegler, M., Remberger, K., and Issinger, O. G. (1994) *Biochem.Biophys.Res.Comm.* 202, 141-147
- (28) Lim, A. C., Tiu, S. Y., Li, Q., and Qi, R. Z. (2004) *J.Biol.Chem.* 279, 4433-4439
- (29) Moreno, F. J., Diaz-Nido, J., Jimenez, J. S., and Avila, J. (1999) *Mol.Cell Biochem.* 191, 201-205
- (30) Avila, J., Ulloa, L., Gonzalez, J., Moreno, F., and Diaz-Nido, J. (1994) *Cell Mol.Biol.Res.* 40, 573-579
- (31) Krieg, M., Haas, R., Brauch, H., Acker, T., Flamme, I., and Plate, K. H. (2000) *Oncogene* 19, 5435-5443
- (32) Hergovich, A., Lisztwan, J., Barry, R., Ballschmieter, P., and Krek, W. (2003) *Nat.Cell Biol.* 5, 64-70



A fluorescence microscopy image of a cell, likely a fibroblast, showing a dense network of microtubules. The microtubules are stained and appear as bright, fibrous structures against a dark background. The cell is roughly elongated and has a central nucleus area that is darker. The microtubules are more concentrated at the periphery of the cell, particularly on the left side.

Chapter 4:

The von Hippel-Lindau tumor suppressor protein influences microtubule dynamics at the cell periphery.

Lolkema MP, Mehra N, Jorna AS, van Beest M, Giles RH, Voest EE
Exp Cell Res. 2004 Dec 10;301(2):139-46

The von Hippel-Lindau tumor suppressor protein influences microtubule dynamics at the cell periphery.

Lolkema MP, Mehra N, Jorna AS, van Beest M, Giles RH, Voest EE
Exp Cell Res. 2004 Dec 10;301(2):139-46

The von Hippel-Lindau protein (VHL) protects microtubules (MTs) from destabilization by nocodazole treatment. Based on this fixed-cell assay with static end points, VHL has been reported to directly stabilize the MT cytoskeleton. To investigate the dynamic changes in MTs induced by VHL in living cells, we measured the influence of VHL on tubulin turnover using fluorescence recovery after photobleaching (FRAP). To this end we engineered VHL-deficient renal cell carcinoma cells to constitutively incorporate fluorescently labeled tubulin and to inducibly express VHL. Induction of VHL in these cells resulted in a decrease of tubulin turnover as measured by FRAP at the cell periphery, while minimally influencing MT dynamics around the centrosome. Our data indicates that VHL changes the behavior of MTs dependent on their subcellular localization implying a role for VHL in cellular processes such as migration, polarization and cell-cell interactions. Here we propose a complementary method to directly measure VHL-induced subcellular changes in microtubule dynamics, which may serve as a tool to study the effect of MT binding proteins such as VHL.

Introduction

In a recent publication, the von Hippel-Lindau (VHL) protein was described to stabilize microtubules (MTs) (1). This finding is significant because it ascribes a novel function for VHL and suggests a mechanism for its tumor suppressor activity. Biallelic inactivation of VHL results in multi-focal tumor formation and is present in the majority of sporadic and inherited renal cell carcinomas (2). MT cytoskeleton dynamics play an important role in various physiological processes such as cell migration, establishing epithelial cell polarity, neurite formation and mitosis. A frequently applied assay to assess whether drugs or proteins affect MT stability uses the microtubule disrupting agent nocodazole. After nocodazole treatment, cells are fixed and stained for acetylated or detyrosinated tubulin to identify the remaining stable MTs. This assay does not depict the dynamic process that underlies MT-stability; rather, it shows an endpoint measurement after nocodazole treatment. The exact nature of the influence of VHL on the MT dynamics described by Hergovich et al. could not be deduced from the static assay as mentioned above (1). We hypothesized that detailing the precise changes in MT dynamics induced by VHL would lend insight to the functional consequences of VHL-loss in the early stages of renal cell carcinoma.

To measure the rate of MT turnover we adapted a well-defined method to study

the dynamics of protein movement in living cells: fluorescence recovery after photobleaching (FRAP) (3). This technique has been previously used to study the behavior of individual MTs using green fluorescent protein (GFP)-labeled α -tubulin (4). Furthermore, using FRAP to measure MT dynamics has been validated extensively in studies involving microinjection of fluorochrome-labeled tubulin (5-8). However, FRAP has not yet been used to assess the effect of drugs or proteins on MT-stabilization. The advent and validation of GFP-labeled tubulin as a tool to study MT dynamics opens the door for studying changes in global MT turnover (4), such as those induced by MT-stabilizing agents.

In this paper we describe a FRAP-based analysis of MT dynamics. We validate our adapted method by showing that (YFP)-labeled α -tubulin (hereafter, tubulin-YFP) incorporates into stable microtubules and that recovery of tubulin-YFP into the bleached region has kinetic properties that can be associated with the properties of microtubule dynamics as previously published. Using this assay we measured changes in MT dynamics by paclitaxel (commonly known as Taxol[®]), a drug known to influence MT stability. To investigate the role of VHL in MT dynamics, we constructed a stable human renal cell carcinoma cell line, which conditionally over-expresses VHL from a tetracycline responsive promoter. After expression of VHL was induced, we registered a change

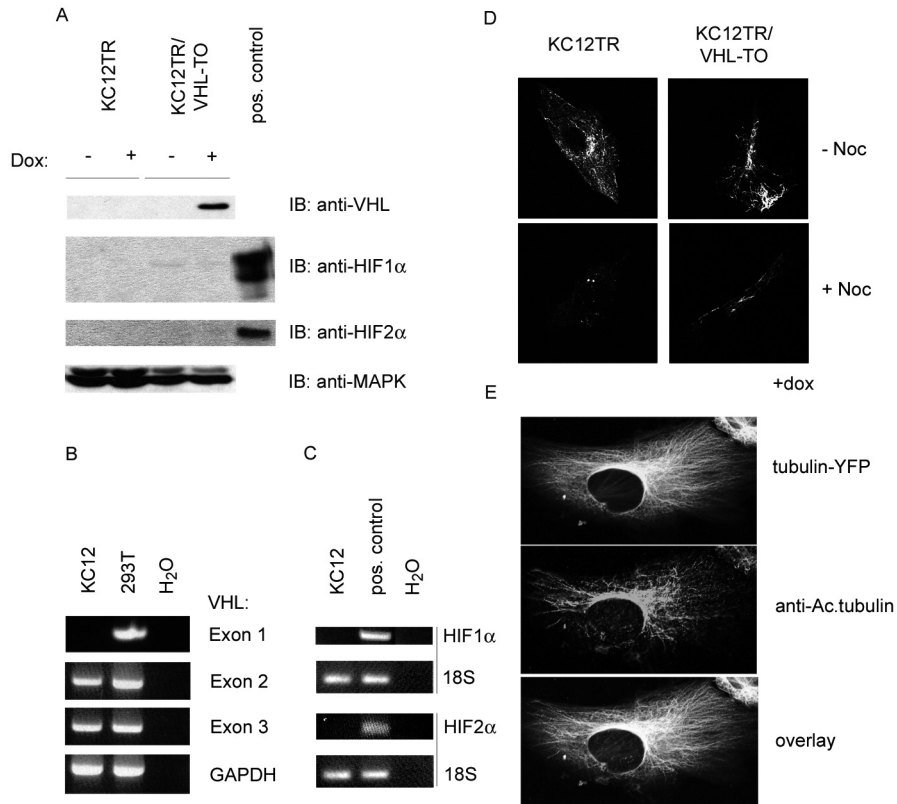


Figure 1: Characterization of KC12RN cell line

(A) Western blot analysis for expression of VHL, HIF1 α and HIF2 α of whole cell lysates of KC12TR or KC12TR/VHL-TO cells stimulated for 16 hrs + or - doxycycline (dox). Upper panel shows western blot analysis of VHL. The second panel shows western blot for HIF1 α with lysate of PC3 prostate carcinoma cell line treated with desferrioxamine as positive control and the third panel shows western blot of HIF2 α with lysate of the VHL deficient 786-O renal carcinoma cell line as a positive control. For loading control the same lysates were submitted to western blot analysis for MAPK (lower panel). (B) KC12 cells have biallelic deletion of VHL exon 1. PCR of genomic DNA with primers specific for the 3 exons of VHL from KC12 and 293T cells. As a positive control for DNA loading a PCR for GAPDH was performed (lower panel). H₂O, contamination control. (C) RT-PCR analysis of HIF α subunits in the KC12 cells. Upper panel shows the RT-PCR for *HIF1 α* with RNA from 293T cells as positive control. The third panel shows RT-PCR for *HIF2 α* with RNA from 786-O cells as a positive control. *18S* is amplified as RNA input control for each experiment (second and fourth panel). (D) KC12TR and KC12TR/VHL-TO cells, all exposed to doxycycline (+dox), were treated with or without nocodazole (noc) for 20 minutes, fixed with methanol and stained for acetylated tubulin. Representative images acquired with the confocal microscope are shown. Noc., nocodazole. (E) KC12RN cells were fixed with methanol and stained for acetylated tubulin. Upper panel shows tubulin-YFP staining, middle panel shows acetylated tubulin staining and lower panel shows the overlay of the two images.

in MT dynamics specifically at the cell periphery. Thus, we have developed a sensitive method to measure real-time changes in MT dynamics, which has allowed us to quantify the MT-stabilizing effect of the tumor suppressor VHL.

Materials and Methods

Expression vectors and cell culturing

KC12 renal cell carcinoma cell line was generously provided by Dr. Oshimura (9) and propagated with RPMI-1640 containing 5% Fetal Calf Serum (FCS), penicillin and streptomycin (Invitrogen Carlsbad, CA). The PC3

prostate cancer and 786-O renal cell carcinoma cell lines were obtained from the ATCC and cultured under the same conditions. The T-REX system (Invitrogen, Carlsbad, CA) was used according to the manufacturer's instructions to generate doxycycline-inducible VHL expressing cells. In short, 10^7 cells were transfected by electroporation with 20 μ g FspI linearized pcDNA₄TR. After 3 weeks of selection, blasticidin (10 μ g/ml) resistant colonies were expanded and transfected with pcDNA₄TO-Luciferase. Two clones showing the strongest induction were chosen. These were subsequently transfected with 20 μ g PvuI linearized full-length VHL, which had been cloned into pcDNA₄TO. After selection on Zeocin (500 μ g/ml), resistant colonies were tested for VHL induction by immunocytochemical staining and western blot after addition of doxycycline and selected for further studies. Selected clones were then further transfected with α -tubulin-YFP (Invitrogen, Carlsbad, CA) and cultured selecting for neomycin (500 μ g/ml) resistant clones.

Reagents and antibodies

Nocodazole, zeocin, blasticidin and neomycin were purchased from Invitrogen, Carlsbad, CA. Further reagents used were: doxycycline (Sigma-Aldrich, St.Louis, MO), paclitaxel (Bristol-Meyers-Squibb, New York, NY), anti-acetylated tubulin (1:500) (monoclonal Ab, Sigma-Aldrich, St.Louis, MO), anti-HIF1 α (1:200) (monoclonal Ab, Beckton Dickinson, San Jose, CA), anti-HIF2 α (1:200) (monoclonal Ab, Beckton Dickinson, San Jose, CA), anti-VHL (1:500) (monoclonal Ab, Beckton Dickinson, San Jose, CA), anti-MAPK (1:3000) (polyclonal Ab, gift of Dr. O. Kranenburg, Dept. of Surgery, University Medical Center Utrecht, The Netherlands).

Western blotting

Samples were examined by SDS-PAGE and subsequent western blotting. Specific protein bands on the western blots were visualized using the appropriate antibodies as indicated in the text. All antibodies were diluted in PBS containing 5% dried skim milk and 0.1% Tween-20. Rabbit anti-Mouse HRP (Pierce, Rockford, IL) (1:20,000) or Swine anti-Rabbit (DAKO, Glostrup, Denmark) (1:3000) were used as secondary antibody after which enhanced chemiluminescence (Perkin Elmer Life sciences, Boston, MA) was used for detection.

Genomic PCR

Genomic DNA was isolated using standard procedures and the PCR of the three exons of VHL was performed using the primers described by Gnarr et al. (10)

RT-PCR

RNA from cell lysates was extracted using RNAbee reagent following the protocol of the manufacturer (Campro Scientific, The Netherlands). cDNA was made using 2 μ g of total RNA and reverse transcribed using Superscript Reverse Transcriptase (Invitrogen, Carlsbad, US) and random hexamers. We used the following primers in our assays: HIF1 α -Fw: 5'-gctgatttggaaccattcctc, HIF1 α -Rev: 5'-gcagcaacgacacagaaact, HIF2 α -Fw: 5'-gaggtgttctatgagctggccc, HIF2 α -Rev: 5'-cttgagggtgacagtacggcc, 18S-Fw: 5'-agttggaggagcattgtc, 18S-Rev: 5'-tattgtcaatctcgggtgg.

Immunofluorescent staining

Cells were washed once with PBS and fixed with 100% ice-cold methanol for 2 minutes at RT, then washed again with PBS. Primary antibodies for staining were used as indicated in the text. Secondary antibodies were goat-anti-mouse Alexa488 (1:200) (DAKO, Glostrup, Denmark) and goat-anti-mouse Alexa 568 (1:200) (DAKO, Glostrup, Denmark). All incubations were done in PBS containing 1% BSA at room temperature in a dark chamber. Staining was visualized on a Zeiss LSM510 confocal imaging unit (Jena, Germany).

Fluorescence recovery after photobleaching (FRAP)

Cells were cultured on 24 mm diameter round coverslips and prepared for imaging on the Zeiss LSM510 confocal imager in a climate box at of 37°C and humidified air containing 5%CO₂. The cells were imaged using the argon laser at approximately 15mW of energy. Images taken for monitoring fluorescence intensity used less than 1% of the laser power and the high-intensity bleaching beam was used at 100% of the laser power in all channels for the argon laser (458nm, 477nm, 488nm, 514nm). The pinhole was adjusted to record slices of approx. 3-6 μ m. In region B (at the cell periphery, see Fig. 2), selecting a larger pinhole resulted in higher percentage of interpretable FRAP patterns. Frames were recorded every 10 seconds for

the dynamics around the centrosome (region A), but taken every 5 seconds to accurately determine the half-life time for the dynamics at the cell periphery (region B). Regions were selected for FRAP according to the cartoon shown in figure 2A. Regions bleached were similar in size. For further calculations we used the parameters and formulas given in Table 1. To be able to determine half-life time we plotted the %Fi vs time and using Sigmaplot software (SPSS, Chicago, IL) we curve-fitted these data with the regression wizard. We chose the 'rise to the max. function' and performed the regression using 3 variables ($f = y_0 + a * (1 - \exp(-b * x))$). From these data we calculated the half-life of fluorescence recovery ($t(1/2)$) from the following function: $t(1/2) = \ln(2)/b$. To correct for loss of global fluorescence that inevitably occurs as a result of imaging, we normalized our data using the mean fluorescence of the entire cell over the time imaged vs. our bleached region of interest (see Table 1 for mathematical formulas). However the two variables occasionally result in a slight increase in the adjusted fluorescence that is measured in the region of interest. Because very mobile proteins will recover 100%, normalizing the data to account for total loss of fluorescence might appear as >100% recovery. All M_f and half-life time data were pooled from at least 3 independent experiments and statistical analyses were performed using a two-tailed Student's T-Test.

Results and discussion

Induction of VHL in KC12 cells affects MTs

To determine the role of VHL in MT dynamics, we constructed cell lines carrying doxycycline-inducible expression plasmids encoding

full-length VHL (KC12 TR/VHL-TO) or an empty plasmid (KC12TR). As the recipient cell line, we chose the human renal cell carcinoma line KC12, which has a known inactivating VHL mutation (9) and is tumorigenic in mouse xenografts. Multiple clones were isolated and tested for inducibility of VHL expression (Figure 1A). VHL protein was not detected in uninduced clones. However, KC12 cells contain a constitutive unbalanced chromosomal translocation resulting in chromosome 3p11-ter loss in one VHL allele in the T-lymphocytes from the VHL patient, and it is possible that the remaining VHL allele is intact. We thus reanalyzed these renal carcinoma cells for the presence of VHL mutations. To begin with, we analyzed the genomic DNA of this cell line by Southern blot analysis using hybridization probes for each three of the three exons of VHL. KC12 cells failed to hybridize a probe comprising the first exon of VHL (data not shown). Probes for the second and third exons, however, hybridized to KC12 genomic DNA. These data suggest that the VHL allele not affected by the $t(3;5)$ has also acquired a somatic deletion of exon 1. Because the first exon of VHL contains the translation initiation site, these mutations would both constitute complete null-alleles. Because biallelic deletion of VHL should also be detectable by a more sensitive PCR amplification, we PCR amplified the 3 exons of VHL and confirmed that exon 1 is deleted in the KC12 cells (Figure 1B). The remaining two exons amplified with expected efficiency (Figure 1B) and showed no sequence abnormalities (data not shown). These data suggest that a somatic mutation occurring in the renal carcinoma of this VHL patient is limited to exon 1 of VHL.

VHL-deficient cells normally express high levels of hypoxia inducible transcription factor alpha (HIF α) under normoxic conditions

Table 1. Formulas used for FRAP calculus

F(ROI)	Mean fluorescence intensity of region of interest (ROI)
F(total cell)	Mean fluorescence intensity of the entire cell
Fi	Average fluorescence before bleaching (5 values averaged)
F ω	Mean fluorescence of last 10 time points recorded in experiments reaching an equilibrium
F(t)n	Normalized fluorescence at time point (t) = $F_t(\text{ROI}) / (F_t(\text{total cell}) / F_i(\text{total cell}))$
F0	F0 = F(t)n directly after bleach
%Fi	Percentage of initial fluorescence = $100 - \{(F_i(\text{ROI}) - F(t)n) / (F_i(\text{ROI}))\} * 100$
Mf	$(F_\omega - F_0) / (F_i - F_0)$
t(1/2)	$t(1/2) = \ln(2)/b$, b is derived from curve fitting as described in the text

(11). We thus determined the levels of HIF1 α and HIF2 α on western blots. Contrary to our expectations given the biallelic inactivation of VHL in KC12 cells we were unable to detect HIF1 α or HIF2 α (Figure 1A). We next performed an RT-PCR to detect whether HIF1 α or HIF2 α were detectable at mRNA levels and we were unable to detect mRNA specific for HIF1 α or HIF2 α in the KC12 cell line (Figure 1C). In this same assay we could readily show mRNA for HIF1 α in 293T cells and HIF2 α in 786-O renal carcinoma cells (Figure 1C). Several mechanisms like promotor methylation or chromosomal deletion could account for the observed lack of HIF. These data infer that KC12 cells system represent a unique cellular system in which to study the HIF-independent function of VHL, as it does not express HIF1 α or HIF2 α but is able

to form tumors in nude mice (9). This finding supports the notion that VHL has a tumor suppressor function that is independent of its ability to regulate HIF α levels (12,13). However, other data has provided evidence for a causative role for HIF2 α in tumorigenesis (14,15). We concluded that any effect of reconstituted VHL in this cell line would be HIF-independent.

We next set out to confirm the positive effect of VHL on MT-stability using the existing method of scoring for stable MTs after nocodazole treatment. We treated KC12TR and KC12TR/VHL-TO cells with doxycycline for 16hrs and exposed them to nocodazole for 20 minutes, fixed them and stained for acetylated tubulin. This assay recapitulated the results of Hergovitch et al. (1), showing that induction of VHL resulted in an increase

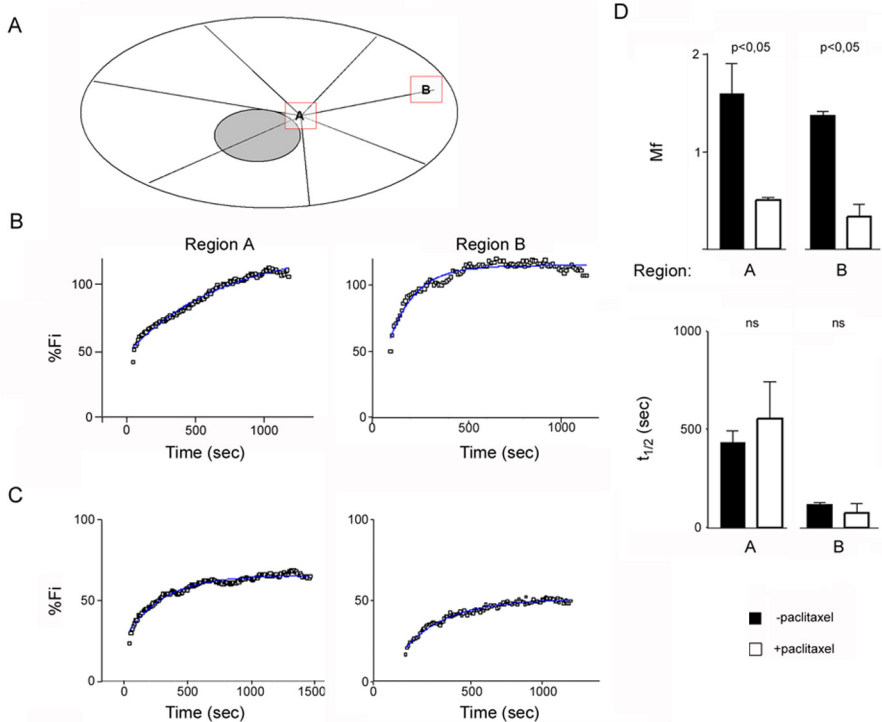


Figure 2: Paclitaxel affects tubulin-YFP turnover as measured by FRAP.

(A) Schematic representation of the regions that were used for FRAP experiments. Lines represent MTs and filled circle represents nucleus. (B) Typical FRAP patterns that were obtained in the different regions in untreated KC12RN cells. The squares are measured points. These are represented as % of initial fluorescence (Fi) vs time in seconds. The solid lines are the curve-fitted lines and are calculated values. (C) Typical FRAP pattern of KC12RN cells after paclitaxel treatment (10 μ M) in the different regions. The representation is identical to Fig. 2B. (D) Bar graph representation of Mf and t(1/2) of non-treated vs paclitaxel-treated cells of the different regions. The error bars represent the standard error of the mean. Statistics using two-tailed Student's t-test are provided above the bars. ns, not significant

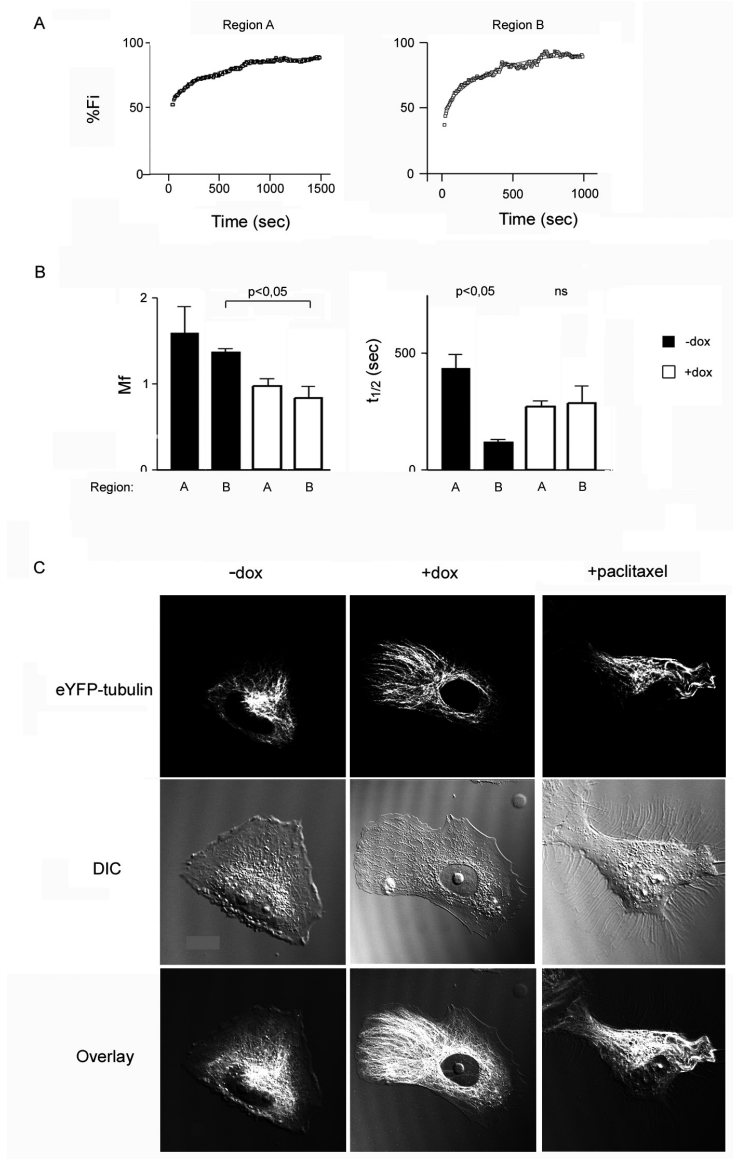


Figure 3: VHL shifts MT-stability towards the cell periphery

(A) Typical FRAP patterns of cells induced with doxycycline (dox) for 16hrs for regions. Every square represents a measurement and the data is given as %Fi vs time in seconds. The solid lines are the curve-fitted lines and are calculated values. ns, not significant. (B) Bar graph representation of calculated Mf and half-life time ($t_{1/2}$). Every bar represents at least 3 independent measurements FRAP region is depicted below the bars. Statistics using two-tailed Student's t-test are provided above the bars. ns, not significant. (C) Confocal slices KC12RN cells. Upper panels: tubulin-YFP directly visualized in living cells. Middle panels: the same cells imaged using differential interference contrast (DIC) microscopy. Lower panels: overlay of tubulin-YFP and DIC image.

of nocodazole resistant MTs as opposed to the KC12TR cells -which lacking the inducible VHL construct- failed to manifest any MT resistance to nocodazole upon exposure to doxycycline (Figure 1D).

For FRAP analysis of MT dynamics we selected a KC12TR/VHL-TO clone that inducibly expresses VHL and stably transfected it with tubulin-YFP. We then selected clones with a uniform expression of tubulin-YFP. Tubulin-YFP expression pattern largely co-localizes with the staining for acetylated tubulin in these cells, suggesting that tubulin-YFP is incorporated into stable MTs (Figure 1E). From these results we concluded that the KC12TR/VHL-TO/tubulin-YFP (dubbed KC12RN) cells represented a suitable model for testing global changes in MT dynamics.

Applying FRAP to measure MT dynamics

To study the dynamic behavior of MTs we next set out to use FRAP of tubulin-YFP. In the KC12RN cells the MT dynamics appeared to differ according to the proximity of the MTs to the centrosome. We thus defined two regions in which subsequent FRAP experiments could be stratified. The first region is defined as the region around the centrosome (region A); the second was defined as a region localized along the cell periphery (region B) (Figure 2A). The mobile fraction (Mf) of tubulin-YFP in cells lacking VHL does not show significant differences in the regions we measured. The half-life time of fluorescence recovery, however, showed a significant decrease in region B; we observed a half-life time (+/-1xSD) ranging from 437 +/- 102 sec. in region A to 78 +/- 38 sec. in region B. These data support the notion that the MTs at the cell periphery are generally more dynamic than around the centrosome. Additionally, the subcellular localization of the MTs with a longer half-life time correlates with the acetylated tubulin staining (Figure 1F). Previously published data on the turnover of MTs during interphase using FRAP did not discriminate between different regions of the cell (4,7). Here we demonstrate for the first time a difference in tubulin turnover in different sub-cellular compartments as measured by the half-life time of fluorescence recovery. This finding and a recent publication on the local effects of stathmin on MT dynamics (16) underscore the importance for stratifying the results of MT turnover data according to their subcellular

localization.

We next addressed whether a known MT stabilizing agent, paclitaxel, could change the FRAP read-out of MT dynamics (17). After 1 hour of paclitaxel treatment we observed significant changes in MT dynamics. In region A as well as region B the Mf decreased significantly with no significant changes in half-life time after paclitaxel treatment (Figure 2C, D). These data show that FRAP analysis of tubulin-YFP can detect the changes in MT dynamics after paclitaxel treatment and that these changes are comparable throughout the entire cell. We used a high paclitaxel dose (10 μ M), which is important for interpreting the effect observed. Occupation of all paclitaxel-binding sites would allow MTs to continue growing but would not permit depolymerization of existing MTs. We thus interpret the changes in Mf to represent the decrease in MT turnover due to the absence of catastrophe. However, the remaining dynamic processes have similar half-life times as before treatment with paclitaxel. These data validated that our modified FRAP-based assay using tubulin-YFP, and allowed us to apply it as a tool for monitoring global changes in MT dynamics.

VHL stabilizes the MTs at the cell periphery

To further investigate the change in MT dynamics induced by VHL we compared KC12RN cells treated with or without doxycycline for 16hrs. Using the same two regions as before in a series of FRAP experiments, we determined the change of MT dynamics after the induction of VHL. We observed that in the presence of VHL, the Mf does not significantly change between the different regions. However, when compared to cells lacking VHL region B showed significant changes; the Mf in region B decreased. The half-life time did not show significant changes between the different sub-cellular regions in the presence of VHL (Figure 3A, B). Furthermore in region A there is a trend towards faster kinetics and lower Mf in the presence of VHL (Figure 3B). The variation of MT-turnover throughout the cell as observed in the absence of VHL is no longer present. These data suggest that the most profound effect of induction of VHL on MT dynamics is localized towards the cell periphery. The dynamics found in

the VHL-proficient cells correlate better with previously published data on MT dynamics as measured by FRAP in cultured cells. The cumulative half-life time we measured in cells expressing VHL was comparable to previously published data (330+/-170 sec. vs 200+/-85 sec) and no differences for sub-cellular localization were noted (7). There also seem to be changes in region A, which show an increase in MT dynamics near the centrosome (Figure 3B). This effect could be a direct destabilizing effect of VHL, however we favor the hypothesis that this effect is secondary to the plus-end stabilizing function of VHL. A change in the MT dynamics at the cell periphery would result in altered MT organization, which could be captured in high-resolution confocal images. These images show the thickening and stabilization of the MTs towards the cell periphery and modified cell shape (Figure 3C). Note that in VHL-proficient cells, the cell shape is flatter and there appears to be a more even distribution of organelles. Together these data suggest that VHL's influence in MT dynamics in interphase KC12RN cells is most prominent at the cell periphery. Furthermore, we confirmed that the microtubule stabilizing function of VHL is independent from its role in regulating the HIF α levels.

Here we directly measure MT turnover as a read-out for quantitatively assessing the role of VHL in MT stability. This assay complements the standard nocodazole resistance assay, but has many additional benefits. This assay does not introduce experimental artifacts through cell fixation and allows real-time evaluation. The extra information obtained by using this assay is useful in assessing the localized change in MT dynamics by endogenous proteins and drug treatments.

VHL appears to have a localized effect at the cell periphery. Physiological processes that involve changes in stability of MTs often require localized changes in MT dynamics. For example, these sorts of MT dynamics might be essential for the formation of parallel MT-arrays such as those observed in polarized epithelial cells or polarizing the MT network in migrating cells (18). It is tempting to speculate that VHL could have a role in processes that require localized changes in MT dynamics such as cell polarization, cell migration and cell-cell interaction. Another interesting finding from this study is that, although VHL is present throughout the cy-

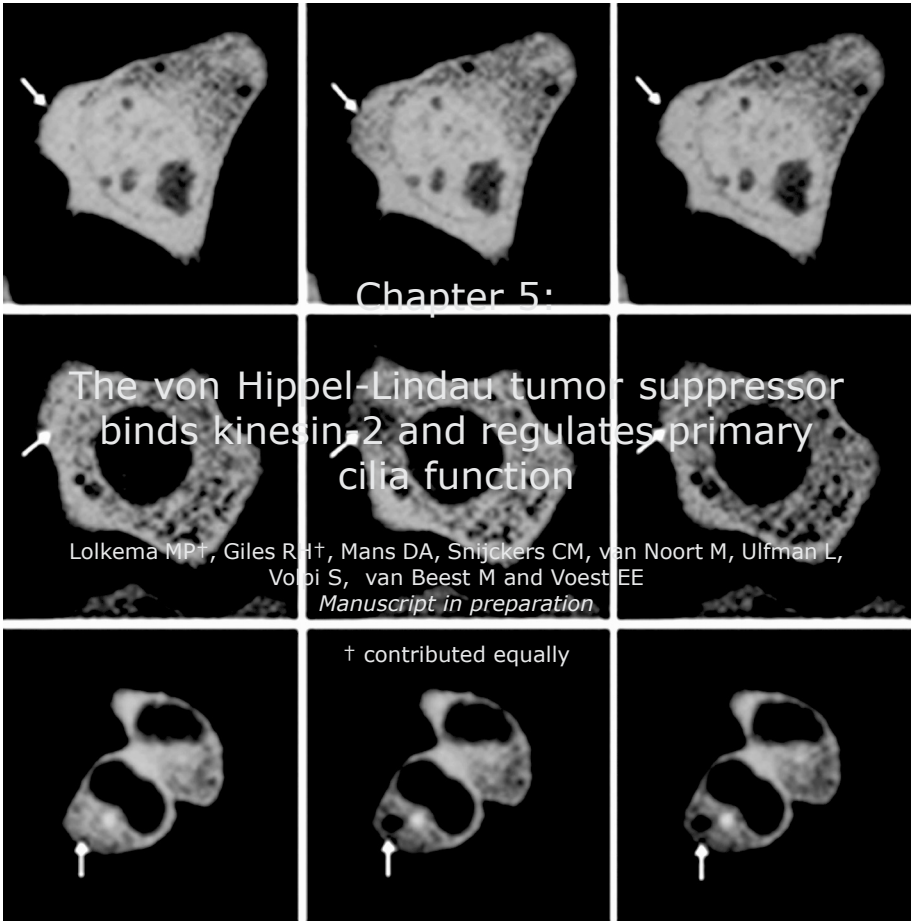
toplasm (19), it can have a localized effect on MT-stability implying the existence of a signal transduction pathway in which VHL is involved to locally stabilize MTs.

Acknowledgements

We would like to thank the members of the Voest lab and especially Luc van Kruisdijk for helpful discussions, reagents and technical assistance. We thank the Dept. of Cell Biology of the University of Utrecht, the Netherlands and especially Prof. Dr. J. Klumperman and Dr. G. Posthuma for their support and use of the live cell imaging station. This work is supported by the Dutch Cancer Society (Grants UU 1999-1879 and UU 1999-2114 to E.V.) and the Dutch Scientific Counsel (NWO) (Grant: 920-03-179 to M.L. and E.V.)

Reference List

- (1) Hergovich, A., Lisztwan, J., Barry, R., Ballschmieter, P., and Krek, W. (2003). *Nat.Cell Biol.* 5, 64-70.
- (2) Lonser, R. R., Glenn, G. M., Walther, M., Chew, E. Y., Libutti, S. K., Linehan, W. M., and Oldfield, E. H. (2003). *Lancet* 361, 2059-2067.
- (3) Lippincott-Schwartz, J., Snapp, E., and Kenworthy, A. (2001). *Nat.Rev.Mol.Cell Biol.* 2, 444-456.
- (4) Shaw, S. L., Kamyar, R., and Ehrhardt, D. W. (2003). *Science* 300, 1715-1718.
- (5) Leslie, R. J., Saxton, W. M., Mitchison, T. J., Neighbors, B., Salmon, E. D., and McIntosh, J. R. (1984). *J.Cell Biol.* 99, 2146-2156.
- (6) Salmon, E. D., Saxton, W. M., Leslie, R. J., Karow, M. L., and McIntosh, J. R. (1984). *J.Cell Biol.* 99, 2157-2164.
- (7) Saxton, W. M., Stemple, D. L., Leslie, R. J., Salmon, E. D., Zavortink, M., and McIntosh, J. R. (1984). *J.Cell Biol.* 99, 2175-2186.
- (8) Edson, K. J., Lim, S. S., Borisy, G. G., and Letourneau, P. C. (1993). *Cell Motil.Cytoskeleton* 25, 59-72.
- (9) Kohno, T., Sekine, T., Tobisu, K., Oshimura, M., and Yokota, J. (1993). *Jpn.J.Clin.Oncol.* 23, 226-231.
- (10) Gnarr, J. R., Tory, K., Weng, Y., Schmidt, L., Wei, M. H., Li, H., Latif, F., Liu, S., Chen, F., Duh, F. M., and . (1994). *Nat.Genet.* 7, 85-90.
- (11) Maxwell, P. (2003). *J.Am.Soc.Nephrol.* 14, 2712-2722.
- (12) Stickle, N. H., Chung, J., Klco, J. M., Hill, R. P., Kaelin, W. G., Jr., and Ohh, M. (2004). *Mol.Cell Biol.* 24, 3251-3261.
- (13) Ohh, M., Yauch, R. L., Lonergan, K. M., Whaley, J. M., Stemmer-Rachamimov, A. O., Louis, D. N., Gavin, B. J., Kley, N., Kaelin, W. G., Jr., and Iliopoulos, O. (1998). *Mol.Cell* 1, 959-968.
- (14) Zimmer, M., Doucette, D., Siddiqui, N., and Iliopoulos, O. (2004). *Mol.Cancer Res.* 2, 89-95.
- (15) Kondo, K., Kim, W. Y., Lechpammer, M., and Kaelin, W. G., Jr. (2003). *PLoS.Biol.* 1, E83.
- (16) Niethammer, P., Bastiaens, P., and Karsenti, E. (2004). *Science* 303, 1862-1866.
- (17) Orr, G. A., Verdier-Pinard, P., McDaid, H., and Horwitz, S. B. (2003). *Oncogene* 22, 7280-7295.
- (18) Musch, A. (2004). *Traffic.* 5, 1-9.
- (19) Duan, D. R., Humphrey, J. S., Chen, D. Y., Weng, Y., Sukegawa, J., Lee, S., Gnarr, J. R., Linehan, W. M., and Klausner, R. D. (1995). *Proc. Natl.Acad.Sci.U.S.A* 92, 6459-6463



The von Hippel-Lindau tumor suppressor binds kinesin-2 and regulates primary cilia function

Lolkema MP[†], Giles RH[†], Mans DA, Snijckers CM, van Noort M, Ulfman L, Volpi S, van Beest M and Voest EE

Manuscript in preparation

† contributed equally

In patients with von Hippel-Lindau (VHL) disease, VHL-/- kidney cysts degenerate into clear-cell renal carcinomas (ccRCC) through unknown mechanisms. The VHL gene product regulates the ubiquitination and subsequent degradation of hypoxia inducible factor (HIF), an important transcriptional activator of the genetic program triggered by hypoxia. Dysregulation of HIF is, however, not sufficient to induce cancer which suggests the presence of alternative functions of VHL. We show here that wild-type VHL binds KIF3A, a component of molecular motor kinesin-2 regulating the assembly and maintenance of primary cilia. We demonstrate that binding KIF3A is important for VHL-mediated microtubule stabilization. Because renal inactivation of any component of kinesin-2 causes cilia defects subsequently leading to cystic kidneys, we investigated the role of VHL in ciliogenesis. VHL localizes to primary cilia in cultured kidney cells. We demonstrate that cultured VHL-/- renal cell carcinoma cells do not tend to develop cilia; however, thick stubby cilia are rapidly assembled upon ectopic re-expression of wild-type -but not mutant alleles of- *VHL* in those same cells. These data show that VHL interacts with the kinesin-2 complex and that this interaction has a functional consequence on ciliogenesis.

Introduction

The rare hereditary von Hippel-Lindau (VHL) disease is caused by heterozygous germline mutations in the VHL gene located on chromosome band 3p25-26 (1). Mutations in VHL kindreds predispose patients to a variety of tumors including renal cell carcinomas, haemangioblastomas of the central nervous system and retina, and pheochromocytomas. These patients also frequently develop multiple cysts in the kidney, pancreas and liver. The occurrence of biallelic somatic *VHL* mutations in about 70% of sporadic renal cell carcinomas fits with Knudson's two-hit model for tumor suppressor genes and suggests that VHL functions as a global gatekeeper of cellular growth in the kidney (1,2).

Many lines of research support a role for VHL as the target recognition moiety of a multiprotein ubiquitin E3 ligase complex, the so-called VHL-EloC-EloB-Cullin2 (VEC) complex. Under normoxic conditions, oxygen-dependent prolyl hydroxylation of hypoxia inducible factor (HIF)- α facilitates VHL binding, followed by ubiquitination, and subsequent proteasomal degradation of HIF α subunits (reviewed in: (3,4)). Two protein products encoded by VHL equally participate in the E3 ligase complex to regulate HIF α , a 30 kDa full-

length protein (p30), and a 19 kDa protein (p19) generated by alternative translation initiation of an internal methionine at position 54 (Fig. 1a) (5,6). The first 53 residues of p30 constitute an acidic domain of unknown function, forming an N-terminal extension to p19. The vast majority of *VHL* mutations are downstream of residue 54 thereby inactivating both isoforms, however, the existence of VHL patient mutations in the acidic domain that do not affect p19 suggest a specific role for p30 in tumor suppression (Giles *et al.*, submitted). Furthermore, phosphorylation of the acidic domain by casein kinase-2 is important for the full tumor suppressor function of VHL (7). Recently, the inactivation of JunB by *VHL* alleles capable of normal HIF regulation has been implicated in the development of pheochromocytoma associated with type 2C VHL disease (8). Thus, while the highly vascularized lesions associated with VHL disease are a result of HIF-induced gene expression of pro-angiogenic factors such as VEGF, careful genetic and functional analysis of the *VHL* gene suggests that the tumor suppressor function of VHL is not solely restricted to its function in regulating HIF.

The heterotrimeric kinesin-2 complex has been implicated in the anterograde ATP-

dependent transport of various cargos along the microtubule (MT) cytoskeleton. Genetic disruption of individual components of the kinesin-2 complex (KIF3A, KIF3B, and KAP3) invariably results in dysfunction of specialized tubulin sensory structures known as primary cilia (9). Moreover, local disruption of KIF3A in the kidney results in ciliogenesis defects and the subsequent development of renal cysts, much like those present in VHL patients (10).

Here, we report that the acidic domain and the MT-binding domain of VHL regulate binding to KIF3A. This binding could be disrupted using a dominant negative KAP3 construct (Δ N-KAP3) unable to bind the kinesin-2 complex (11). The interaction between VHL and KIF3A does not influence the known function of VHL in regulating HIF α levels nor is KIF3A a target for the VEC complex mediated polyubiquitination. Our data suggest that KIF3A mediates the binding of VHL to MTs. Moreover, disrupting the interaction between VHL and kinesin-2 influences the mobility of VHL. Furthermore, we show that the interaction between VHL is essential for the function of primary cilia. This interaction not only assigns the first function of VHL in which the acidic domain is implicated, but it provides a molecular mechanism for the MT-stabilizing function of VHL and suggests a role for VHL in ciliogenesis.

Materials and Methods

Construction of plasmids

The VHL bait for Yeast-two-Hybrid was generated by cloning VHL cDNA by one-step PCR in the Gal4 DNA-binding domain containing vector pMD₄ (kind gift of Dr. L. van 't Veer). All eukaryotic expression constructs were generated using pcDNA₃-derived vectors (Promega, Madison, WI) containing either a N-terminal Myc- or Vsv-tag and standard cloning techniques. GFP-fusion constructs were generated by cloning into pEGFP-C1 (Clontech, Palo Alto, CA). The KIF3A construct (kind gift of Dr. L. Goldstein), Δ N-KAP3 construct (kind gift of Dr. T. Akiyami), the VHL- Δ 95-123, VHL-Y112H construct (kind gift of Dr. W. Krek), the dsRED- γ -tubulin construct (kind gift of Dr. J. Ellenberg) were requested and cloned into the appropriate vectors.

Yeast-Two-Hybrid Screen

The Yeast-two-Hybrid screen was performed

according to the Matchmaker protocol (Clontech, Palo Alto, CA) using a human fetal brain cDNA library (Matchmaker, Clontech, Palo Alto, CA). The library was co-transformed with the VHL bait plasmid into *Saccharomyces cerevisiae* strain Hf7c. Library plasmids were recovered from His⁺/LacZ⁺ clones and tested for the absence of interaction with irrelevant baits and sequenced.

Immunoprecipitations

Approximately 1×10^6 cells were lysed in 400 μ l Triton lysis buffer (20 mM TRIS; 1% Triton-X-100; 140 mM NaCl; 10% Glycerol; at pH 8.0) containing 'complete' cocktail of protease inhibitors (Roche, Basel, Switzerland). Cell remnants were spun down by 5 min centrifuging at 4°C. α -VHL (1.5 μ g of IG32; BD-Pharmingen, San Diego, CA) was coupled to protein A/G agarose beads (7.5 μ l; Santa Cruz Biotechnology, Santa Cruz, CA) and added to 200 μ l of cleared lysate. For endogenous IPs, 2 ml cell lysate (10×10^6 cells) was used with 25 μ l protein A/G agarose beads pre-coupled to 7.5 μ g α -VHL or 7.5 μ g α -KIF3A (BD-Transduction Labs, San Diego, CA). The IP reactions were incubated overnight at 4°C, washed three times with Triton lysis buffer and analyzed by western blotting. All IPs were repeated in at least three independent experiments.

Western blot

Specific protein bands were visualized using the following antibodies: α -Myc (9E10, hybridoma supernatant 1:5), α -Vsv (P4D5, hybridoma supernatant 1:5), α -KIF3A (1:500; BD-Transduction Labs, San Diego, CA) or α -MAPK (1:3000) (polyclonal Ab, kind gift of Dr. O. Kranenburg) as indicated in the text. All antibodies were diluted in PBS containing 5% milk and 0.1% Tween-20. Rabbit α -mouse HRP (1:20,000; Pierce, Rockford, IL) or Swine α -Rabbit HRP (1:3000; DAKO, Glostrup, Denmark) provided the secondary antibody after which enhanced chemiluminescence (Perkin Elmer Life Sciences, Boston, MA) was used for detection.

Reporter assay

To generate the HRE-luciferase reporter construct, we used the following wild-type HRE oligonucleotide (W18) of the 3'-enhancer of the human erythropoietin gene (12) in triplicate in front of a minimal TK promoter and the Luciferase Gene in the vector pBILuc: C(TACGTGCT)GC(TACGTGCT)GC(TACGTGCT)

T)G (where the HRE is in parentheses and the core bases essential for HIF binding are underlined). The vector pBILuc is derived from pBICat₂ (13) in which the Cat gene has been replaced by Luciferase out of pTopFlash (14). As a negative control, a similar construct with the M28 fragment (12) was constructed in which three altered nucleotides completely abrogate HIF-binding: CTCAAT-GCTGCTCAATGCTGCTCAATGCTG 3' (where the mutated core bases are underlined). HEK293T cells were plated 18 hours prior to transfection by Fugene6 (Roche, Basel, Switzerland) according to the manufacturer's instructions. The following amounts of plasmids were transfected in HEK293T cells: 50 ng HRE-Luc or Mut-Luc in combination with 5 ng of the renilla internal control CMV-pRNL (Promega, Madison, WI), and 100 ng wild-type HIF1 α as indicated in the text. The total amount of DNA transfected in all reporter assays was adjusted to 500 ng with pcDNA₃. Luciferase activities were measured 24-36 hours after transfection using the DUAL luciferase system according to the manufacturer's protocol (Promega, Madison, WI). Luciferase activity was normalized relative to renilla.

Microtubule co-sedimentation assay

Transfected HEK293T cells were lysed in PTN buffer (10 mM Pipes, 30 mM TRIS, 50 mM NaCl, 1 mM EGTA, 1.25 mM EDTA, 1 mM DTT, 1% Triton-X-100, and protease inhibitors at pH 6.3). The lysates were pre-cleared by centrifugation at 100,000g for 45 min. at 25°C. The co-sedimentation assay was performed using the MAP Spin-down Biochem Kit (Cytoskeleton, Denver, CO), with the following adjustments: after polymerization, microtubules were spun down at 100,000g for 30 min at 25°C. The pelleted microtubules were resuspended in the pre-cleared lysates containing 50 μ M paclitaxel and incubated at room temperature for 30 min. The samples were then loaded onto 100 μ l of the kit's cushion buffer and centrifuged at 100,000g for 40 min. Pre-cleared total lysates, supernatant and pellet fractions were analyzed by western blotting.

Live cell imaging

Transfected N1E-115 neuroblastoma cells were visualized on a Zeiss LSM 510 confocal scanning microscope (Carl Zeiss, Jena, Germany) fitted with a climate control chamber maintaining humidified 37°C and 5% CO₂.

A circular region of interest with 10 mm radius was photobleached with 80 pulses of approximately 15 mW laser intensity after which the cell was followed by time-lapse imaging (every 0.25 sec, total 400 frames). The pre-bleach fluorescence intensity (F_i) was defined as the mean of 15 images before photobleaching. Total cell fluorescence was measured over time and used to normalize the data as described before (15). All values were calculated as percentage F_i . The recovery fluorescence (F_ω) was defined as the mean of the 15 last scans. The mobile fraction (M_f) was calculated using the following equation: $M_f = (F_\omega - F_0) / (F_i - F_0)$ (15). All experiments were repeated independently on at least three separate days. For co-transfection assays we used equivalent doses of the co-transfected plasmids unless otherwise stated in the figure legends.

Immunofluorescent staining

Cells were washed once with PBS and fixed with 100% ice-cold methanol for 2 minutes at RT, then washed again with PBS. Primary antibodies for staining were used as indicated in the text: α -VHL (Ig32; BD-Pharmingen, San Diego, CA), α -acetylated tubulin (Sigma-Aldrich, St.Louis, MO) and α -glutamylated tubulin (GT335, Gift from B. Edde and C. Janke, 1:2000). Secondary antibody was goat-anti-mouse Alexa 568 (1:200) (DAKO, Glostrup, Denmark). All incubations were done in PBS containing 1% BSA at room temperature in a dark chamber. Staining was visualized on a Zeiss LSM510 confocal imaging unit (Jena, Germany).

Ca²⁺ microfluorimetry

We grew kidney epithelial cells on uncoated 24x60 mm glass coverslips for at least 4 days to full confluence. The experimental setup for flow has previously been described in detail (16). Briefly, we incubated cells for 30 min with the Ca²⁺ sensitive probe Fura2-AM (5 μ M) at 37°C. We then washed cells three times to remove excess Fura2-AM and placed them in a perfusion chamber with a thickness of 0.025 cm. in HEPES buffer (pH 7.4) containing 132 mM NaCl, 4.2 mM, NaHCO₃, 5.9 mM KCl, 1.4 mM MgSO₄, 1.2 mM Na₂HPO₄, 1.6 mM CaCl₂, 11 mM dextrose and 10 mM HEPES buffer. We captured paired Fura images every 4s at excitation wavelengths of 340 nm and 380 nm. After equilibration in the microscopy media for at

least 5 min, we then stimulated the primary cilia of these cells at a fluid shear stress of $0.75 \text{ dyne cm}^{-2}$. We radiometrically calculated the Ca^{2+} level relative to the baseline value using R_{min} and R_{max} values of 0.3 and 6.0, respectively. Freshly diluted thrombin ($1 \mu\text{M}$) produced a robust $[\text{Ca}^{2+}]$ response in these cells and was used to determine the maximum response (upper baseline). Cells were incubated with $10 \mu\text{M}$ nocodazol for 30 minutes at 37°C prior to microfluorimetry as indicated.

Results

KIF3A and VHL are interacting proteins

We performed a yeast-two-hybrid screen of a human fetal brain cDNA library with the full-length VHL protein as bait. Among the 8 clones that appeared to robustly bind VHL in this assay we found chaperonin CCT η , a chaperone protein known to bind to VHL and is involved in the correct folding of VHL into the elongin B/C complex (17). These results indicated that we had detected possible VHL binding proteins and we selected a cDNA encoding the C-terminal portion of the kinesin-2 subunit KIF3A for further analysis. We re-transformed yeast with the KIF3A construct with 4 different VHL bait constructs: full length (VHL_{fl}), β -domain: ranging from aa 1-

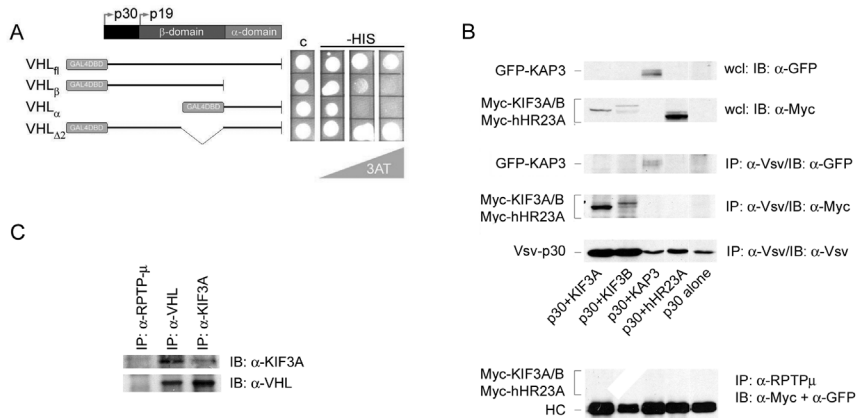


Figure 1: VHL binds KIF3A and other members of the kinesin-2 complex.

(A) Yeast-two-Hybrid assay. Left panel shows the schematic representation of the VHL constructs that were used as bait in a Yeast-two-Hybrid assay with KIF3A as prey. Above this panel, a schematic representation of the VHL protein is given showing the acidic domain (left box), β -domain (middle box) and α -domain (right box) and the translation initiation sites for the two different isoforms of VHL: p30 and p19. Right panel shows the colony growth of transformed yeast under increasing stringency, which is achieved using increasing concentrations of 3AT on agar plates without histidine. The first lane in the right panel (c) shows the control colony in the presence of histidine. Gal4 DNA binding domain fused to (from top to bottom) full-length VHL (VHL_{fl}), a deletion construct of containing only the HIF-binding VHL β -domain (VHL_{β}), a deletion construct of containing only the elongin-C binding VHL α -domain (VHL_{α}), or a deletion construct of VHL lacking exon 2 ($\text{VHL}_{\Delta 2}$). -HIS, without histidine; 3AT, 3-aminotriazole. (B) Overexpression IP of lysates of transfected HEK293T cells. The cells were co-transfected with Myc-KIF3A, Myc-KIF3B, GFP-KAP3 or Myc-hHR23A and Vsv-p30 as described under the different lanes. Top two panels show western blot of whole cell lysates for respectively GFP-tagged and Myc-tagged proteins. The third and fourth panels show recovery for respectively GFP-tagged and Myc-tagged proteins from the anti-Vsv IP. The fifth panel shows recovery of Vsv-VHL from the anti-Vsv IP. The lower panel shows the recovery for the aspecific IP using α -RPTP μ antibodies. Irrelevant lanes were removed for clarity. Wcl, whole cell lysate; IB, immunoblot; IP, immunoprecipitation. (C) Endogenous IP in HEK293T cells. Upper panel shows western blot stained for endogenous KIF3A after recovery of an specific IP using α -RPTP μ (lane 1), an IP for VHL (lane 2) and an IP for KIF3A (lane 3). Lower panel shows the same samples on western blot stained for VHL. IB, immunoblot; IP, immunoprecipitation.

178 (VHL_B), α -domain: ranging from aa 178-213 (VHL _{α}) and Δ exon2: lacking the region from aa 137-178 (VHL _{Δ 2}). In this assay the major determinants for binding of VHL to KIF3A seem to be located in the first exon of VHL ranging from aa 1-136 (Fig. 1a). Interaction was validated by co-immunoprecipitation (IP) using cell lysates containing exogenous Vsv-tagged VHL (p30) and Myc-tagged KIF3A (Fig. 1b; first lane). As a specificity control, we used a Myc-tagged cDNA from hHR23A (Rad23A), a nucleotide excision repair protein with no known link to VHL (18). Indeed, IP using an antibody against Vsv-VHL specifically co-immunoprecipitated the Myc-tagged KIF3A protein whereas the Myc-tagged hHR23A was not detected (Fig. 1b; fourth lane). Moreover, IP using an antibody for an irrelevant protein in this system: RPTP- μ , a transmembrane protein with phosphatase activity that is not expressed in these cells, does not retrieve any of the overexpressed proteins (Fig. 1b; lower panel). IP of exogenous VHL resulted

in co-precipitation of the other two components of the kinesin-2 complex: KIF3B and KAP3, suggesting that VHL is able to bind all three members of the kinesin-2 complex either directly or indirectly (Fig. 1b; second and third lane). Although it seems from the data shown here that KIF3B binds less to VHL than KIF3A, repeated experiments showed that this effect is dependent on transfection efficiency of KIF3B (data not shown). Because overexpressed proteins do not represent physiological circumstances, we performed IPs using cell lysates of untransfected cells to determine whether these proteins are present in an endogenous complex. Using an α -VHL antibody we readily pulled down KIF3A from HEK293T cells and using an α -KIF3A antibody we readily pulled down VHL, while an irrelevant antibody did not retrieve either VHL or KIF3A (Fig. 1c). As compared to overexpression IPs (Fig. 1b) the retrieval of both VHL and KIF3A in the endogenous IP are remarkably high. This supports the notion that the binding of

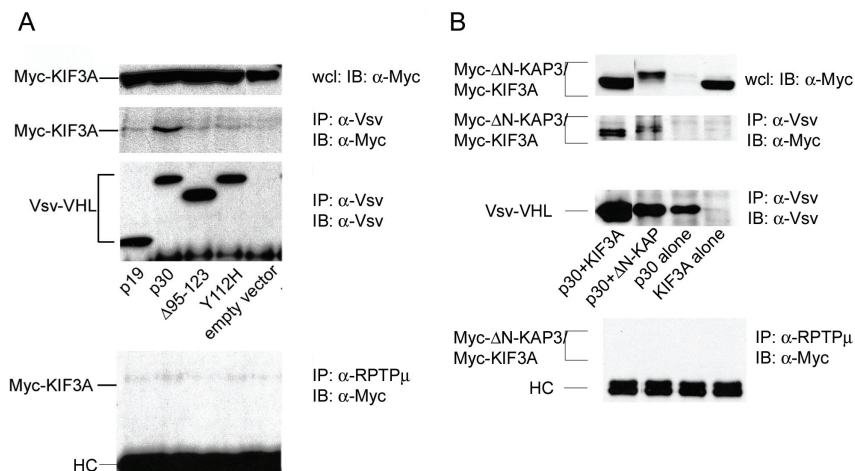


Figure 2: Characterization of binding between VHL and KIF3A

(A) Overexpression IP of lysates of transfected HEK293T cells. Cells were transfected with p30, p19, Δ 95-123 or Y112H and KIF3A as indicated under the lanes. The upper panel shows the western blot of the whole cell lysates as a control for the transfection efficiency of KIF3A. The second panel shows the recovery of the IP for VHL using an α -Vsv antibody, stained for KIF3A using an α -Myc antibody. The third panel shows recovery of the different VHL mutants after IP for the Vsv-tag. The lower panel represents the recovery of an aspecific IP using α -RPTP μ antibodies stained for KIF3A using the α -Myc antibody. Irrelevant lanes were removed for clarity. IB, immunoblot; IP, immunoprecipitation; HC, immunoglobulin heavy chain. (B) Overexpression IP of lysates of transfected HEK293T cells. Cells were transfected with p30 and KIF3A or Δ N-KAP3 as indicated under the lanes. The upper panel shows a western blot analysis of the transfection efficiency for KIF3A and Δ N-KAP3 in which Δ N-KAP3 runs slightly higher than KIF3A. The second panel shows the recovery of KIF3A and Δ N-KAP3 after IP for VHL using an α -Vsv antibody. The third panel shows the recovery of VHL after an IP using the α -Vsv antibody. The lower panel shows the recovery after aspecific IP using an α -RPTP μ antibody. Irrelevant lanes were removed for clarity. IB, immunoblot; IP, immunoprecipitation; HC, immunoglobulin heavy chain.

VHL to KIF3A is strong in the endogenous situation. These data argue for the participation of VHL in a protein complex containing KIF3A, KIF3B and KAP3, otherwise known as the kinesin-2 complex.

Characterizing the binding of VHL to the kinesin-2 complex

We further characterized the binding of VHL to KIF3A by testing two deletion variants of VHL: the naturally occurring p19 isoform of VHL, generated by an alternative translation initiation site at residue 54, and the $\Delta 95-123$ mutant of VHL ($\Delta 95-123$) described by Hergovich et al. defining the region regulating MT stabilization (19). Overexpression IP of either the p19 or $\Delta 95-123$ both significantly diminished co-precipitation of KIF3A, indicating that the acidic domain as well as the MT-binding domain are important regions for KIF3A binding (Fig. 2a; first and third lanes). These data suggested that the microtubule stabilizing function of VHL could be mediated by KIF3A. Therefore, we tested the mutant Y112H VHL allele reported to be deficient in stabilizing microtubules; this mutation is associated with type 2A VHL disease. We found that this type 2A mutation was less able to bind KIF3A (Fig. 2a; fourth lane). This led us to hypothesize that the microtubule stabilizing function of VHL could be due to its interaction with the kinesin-2 complex.

Interfering with the binding of VHL to the kinesin-2 complex: the ΔN -KAP3 construct

To further study the nature of the binding of VHL to the different subunits of the heterotrimeric kinesin-2 complex, we tested whether the ΔN -KAP3 construct described by Jimbo et al. could bind to VHL. ΔN -KAP3 binds to APC, a target for kinesin-2-dependent transport, but fails to bind to the other members of the kinesin-2 complex, thereby disrupting the functional interaction between APC and the kinesin-2 complex (11). We immunoprecipitated exogenous Vsv-VHL and specifically recovered Myc-tagged ΔN -KAP3 (Fig. 2b; second lane), allowing us to similarly employ this construct as a dominant negative inhibitor of VHL-kinesin-2 binding. Furthermore it indicates that VHL binds KAP3 independent of its binding to KIF3A.

The kinesin-2 complex mediates MT-binding of VHL

Next we addressed the possibility that association of VHL with the kinesin-2 motor complex mediates the binding of the full-length VHL isoform (p30) to MTs. To this end we performed a MT co-sedimentation assay with lysates of HEK293T cells transfected with Vsv-p30. Our data indeed demonstrate binding of p30 to MTs (Fig. 3a, upper panel), supporting data produced by Hergovich et al (19). To determine whether the binding of VHL to MTs is direct or indirect we performed a similar assay using highly purified tubulin and in vitro translated VHL. In this assay we were not able to show direct binding of p30 to microtubules (Fig. 3a, middle panel). However, Hergovich et al. (19) proposed that the binding of VHL to MTs is direct. The discrepancy between our data and the proposition that VHL binds directly to MTs might be explained by different protocols used in the two studies; we used an additional sucrose cushion in the co-sedimentation assay. This sucrose cushion serves as a den-

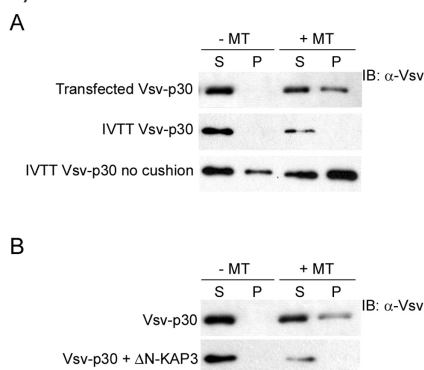


Figure 3: VHL binds to microtubules through its interaction with the kinesin-2 complex.

(A) MT co-sedimentation assay. Upper panel, Vsv-p30 transfected into HEK293T cells recovered from supernatant (S, left lane) or pellet (P, second lane) without the addition of MTs (- MT) and supernatant (S, third lane) or pellet (P, last lane) in the presence of MTs (+MT). Middle panel, same assay performed using in vitro translated (IVTT) p30. Lower panel, same assay repeated without the recommended cushion buffer using the IVTT p30. (B) MT co-sedimentation assay using lysates of transfected HEK293T cells. Upper panel shows recovery of Vsv-p30 using HEK293T cells transfected with only Vsv-p30 (similar organization as described Fig. 2A). Lower panel, recovery of Vsv-p30 using HEK293T cells transfected with both Vsv-p30 and ΔN -KAP3.

sity gradient separating the lysate from the pellet and increasing the specificity of the spun down fraction. To address the different outcomes, we directly compared the two methods with *in vitro* translated p30 in the presence or absence of a sucrose cushion separation. In the absence of the sucrose cushion we found more VHL in the pellet with MTs than in the pellet without MTs (Fig. 3a, lower panel). However, using the more stringent assay (with sucrose cushion) we found no direct interaction between MTs and VHL (Fig. 3a, middle panel). These data indicate that an endogenous factor present in the cell lysates of the first experiment (Fig. 3a, upper panel), e.g. endogenous kinesin-2, enhances the binding of VHL to MTs as measured by this assay.

To specifically address whether kinesin-2 mediates VHL-MT binding, we tested the ability of Δ N-KAP3 to disrupt the binding of p30 to MTs. We co-transfected VHL and Δ N-KAP3 in HEK293T cells and found that the MT co-sedimentation of p30 was greatly reduced in the presence of Δ N-KAP3 (Fig. 3b). All relevant plasmids were expressed as detected by western blot (data not shown). In conclusion, our data suggest that p30 - at least in part- binds MTs via its interaction with the kinesin-2 complex.

As Hergovich et al. suggested that the binding between VHL and MTs results in increased stability of microtubules we determined whether Δ N-KAP expression would abrogate the increased stability of MTs induced by VHL. Using a previously described method of measuring MT-stability using live cell imaging and fluorescence recovery after photobleaching (FRAP) (15) we determined that indeed Δ N-KAP specifically inhibited VHL mediated MT-stability (supplemental Figure 1). These data support the notion that the interaction between VHL and the kinesin-2 complex indeed regulates the interaction between VHL and MTs.

VHL is a highly mobile protein

We next sought to determine whether the kinesin-2 complex actively transports VHL. To this end we constructed fusions of the green-fluorescent protein (GFP) to p30 (GFP-p30) and to p19 (GFP-p19), which were transfected into N1E-115 neuroblastoma cells as these cells express detectable levels of endogenous KIF3A (data not shown). To validate our construct, we performed IPs

and confirmed that GFP-p30 bound to KIF3A (data not shown). Furthermore, examining methanol-fixed coverslips of GFP-p30 expressing cells revealed the same perinuclear, vesicular structures as described by Hergovich et al. (data not shown) (19). However, in living cells we observed that GFP-p30 localizes predominantly to the cytoplasm and has a seemingly random distribution (Fig. 4a, second panel, left image). To study the dynamics of VHL localization we performed live cell imaging and fluorescence recovery after photobleaching (FRAP) experiments (20). The FRAP pattern of GFP-p30 differed only slightly from that of GFP indicating that GFP-p30 is a highly mobile protein much like GFP (Fig. 4a and b).

The binding of VHL to KIF3A alters its mobility after ATP depletion

As the processive movement of kinesin-2 molecules along microtubules is dependent on the presence of ATP, we performed the same FRAP assay after intracellular ATP-depletion using sodium azide and 2-deoxyglucose. As opposed to GFP, we found that GFP-p30 acquired a dramatic decrease in its mobility after ATP depletion as seen by time-lapse photography (Fig. 4a). The degree of mobility can be determined by calculating the mobile fraction (Mf), which represents a ratio of absolute fluorescence recovery after photobleaching (Fig. 4c). Next, we made a construct fusing GFP to KIF3A (GFP-KIF3A) and examined its mobility before and after ATP depletion. Like GFP-p30, GFP-KIF3A had a dramatic decrease in Mf after ATP depletion (Fig. 4c). In the absence of ATP, a large portion of the GFP-p30 redistributed to a perinuclear site resembling the microtubule-organizing center (MTOC). To confirm this observation we co-transfected GFP-p30 with ds-RED-labeled γ -tubulin, a major component of the MTOC, and found that after ATP depletion, GFP-p30 co-localizes with ds-RED- γ -tubulin in living cells (Fig. 4d). We thus concluded that after ATP-depletion a large portion of the GFP-p30 is immobilized at the MTOC. GFP-KIF3A responded in an identical manner after ATP depletion (data not shown). ATP depletion did not change the viability of the cells. After reconstitution with normal medium, mobility of GFP-p30 was fully recovered as measured by FRAP (data not shown) as well as the random cytoplasmic localization.

We next asked whether the VHL variants unable to bind KIF3A (Fig. 2a) would display similar behavior in this assay. We began by measuring the mobility of GFP-p19 and GFP- Δ 95-123 before and after ATP depletion and found the Mfs for these VHL constructs were not reduced (Fig. 4b). We subsequently tested whether the type 2A patient-derived Y112H mutation would react differentially to ATP depletion. For these purposes we generated GFP-Y112H. Like GFP-p30, GFP-Y112H is a highly mobile protein under normal conditions. However, unlike GFP-p30, GFP-Y112H was less responsive to ATP depletion, with an Mf of 0.70 +/- 0.21 (S.D.) which is significantly higher than GFP-p30 at 0.42 +/- 0.16 ($p < 0.01$) (Fig. 4e). We conclude from these experiments that the binding of VHL to KIF3A correlates with a decrease in mobility after ATP depletion. We next asked whether binding of VHL to the Δ N-KAP3 construct would interfere with the decrease in mobility of GFP-p30 after ATP depletion. Interestingly, upon depleting ATP from cells that were transfected with both the Δ N-KAP3 construct and GFP-p30, the Mf of GFP-p30 did not significantly change (Fig. 4e).

The interaction between VHL and the kinesin-2 complex does not affect proteasomal degradation

To determine the consequence of VHL/kinesin-2 interaction, we examined VHL's well-known function as an E3 ubiquitin ligase. We found that KIF3A is not a target for proteasomal degradation by poly-ubiquitination, as cellular levels do not accumulate after treatment with MG132, an inhibitor of proteasomal degradation (Fig. 5a). Furthermore, disrupting the binding between VHL and KIF3A using the Δ N-KAP3 construct did not change the expression levels of HIF1 α in HEK293T cells in the presence or absence of desferoxamine (DFO), an iron chelator known to stabilize HIF1 α (Fig. 5b). Next, we tested whether the HIF mediated transcription would be affected by the overexpression of Δ N-KAP3. We transfected HEK293T cells with a reporter construct with 3 HRE sequences in front of a luciferase reporter and its control with 3 mutated HRE sequences. In this assay we were unable to detect any changes in HIF reporter activity as a consequence of Δ N-KAP3 overexpression although we tested three different concentrations of Δ N-KAP3 (Fig. 5c/d). Therefore, we con-

cluded that the interaction between VHL and the kinesin-2 complex is not involved in HIF regulation, nor does the kinesin-2 complex undergo VHL-mediated polyubiquitination.

VHL localizes to cilia and is important for ciliogenesis

The kinesin-2 complex has been implicated in the generation and function of primary cilia (9). Primary cilia protrude from the apical surface cells into the tubular lumen contain ordered microtubules that are composed of acetylated α -tubulin, deetyrosinated tubulin, and glutamylated tubulin (21). To examine whether VHL could be involved in ciliogenesis we performed immunofluorescence studies on KC12TR/VHL-TO and KC12 parental cells. The KC12TR/VHL-TO renal cell carcinoma cell line has previously been described and carries a doxycycline-inducible plasmid encoding the full length VHL cDNA (15). These cells were grown to confluence in the presence or absence of doxycycline and stained for VHL. The stable microtubule network was counterstained with a monoclonal antibody recognizing acetylated or glutamylated tubulin. We found that KC12 parental cells (with or without doxycycline) and KC12 TR/VHL-TO cells not treated with doxycycline do not generally form primary cilia; however, a striking increase in the number of cilia was observed after induction with doxycycline. Furthermore, VHL was clearly located in the cilia (Fig. 6a). We next evaluated the cellular architecture of MDCK and freshly isolated baby mouse kidney cells by co-staining for acetylated tubulin and VHL. In addition to general cytoplasmic staining, cilia localization of endogenous VHL was confirmed for both cell types (Fig. 6b). Because KC12 cells devoid of VHL appeared to have so few cilia, we screened for the frequency of primary cilia in confluent KC12TR/VHL-TO and KC12TR cell cultures in the presence or absence of doxycycline using immunofluorescence antibody against acetylated tubulin and confocal microscopy. Induction of VHL expression by doxycycline treatment was confirmed by western blot and immunofluorescence (not shown). One thousand interphase cells (determined by DAPI) were examined for each cell type. Low numbers of cilia were observed in the KC12TR cell line irrespective of doxycycline treatment: 44 cilia (no doxycycline) vs 61 (doxycycline). Similarly, of 1000 KC12TR/VHL-TO interphase untreated cells, 83

cilia were counted. However, inducing these cells with doxycycline, thereby inducing VHL, elevated the frequency of primary cilia to 566/1000 interphase cells (Fig. 6c). This experiment was performed twice independently and the data pooled. No signal was detected when cells were incubated with the secondary antibody alone.

Cilia induced by VHL overexpression are functional: intracellular calcium influx.

In the kidney, urine flow bends primary cilia on the luminal surfaces of renal tubule cells, rapidly resulting in a localized influx of calcium through ion channels, which is subse-

quently amplified by calcium-induced release of calcium from intracellular stores (22). We measured calcium signalling in KC12TR and KC12TR/VHL-TO cells to explore whether the mechanotransduction events triggered by flow are sensitive to levels of VHL. To this end, confluent cultures of KC12TR cells and KC12TR/VHL-TO treated with or without doxycycline were incubated with Ca^{2+} -sensitive fluorescence probe Fura-2/AM. The cells were then placed in a perfusion chamber under steady flow as previously described (16). Spectrofluorometric analysis allows a quantitative analysis of intracellular $[Ca^{2+}]$. We observed that only KC12 cells re-expressing VHL were capable of

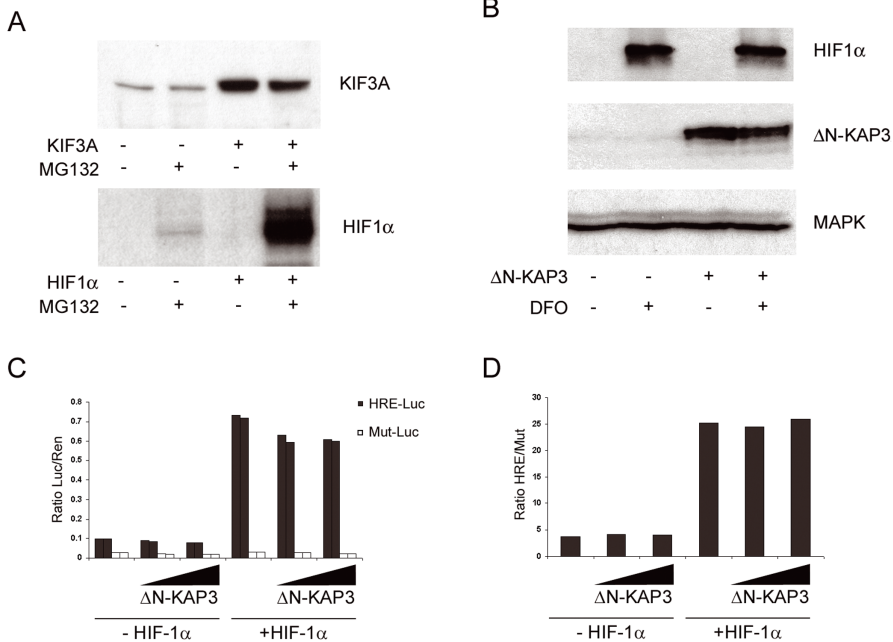


Figure 5: VHL-Kinesin-2 interaction does not involve ubiquitination or HIF signaling.

(A) Western blot of KIF3A and HIF1α before and after MG132 treatment. Upper panel shows western blot for KIF3A from 293T cells, left lanes 1-2 show endogenous KIF3A, lanes 3-4 show transfected KIF3A. Lanes 2 and 4 are treated for 8 hours with 5 μM MG132, a proteasome inhibitor. Lower panel shows similar experiment with endogenous vs. transfected HIF1α. (B) Western blot for HIF1α in the presence or absence of Myc-ΔN-KAP3. Upper panel shows endogenous HIF1α expression in HEK293T cells, lanes 1 and 3 are untreated; lanes 2 and 4 were treated for 4 hours with DFO. Lanes 1-2 were transfected with an empty plasmid and lanes 3-4 were transfected with the Myc-ΔN-KAP3. The middle panel shows the expression of the Myc-ΔN-KAP3. Lower panel is the loading control using MAPK. (C) Synthetic reporters containing a Hypoxic Response Element (HRE) in triplicate or its mutated variant were transfected in HEK293T cells either alone or in combination with ΔN-KAP3 and/or HIF1α. The amount of ΔN-KAP3 cDNA used was 30ng, 100ng and 300ng. Luciferase values were normalised against control renilla values and plotted on the y-axis. Black bars represent the loading control reporter of a Hypoxic Responsive Element (HRE) in triplicate in front of the minimal TK promoter. Open bars represent values using the mutated promoter. (D) Ratios of normalised mean luciferase values of wildtype promoter over the mutated promoter as are depicted in Fig. 5C.

recapitulating the significant calcium response (77%) observed with thrombin stimulation as compared to the same cells transfected with empty plasmids and induced with doxycycline (1.6%) or cells uninduced with doxycycline (1.2%) (Fig. 6d). KC12TR/VHL-TO cells induced with doxycycline and then treated with 10 μ M nocodazole neutralized this effect. These data indicate that VHL, as has been reported for kinesin-2, has a function in ciliogenesis and that the intracellular signaling derived from the primary cilia is dependent on the presence of VHL.

VHL regulation of primary cilia depends on kinesin-2

Kinesin-2-mediated anterograde intra-flagellar transport (IFT) is essential for the assembly and maintenance of cilia in various cell types. Because our results suggest that VHL also regulates cilia assembly, we sought to answer whether this function was dependent on the interaction with kinesin-2. VHL-deficient KC12 cells were transiently transfected with constructs GFP-p30, GFP-KIF3A GFP- Δ 95-123, GFP-Y112H and GFP and cultured to confluence for 3-4 days. After methanol-fixation and counterstaining with anti-acetylated tubulin or anti-glutamylated tubulin, interphase cells were analyzed by confocal microscopy for the presence of primary cilia in GFP-positive cells. If the tubulin staining clearly indicated the presence of a cilium, it was closely examined for GFP signal, to determine the presence of the GFP-labelled VHL allele. Two cilia were observed in the 55 KC12 cells transfected with GFP alone, which is consistent with the background cilia frequency observed in these cells. Neither of these cilia showed GFP staining in the tip of the cilia. In contrast, most cells transfected with GFP-KIF3A (49/60) had cilia, all of which showed clear GFP staining. Not surprising considering the response of the KC12TR/VHL-TO cells, more than half (64/104) of the KC12 cells transfected with GFP-p30 produced easily detectable cilia. Of the 236 GFP- Δ 95-123 transfected cells 39 cilia (17%) were observed, with no positive staining for GFP and of 108 GFP-Y112H positive cells analysed, 12 cilia (11%) were observed, and only one of these cilia had green staining. These data suggest that the binding between VHL and kinesin-2 is impor-

tant for ciliogenesis and targets VHL to the tip of the cilia.

Discussion

The data presented here provide evidence that VHL binds the MT-based heterotrimeric kinesin-2 motor complex by interacting directly with KIF3A and possibly KAP3. Furthermore the third component of the kinesin-2 complex: KIF3B, could also be found in a complex with VHL, indicating that VHL probably interacts with a functional kinesin-2 complex. The acidic domain of VHL and the MT-binding region ranging from residues 95-123 within the first exon of VHL are important for this binding. The type 2A mutant Y112H is deficient in binding KIF3A. These findings correlate well with the regions and mutations described by Hergovich et al. as being deficient in stabilizing microtubules (19). A significant portion –if not all– of the binding of VHL to MTs is mediated through this interaction. Kinesin-2 binding does not involve the ubiquitin ligase-associated function of VHL, but instead regulates VHL mobility. Similar to the kinesin-2 family members, VHL seems to play a role in the generation and/or maintenance of functional primary cilia.

Patients suffering from the von Hippel-Lindau disease develop multiple cystic manifestations especially in the kidney, pancreas and in rare instances in the endolymphatic sac (1). Most patients demonstrate multiple renal cysts (23), which is almost invariably correlated with the “second hit” inactivating the wild-type VHL gene (24). Renal cysts are common in the general population and are rarely clinically significant; however, in VHL patients they have a significant predilection to degenerate to conventional clear cell RCC, the leading cause of death in patients with VHL disease (35-75% prevalence in one autopsy series) (25). In VHL patients, there is considered to be progression from simple cysts with a single layer of tubular epithelium, to atypical cysts demonstrating diffuse epithelial hyperplasia with stratification to three or more cell layers, to either cystic or solid RCCs (23). Uncovering the cause for the cystic phenotype in VHL patients would increase our understanding of an important event in the development of ccRCC.

Primary cilia extend like antennae from the surface of most eukaryotic cells, where they function as environmental sensors.

These specialized microtubule organelles contain an axoneme core, which serves as scaffolding for microtubule-based molecular motors. Mechanical forces bending primary cilia in response to fluid flow in kidney tubules elevate cellular $[Ca^{2+}]$ and activate signal transduction (22). Mutations in at least a dozen different genes involved in cilia assembly or maintenance have now been implicated with the development of cystic kidneys in humans, mice, rats, and zebrafish (26), including components of kinesin-2. Known genes leading to polycystic kidney disease like PKD1 and PKD2 have been implicated in cilia function and generation (27). Therefore the cystic phenotype of VHL patient could be explained by our finding that VHL affects ciliogenesis.

Targeted deletion of Kif3a in murine renal epithelium results in polycystic disease characterized by lack of primary cilia (10). A similar experiment inactivating VHL in the kidney has been performed for the VHL coKO mice, however these mice developed a phenotype of hemangiomas and overexpression of hypoxia dependent factors such as EPO and VEGF, and only in a low frequency they developed renal cysts (28). These data seemingly contradict a prominent function for VHL in the development of renal cysts in mice. However, the clinical findings in patients might clarify this apparent discrepancy. Type 2A patients have a low predisposition for ccRCC and the corresponding mutated alleles produce VHL mutants that are deficient in stabilizing microtubules and localizing to cilia. A possible explanation for these observations is that there are at least two independent functions for the VHL gene: regulating ciliogenesis and controlling HIF levels. In the majority of patients where missense mutations are introduced (e.g. type 2B patient mutations), *in vitro* studies have shown that these VHL mutants retain some microtubule stabilizing function but lose their ability to regulate HIF. Alternatively, type 2A mutations such as Y112H lose both functions simultaneously (19,29). It is conceivable that a total loss of VHL-mediated ciliogenesis could fail to confer survival benefit in the kidney environment. We believe that these data collectively suggest a model whereby residual VHL-mediated ciliogenesis is important for generating the cystic

phenotype observed in VHL patients and consequently affects their risk for developing ccRCC.

Acknowledgements

We would like to thank all members of the lab and especially Dr. M. Gebbink, Dr. J. Neefjes, and Dr. N. Galjart for helpful discussions. We thank the Dept. of Cell Biology of the University of Utrecht, the Netherlands and especially Prof. Dr. J. Klumperman and Dr. G. Posthuma for their support and use of the live cell imaging station, and Drs. Edde and Janke of the CRBM, Montpellier, France for the GT335 antibody. This work is supported by the Dutch Cancer Society (Grants UU 1999-1879 and UU 1999-2114 to E.V.) and the Netherlands Scientific Organization (NWO) (Grants: 920-03-179 to M.L. and E.V., and VIDI grant 016.066.354 to R.G.).

References:

1. Lonser, R. R., Glenn, G. M., Walther, M., Chew, E. Y., Libutti, S. K., Linehan, W. M., and Oldfield, E. H. (2003) *Lancet* 361(9374), 2059-2067
2. Kim, W. Y., and Kaelin, W. G. (2004) *J Clin Oncol* 22(24), 4991-5004
3. Kaelin, W. G., Jr. (2004) *Clin Cancer Res* 10(18 Pt 2), 6290S-6295S
4. Pugh, C. W., and Ratcliffe, P. J. (2003) *Semin Cancer Biol* 13(1), 83-89
5. Iliopoulos, O., Ohh, M., and Kaelin, W. G., Jr. (1998) *Proc Natl Acad Sci U S A* 95(20), 11661-11666
6. Schoenfeld, A., Davidowitz, E. J., and Burk, R. D. (1998) *Proc Natl Acad Sci U S A* 95(15), 8817-8822
7. Lolkema, M. P., Gervais, M. L., Snijckers, C. M., Hill, R. P., Giles, R. H., Voest, E. E., and Ohh, M. (2005) *J Biol Chem* 280(23), 22205-22211
8. Lee, S., Nakamura, E., Yang, H., Wei, W., Linggi, M. S., Sajan, M. P., Farese, R. V., Freeman, R. S., Carter, B. D., Kaelin, W. G., Jr., and Schlisio, S. (2005) *Cancer Cell* 8(2), 155-167
9. Scholey, J. M. (2003) *Annu Rev Cell Dev Biol* 19, 423-443
10. Lin, F., Hiesberger, T., Cordes, K., Sinclair, A. M., Goldstein, L. S., Somlo, S., and Igarashi, P. (2003) *Proc Natl Acad Sci U S A* 100(9), 5286-5291
11. Jimbo, T., Kawasaki, Y., Koyama, R., Sato, R., Takada, S., Haraguchi, K., and Akiyama, T. (2002) *Nat Cell Biol* 4(4), 323-327
12. Wang, G. L., and Semenza, G. L. (1993) *Proc Natl Acad Sci U S A* 90(9), 4304-4308
13. Luckow, B., and Schutz, G. (1987) *Nucleic Acids Res* 15(13), 5490
14. Korinek, V., Barker, N., Morin, P. J., van Wichen, D., de Weger, R., Kinzler, K. W., Vogelstein, B., and Clevers, H. (1997) *Science* 275(5307), 1784-1787
15. Lolkema, M. P., Mehra, N., Jorna, A. S., van Beest, M., Giles, R. H., and Voest, E. E. (2004) *Exp Cell Res* 301(2), 139-146
16. Ulfman, L. H., Joosten, D. P., van der Linden, J. A., Lammers, J. W., Zwaginga, J. J., and Koenderman, L. (2001) *J Immunol* 166(1), 588-595
17. Feldman, D. E., Thulasiraman, V., Ferreyra, R. G., and Frydman, J. (1999) *Mol Cell* 4(6), 1051-1061
18. van der Spek, P. J., Visser, C. E., Hanaoka, F., Smit, B., Hagemeijer, A., Bootsma, D., and Hoeijmakers, J. H. (1996) *Genomics* 31(1), 20-27
19. Hergovich, A., Lisztwan, J., Barry, R., Ballschmieter, P., and Krek, W. (2003) *Nat Cell Biol* 5(1), 64-70
20. Lippincott-Schwartz, J., Snapp, E., and Kenworthy, A. (2001) *Nat Rev Mol Cell Biol* 2(6), 444-456
21. Poole, C. A., Zhang, Z. J., and Ross, J. M. (2001) *J Anat* 199(Pt 4), 393-405
22. Praetorius, H. A., and Spring, K. R. (2001) *J Membr Biol* 184(1), 71-79
23. Van Poppel, H., Nilsson, S., Algaba, F., Bergerheim, U., Dal Cin, P., Fleming, S., Hellsten, S., Kirkali, Z., Klotz, L., Lindblad, P., Ljungberg, B., Mulders, P., Roskams, T., Ross, R. K., Walker, C., and Wersall, P. (2000) *Scand J Urol Nephrol Suppl* 205, 136-165
24. Lubensky, I. A., Gnarra, J. R., Bertheau, P., Walther, M. M., Linehan, W. M., and Zhuang, Z. (1996) *Am J Pathol* 149(6), 2089-2094
25. Evans, J. P., and Skrzynia, C. (2002) von Hippel-Lindau Disease. In:
26. Pazour, G. J. (2004) *J Am Soc Nephrol* 15(10), 2528-2536
27. Pan, J., Wang, Q., and Snell, W. J. (2005) *Lab Invest* 85(4), 452-463
28. Haase, V. H. (2005) *Semin Cell Dev Biol*
29. Clifford, S. C., Cockman, M. E., Smallwood, A. C., Mole, D. R., Woodward, E. R., Maxwell, P. H., Ratcliffe, P. J., and Maher, E. R. (2001) *Hum Mol Genet* 10(10), 1029-1038

Figure 4: Decreased mobility after ATP depletion of GFP-p30 correlates with binding to the kinesin II complex

(A) Time-lapse photographs of N1E-115 cells transfected with GFP (upper row) or GFP-p30 (middle and bottom rows) and submitted to fluorescence recovery after photobleaching (FRAP) experiments. Images were acquired 0.25 seconds before bleaching (left column), directly after bleaching ($t=0$, middle column), and 50 seconds after bleaching (right column). White arrows indicate approximate region of bleaching. Cells in bottom row were subjected to ATP depletion for at least 30 minutes using sodium azide and deoxyglucose. (B) Fluorescence recovery after photobleaching (FRAP) experiment. This graph depicts the %Fi, which represents the percentage of initial fluorescence as calculated from 3 independent measurements pooled into 1 line. The error bars represent the standard error of the mean of each time point. The open squares represent the data generated using GFP transfected into NE1-115 cells and the closed squares represent the data generated using GFP-p30 transfected into NE1-115 cells. (C) FRAP-derived mobility (Mf) values of GFP-tagged variants of VHL (top of graph) in transfected N1E-115 cells. Each square represents an individual measurement before (filled squares) or after ATP depletion (open squares). Horizontal line in each experiment represents the mean value. Significance of mobility decrease after ATP depletion was calculated using a two-tailed Students T-Test, and is depicted below the graph. Mf, mobile fraction; N/A, not applicable (mobility did not decrease); NS, not significant. (D) Live cell images of N1E-115 cells co-transfected with CFP-p30 (left panel) and dsRED- γ -tubulin (middle panel) after ATP depletion. Right panel, image overlay. (E) FRAP-derived Mf values for GFP-p30 in the presence or absence of Δ N-KAP3 overexpression as indicated above the graph. Each square represents an individual measurement before (filled squares) or after ATP depletion (open squares). Horizontal line in each experiment represents the mean value. Significance of mobility decrease after ATP depletion was calculated using a two-tailed Students T-Test, and is depicted below the graph. Mf, mobile fraction

Figure 6: VHL is necessary for cilia development and function in KC12 renal cell carcinoma cells.

(A) KC12TR/VHL-TO cells were induced to express VHL with doxycycline and grown to confluency. Cells were fixed using ice-cold methanol and stained for acetylated tubulin (red) and for VHL using Ig32 (green). We show a maximal Z-projection of a Z-stack depicting a representative cell made using a Zeiss LSM510 confocal microscope. (B) MDCK cells were grown to confluency and stained for endogenous VHL using Ig32. In this sample no counterstain was used and the gray dots represent VHL staining. We show a 3D-image with 3 projections from different angles made using a Zeiss LSM510 confocal microscope. Arrows show the VHL staining in a cilium. (C) Primary cilia formation was counted in KC12 parental and KC12TR/TO cells. Depicted is the number of cells positively identified as carrying intact cilia from 1000 counted cells that were identified using DAPI. Data was acquired at least 2 different time points for each cell type and pooled. (D) KC12TR cells and KC12TR/VHL-TO cells were induced to express VHL with doxycycline (top of graph) and grown to confluency and used in a Ca^{2+} influx experiment. The graph depicts the % of the maximal Ca^{2+} influx as measured by thrombin response. As shown under the graph we measured in the presence or absence of flow.

Figure 4

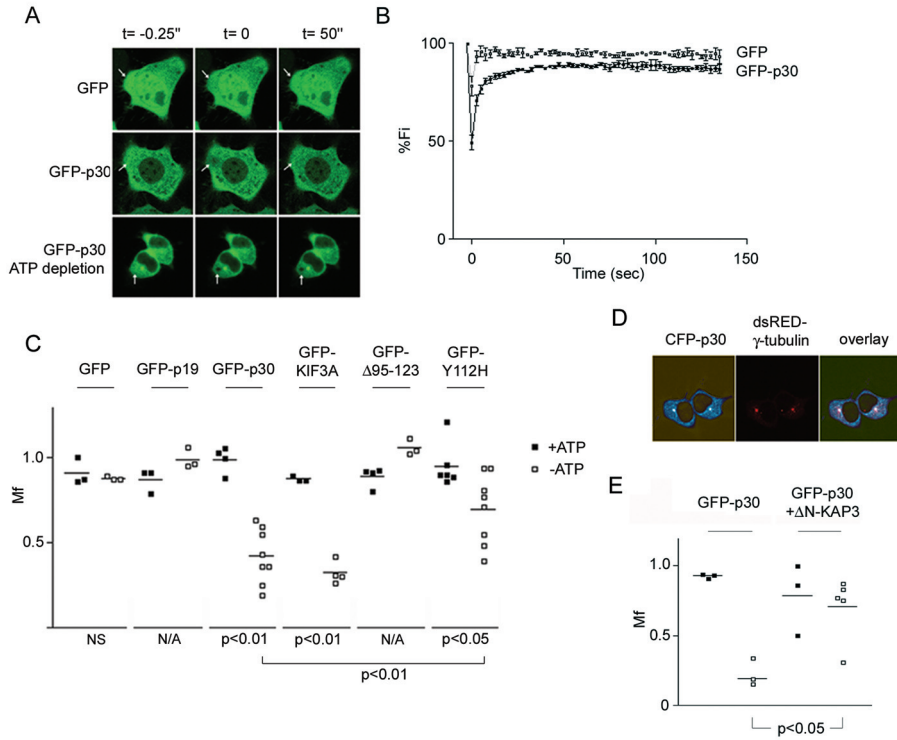
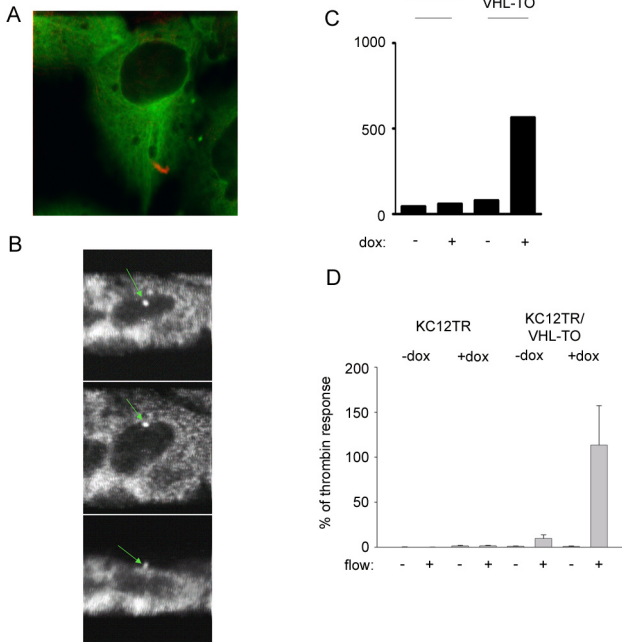


Figure 6



HIF

Chapter 6:

Interplay between VHL/ HIF1 α and Wnt/ β -catenin pathways during colorectal tumorigenesis

Giles RH, Lolkema MP, Snijckers CM, Belderbos M, van der Groep P, van Beest M, van Noort M, Goldschmeding R, van Diest PJ, Clevers H, Voest EE

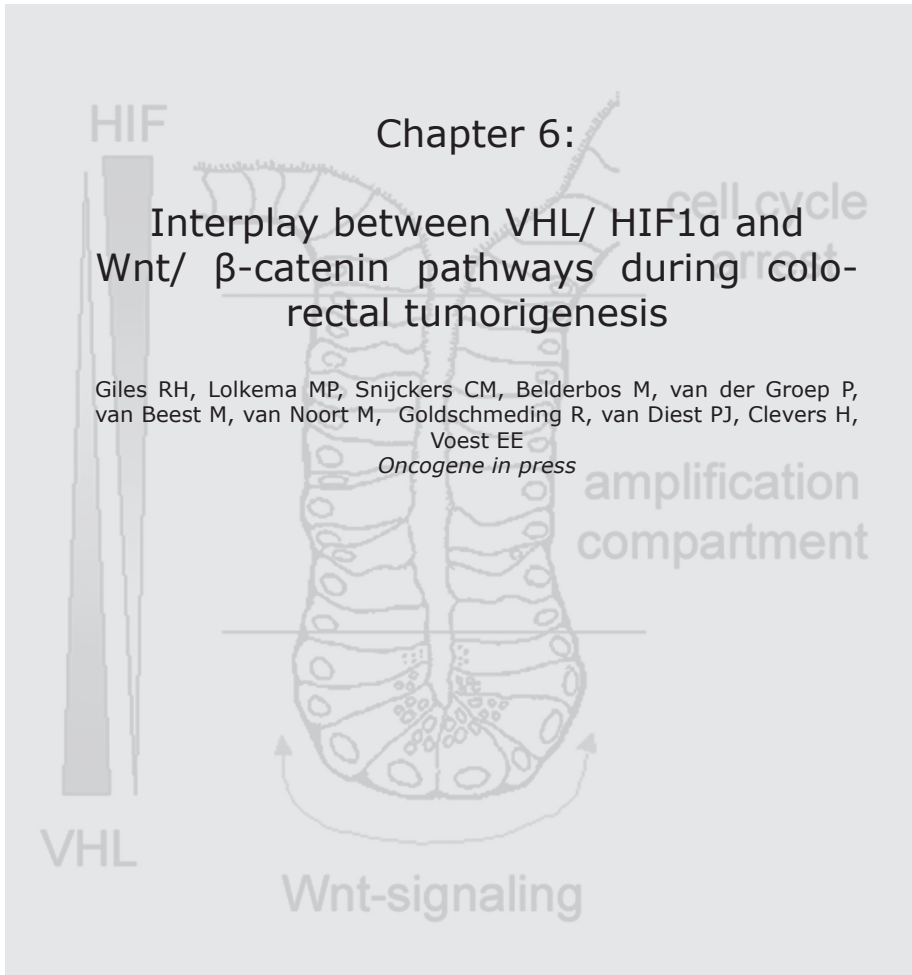
Oncogene in press

VHL

Wnt-signaling

amplification compartment

cell cycle arrest



Interplay between VHL/ HIF1 α and Wnt/ β -catenin pathways during colorectal tumorigenesis

Giles RH, Lolkema MP, Snijckers CM, Belderbos M, van der Groep P, van Beest M, van Noort M, Goldschmeding R, van Diest PJ, Clevers H, Voest EE

Oncogene in press

Activation of the Wnt signaling pathway initiates the transformation of colorectal epithelial cells, although the transition to metastatic cancer requires angiogenesis. We have investigated the expression of VHL in intestinal epithelial derived cells and intestines from humans and mice. Here we show that VHL expression is regulated by TCF4 in colorectal cancer (CRC) cell lines and consistent with other Wnt targets, immunohistochemistry of VHL in normal adult intestine reveals restricted expression to the proliferative compartment at the bottom of intestinal crypts. VHL is overexpressed in intestinal polyps from Familial Adenomatous Polyposis patients. Accordingly, Vhl is completely absent from the proliferative intestinal pockets of Tcf4 $^{-/-}$ perinatal mice. We observed complementary staining of the hypoxia inducible factor (HIF)1 α to VHL in normal intestinal epithelium as well as in all stages of CRC. Although we observed upregulated levels of VHL in very early CRC lesions –presumably due to activated Wnt signaling– a clear reduction of VHL expression is observed in later stages of CRC progression, coinciding with stabilization of HIF1 α . Because loss of VHL in later stages of CRC progression results in stabilization of HIF, these data provide evidence that selection for VHL down-regulation provides a pro-angiogenic impulse for CRC progression.

Introduction

Colorectal cancer (CRC) is one of the most common causes of cancer in the Western world. The sequence of multiple genetic events that occur in the transition from normal mucosa to cancer cells is subject to extensive research. Greater than 90% of all CRCs have an activating mutation of the canonical Wnt signaling pathway, ultimately leading to β -catenin/TCF4-mediated gene transcription. Downstream targets of the Wnt signaling pathway, such as the *Myc* oncogene, collectively form a genetic program enabling an intestinal epithelial cell to transform to a cancer phenotype (1). In addition to the genetic changes within the cancer cell, exponential growth requires a supportive micro-environment. In CRC, tumor-induced formation of new capillaries from pre-existing vasculature –angiogenesis– often marks the adenoma/carcinoma transition (2,3). This angiogenic switch during tumor growth provides increased oxygen and nutrient supplies to the tumor and has been correlated with invasive tumor growth and progression to a metastatic phenotype. Because angiogenesis represents a powerful control point in tumor development, investigation of the physiological mechanisms underlying this process in CRC has direct relevance to the development of future therapeutics. Both preclinical and clinical

evidence indicate that vascular endothelial growth factor (VEGF) plays an important role in the angiogenic switch of colorectal cancer. This insight has led to the widespread use of cyclooxygenase-2 inhibitors –which inhibit VEGF– to prevent the formation of polyps and cancer in familial adenomatous polyposis (FAP), hereditary non-polyposis colon cancer, and sporadic colorectal cancer (4). The recent approval of bevacizumab, an anti-VEGF antibody, for advanced colorectal cancer also underscores the relevance of VEGF in survival and progression of disease (5). In addition, several clinical trials with anti-VEGF approaches are underway both in the adjuvant and metastatic disease setting (5). Taken together these findings support the central role of VEGF in colorectal cancer progression.

One of the best-documented transcriptional regulators of VEGF is the hypoxia inducible factor 1 α (HIF1 α). Under normoxia HIF1 α is rapidly degraded, a process that occurs under the control of the tumor suppressor gene von Hippel-Lindau (VHL). VHL forms a multiprotein complex with elongin C, elongin B, Cul-2, and Rbx-1 [(VEC), reviewed by Maynard and Ohh (6)]. VEC functions as an E3 ubiquitin ligase to target HIF1 α for polyubiquitination and subsequent degradation by the 26S proteasome (7-9). VHL functions as the target recognition moiety of the VEC complex and specifically recognizes

prolyl-hydroxylated HIF1 α subunit (10,11). This post-translational modification of HIF1 α requires oxoglutarate, iron and oxygen (10-12). Thus, ubiquitin-mediated destruction of HIF1 α occurs selectively under normoxic conditions whereas hypoxia results in stabilization and transcriptional activity of HIF. Accordingly, biallelic inactivation of the VHL gene through mutation, deletion, or promoter silencing generally leads to the stabilization of HIF1 α and thereby promotes the up-regulation of numerous HIF1-target genes, resulting in an inappropriate triggering of the hypoxic response under normal oxygen tension (6). This is best observed in patients with von Hippel-Lindau disease, an inherited autosomal dominant cyst and cancer syndrome. Clinically, tumors lacking VHL secrete high levels of VEGF and other pro-angiogenic factors and manifest as highly vascularized lesions (13,14) such as hemangioblastomas and clear cell renal cancer.

The observation that VEGF plays an important role in colorectal cancer progression together with our earlier findings that VHL is abundantly expressed in colonic mucosa (15) formed the basis for our hypothesis that aberrant regulation of VHL contributes to the angiogenic switch in colorectal cancer. Here we report that the VHL tumor suppressor gene acts as a physiological Wnt target in the intestines. Although we observed upregulated levels of VHL in very early CRC lesions –presumably due to active Wnt signaling- a very clear reduction of VHL expression is observed in later stages of CRC progression, coinciding with stabilization of HIF1 α and induction of a hypoxic response in these tumors. Thus, correlative data and biological plausibility support a role for VHL down-regulation in the angiogenic switch in CRC progression. Furthermore, understanding the regulation of VHL levels may provide an alternative approach to inhibit angiogenesis.

Material and methods

Cell culture and treatment

LS174T (ATCC number CL-188) were cultured in RPMI 1640 supplemented with 10% FCS. The T-REX system (Invitrogen, Carlsbad, CA) was used according to the manufacturer's instructions to generate doxycycline inducible dn-TCF4 expressing cells (L8) as previously described (16). To inhibit

GSK3 β activity, 293T cells were grown to 70% confluency and 20mM LiCl (Sigma) was added to the medium for 4 hours prior to lysis. Conditioned medium from parental (mock-transfected) and Wnt3a-transfected mouse fibroblast L cells was prepared as described (17) and was used to stimulate 293T cells for 16 hours before harvesting cells.

Reporter assays

To generate the HRE-luciferase reporter construct (HRE-Luc), we used the following wild-type HRE oligonucleotide (W18) of the 3'-enhancer of the human erythropoietin gene (18) in triplicate in front of a minimal TK promoter and the Luciferase gene in the vector pBILuc: C(TACGTGCT)GC(TACGTGCT)GC(TACGTGCT)G (where the HRE is in parentheses and the core bases essential for HIF binding are underlined). The vector pBILuc is derived from pBICat₂ (19) in which the Cat gene has been replaced by Luciferase out of pTopFlash (20). As a negative control, a similar construct (Mut-Luciferase, or Mut-Luc) with the M28 fragment (18) was constructed in which three altered nucleotides completely abrogate HIF-binding: CTCAATGCTGCTCAATGCTGCTCAATGCTG 3' (where the mutated core bases are underlined). 293T cells were plated 18 hours prior to transfection by Fugene6 (Roche, Basel, Switzerland) according to the manufacturer's instructions. The following amounts of plasmids were transfected in 293T cells: 50 ng HRE-Luc or Mut-Luc in combination with 5 ng of the renilla internal control CMV-pRNL (Promega, Madison, WI), and 100 ng wild-type HIF1 α as indicated in the text. The total amount of DNA transfected in all reporter assays was adjusted to 500 ng with pcDNA₃. Luciferase activities were measured 24-36 hours after transfection using the DUAL luciferase system according to the manufacturer's protocol (Promega, Madison, WI). Luciferase activity was normalized relative to renilla.

Western blotting

Samples were examined by SDS-PAGE on 10% acrylamide gels and subsequent western blotting. Specific protein bands on the western blots were visualized using supernatant from an in-house produced anti-VHL monoclonal hybridoma specifically recognizing the C-terminus of VHL (1B3B11) generated using a protocol we have previously described (21). Hybridoma supernatant was diluted 1:5 in PBS containing 5% milk and

0.1% Tween-20. Rabbit anti-Mouse HRP (Pierce, Rockford, IL) (1:20,000) was used as secondary antibody after which enhanced chemiluminescence (Perkin Elmer Life Sciences, Boston, MA) was used for detection.

RT-PCR

RNA from cell lysates was extracted using RNAbee reagent (Campro Scientific, Veenendaal, The Netherlands) following the protocol of the manufacturer. cDNA was made using 2 μ g of total RNA and reverse transcribed using Superscript Reverse Transcriptase (Invitrogen, Carlsbad, US) and random hexamers. Gene-specific cDNA fragments were amplified by 25 cycles of PCR consisting of 1 min. at 95 °C, 1 min. at 55 °C and 2 min. at 72 °C. PCR fragments were analyzed by DNA gel electrophoresis. We used the following primers in our assays: VHL-Fw: 5'-gctaccgaggtcaccttgg, VHL-Rev: 5'-tgtgtcagccgctccag-gtc, VEGF-Fw: 5'-cgaaacatgaacttctctgc, VEGF-Rev: 5'-ccactctgctgatgattctgc, EphB2-Fw: 5'-cgtgactgcagcagcatc, EphB2-Rev: 5'-cagtagagcttgatgggtac, 18S-Fw: 5'-agttggtggagcgatttgc, 18S-Rev: 5'-tattgctcaatctcgggtg.

Tissue sample preparation and immunohistochemistry

Samples of small intestine or colon were obtained immediately after excision biopsy procedures from patients treated at the University Medical Center Utrecht, The Netherlands and fixed in neutral 4% buffered formaldehyde at 4°C for 24 hours. Individual segments were embedded in paraffin and sectioned (4-5 μ m). Informed consent to anonymously use leftover patient material for scientific purposes was a standard item in the treatment contract with the patients. None of the patients with colorectal cancer had received any preoperative therapy. Paraffin sections were mounted on silane-coated slides and baked in an oven at 57°C the night before the staining was performed to avoid de-attachment of the tissue. Following dewaxing and hydration, sections were pretreated with peroxidase blocking buffer (1.5% H₂O₂ in methanol) for 20 minutes at room temperature. Antigen retrieval was performed by boiling samples in Na-citrate buffer (10 mM, pH 6.0). After 20 minutes, the boiling pan was allowed to slowly cool down to room temperature. Incubation of vVHL (Ig32, diluted 1:100, Transduction

Labs/Pharmigen, Alphen aan den Rijn, the Netherlands) was performed in 10% normal goat serum in PBS overnight at 4°C. In all cases, the Powervision poly HRP goat-anti-mouse IgG (Immunologic, Duiven, the Netherlands) was used as a secondary reagent. Stainings were developed using DAB (brown precipitate) and then counterstained with hematoxylin and mounted. To exclude cross-reactivity of Ig32 with other Wnt-signaling targets, we pre-incubated this antibody for 30 minutes with 2.5 μ g recombinant VHL, which completely abrogated all signal in the intestine (not shown). Anti-HIF1 α immunohistochemistry was performed as we have previously described (22). Samples for β -catenin staining were fixed in 10% neutral buffered formalin for 12 hours at 4°C. Following dewaxing and hydration, sections were pretreated with peroxidase blocking buffer for 20 minutes at room temperature. Antigen retrieval was performed by boiling samples in Tris/EDTA (40 mM/1mM, pH 8.0) buffer for 50 minutes in a cooking pan. After this period, the pan was allowed to slowly cool down to room temperature. Samples were blocked with 1%BSA/PBS for 20 minutes, washed 3 times in PBS and incubated with anti-C-terminus β -catenin antibody (diluted 1:50, Transduction Labs/Pharmigen, Alphen aan den Rijn, the Netherlands) in 0.05% BSA/PBS for 2 hours at room temperature. Detection of the primary antibody was performed using the Powervision poly HRP goat-anti-mouse IgG (Immunologic, Duiven, the Netherlands) for 1 hour at room temperature. The stainings were visualized with DAB. Nuclei were counterstained with hematoxylin.

Results

VHL responds to Wnt signaling

To investigate the role of the tumor suppressor *VHL* in colorectal cancer we checked whether CRC cell lines harbored mutations in the *VHL* gene. For this purpose we sequenced the entire open reading frame of *VHL* in a number of CRC cell lines and found them all to be wild-type for *VHL* despite variable expression levels (data not shown). One cell line in particular was found to express high levels of VHL: LS174T. These LS174T CRC cells also show high levels of constitutive β -catenin/TCF-driven transcription due to stabilizing mutations in β -catenin (16). We

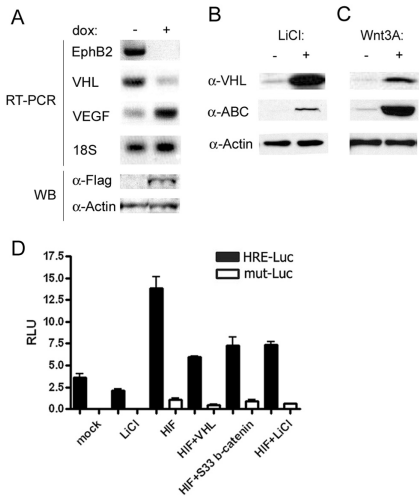


Figure 1. VHL is a β -catenin/TCF target in vitro.

(A) Top four panels show RT-PCR analysis of the expression levels of EphB2, VHL, VEGF, and 18S (input control) mRNAs in L8 cells. Cells were induced for 24 hours with doxycycline (dox; 1 μ g/ml). Lower two panels show western blot analysis of the protein expression levels of FLAG-tagged dn-TCF4 (α -FLAG) and the loading control actin. This figure shows a representative image of 3 independent experiments with similar outcome. WB; western blot. (B) Western blots of 293T cell lysates at baseline (-) or after 5 hr treatment with 20mM LiCl (+). Top panel, VHL protein levels; middle panel, non-phosphorylated activated β -catenin (ABC) as a positive control for activated Wnt signaling; lower panel, loading control actin. This figure shows a representative image of 2 independent experiments with similar outcome. (C) Soluble Wnt3A stimulates VHL levels. Western blot of VHL protein levels in 293T cell lysates after 16 hrs cultured with conditioned medium from either mouse L fibroblasts transfected with an empty plasmid (-) or with a plasmid expressing soluble Wnt3A ligand (+). Middle panel shows the positive control for activated Wnt signaling: non-phosphorylated activated β -catenin (ABC). Lower panel shows the loading control actin. This figure shows a representative image of 2 independent experiments with similar outcome. (D) The transcriptional activity of HIF1 α is reduced by β -catenin. 293T cells were co-transfected with HIF1 α luciferase reporter constructs with either three tandem HIF1 α response elements (HRE-Luc, filled bars) or three HREs with a single mutation (Mut-Luc, empty bars) and with the combinations of empty vector (mock), HIF1 α , VHL, stable dominant positive S33 β -catenin and LiCl as indicated. Relative luciferase units (RLU) are normalized with renilla to take transfection efficiency into account. Experiments were performed in duplicate and repeated at three independent time points. Bars show the standard error of the mean.

used LS174T cells that were engineered to express dominant-negative TCF4 (dn-TCF4) under the control of a doxycycline-inducible promoter (dubbed L8). dn-TCF4 does not bind β -catenin and acts as a potent inhibitor of the endogenous β -catenin/TCF complexes present in CRC cells. Thus upon induction with doxycycline, L8 cells abrogate all transcription mediated by β -catenin/TCF complexes (16), essentially shutting off the Wnt signaling cascade. To investigate the influence of Wnt signaling on VHL levels in these cells, we performed RT-PCR for VHL with RNA derived from L8 cells either at baseline or after stimulation with doxycycline for 16 hours. As has been previously published (23), transcript levels of the well-characterized Wnt target the tyrosine kinase receptor EphB2 were greatly diminished by treating this cell system with doxycycline (Fig. 1A, top panel). To our surprise, however, VHL transcript levels responded similarly (Fig. 1A, second panel). Because numerous studies have established that VHL inactivation results in increased transcriptional activation of VEGF, we also performed RT-PCR for VEGF in the same experiment. Contrary to VHL, VEGF levels increased 3.3-fold after treatment of L8 cells with doxycycline (Fig. 1A, third panel), indicating an intact response to VHL downregulation. Doxycycline alone had no effect on VHL levels in LS174T cells transfected with empty vectors (not shown). We amplified 18S as an appropriate control for cDNA input (Fig. 1A, fourth panel) because, unlike several housekeeping genes, transcript levels are not influenced by fluctuating VHL or HIF1 α levels (24,25), nor are they affected by β -catenin/TCF activity. Ample product was observed in RT-PCR using plasmids containing cDNA sequences as primer controls and no product was detected in the absence of cDNA template for each primer pair (not shown). To verify the induction of dn-TCF4 in this experiment we prepared protein lysates from a portion of the L8 cells and tested the expression of the Flag-tagged dn-TCF4 construct using western blot analysis. Anti-Flag staining shows a specific band at the expected height of 85 kDa only in the cells induced with doxycycline (Fig. 1A, fifth panel) despite equal protein loading as indicated by anti- β -actin staining of the same blot (Fig. 1A, lowest panel). We concluded from this experiment that blocking β -catenin/TCF affects VHL transcript levels in a manner suggestive of a Wnt signaling target.

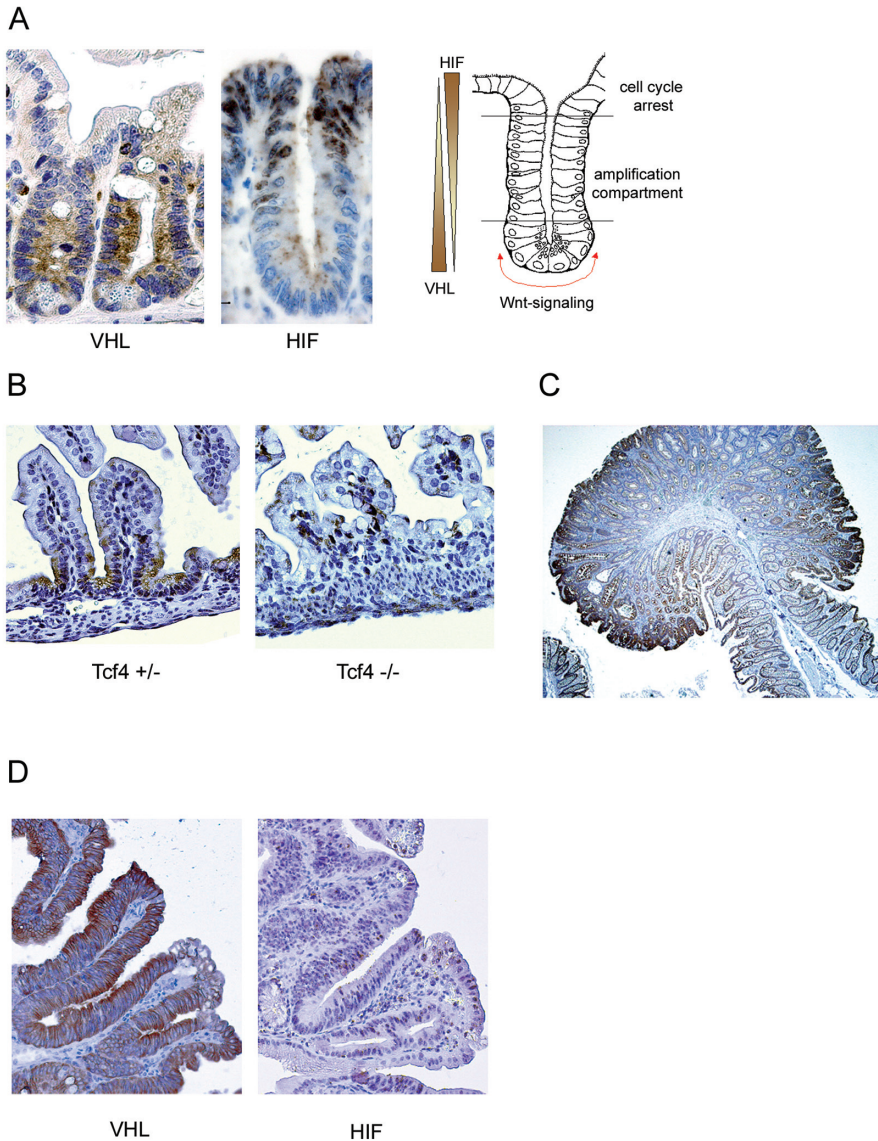


Figure 2: VHL is an in vivo target of Wnt signaling.

(A) Immunohistochemical analysis of VHL and HIF1 α in the small intestine reveals that VHL expression is restricted to the cells in the intervillus regions (left) while HIF1 α (middle) is expressed in a complementary pattern by the adjacent cells in the villus. Stainings were developed using DAB (brown precipitate) and counterstained with hematoxylin (blue nuclei). A cartoon (right) illustrates the position of the putative Wnt signal, the amplification compartment with proliferating cells and the arrested and differentiated cells located toward the intestinal lumen. (B) VHL is expressed in the intervillus regions of Tcf4^{+/-} embryos (left) but is completely absent in Tcf4^{-/-} littermates stained in parallel (right). (C) Immunohistochemistry of VHL in a FAP patient polyp shows elevated expression of VHL. (D) Early lesions from FAP patients show overexpression of VHL by immunohistochemistry (left), but limited or no immunohistochemical staining for HIF1 α (right).

We subsequently performed experiments to test whether VHL levels could respond to upstream Wnt signaling. Initially, we tested the effects of 20 mM LiCl on endogenous VHL levels in 293T cells; LiCl inhibits GSK3 β and mimics Wnt signaling by allowing non-phosphorylated β -catenin levels to accumulate (26). Stimulation with LiCl for five hours markedly increased the amounts of endogenous VHL in 293T cells detected by immunoblotting (Fig. 1B, upper panel), and likewise increased expression of the active signaling pool of non-phosphorylated β -catenin (ABC, Fig. 1B, middle panel) as has been previously reported in these cells (27). To substantiate this finding, we determined whether soluble Wnt3a protein could also regulate VHL levels. To this end, we stimulated 293T cells overnight with conditioned medium derived from mouse fibroblast L cells secreting Wnt3a (17). Accumulation of non-phosphorylated β -catenin (Fig. 1C, middle panel) served again as control for activation of the pathway. Consistent with the previous data, Wnt3a stimulation also resulted in VHL accumulation (Fig. 1C, upper panel), indicating that VHL is downstream of an intact Wnt-signaling pathway. Actin levels were used as a control for equal protein loading for all experiments.

Wnt signaling regulates VEGF through VHL and HIF1 α

The RT-PCR data (Fig. 1A) suggested that VHL regulation by β -catenin/TCF affects HIF1 α transcriptional activity, as seen by VEGF induction. To investigate the direct influence of β -catenin/TCF on HIF activity, we performed a HIF1 α reporter assay. We generated a luciferase reporter construct to carry three tandem hypoxia response elements derived from the promoter of the erythropoietin gene (HRE-Luc) or three HREs with three nucleotide mismatches (Mut-Luc). 293T cells were co-transfected with either the HRE-Luc or the Mut-Luc reporter plasmids and with the combinations of empty vector (mock), HIF1 α , VHL, and constitutively active S33 β -catenin as indicated in Fig. 1D. All samples were co-transfected with renilla as an internal transfection control. The mock transfection illustrates the background levels of HIF1 α activity in 293T cells which is increased by approximately 4-fold upon transfection of HIF1 α . As

expected, co-transfection of VHL with HIF1 α greatly reduced HIF1 α activity, which was mirrored by co-transfecting constitutively active S33 β -catenin. Mut-Luc background levels remained low, indicating a HIF1 α -specific effect. These data suggest that upregulation of VHL by β -catenin/TCF reduces HIF1 α activity. Furthermore we used LiCl as an activator of endogenous-Wnt signaling and as expected, the addition of LiCl to the HIF1 α -reporter assay resulted in a similar downregulation of HIF1 α activity compared to the overexpression of VHL (Fig. 1D).

By deduction, our data suggest that Wnt signaling would fail to decrease HIF activity in VHL $^{-/-}$ cell lines. In an attempt to address this question, we stimulated renal cell carcinoma cell lines 786-0, KC12, or RCC4 (all VHL mutant) cell lines with LiCl; however, none of these cell lines upregulated activated β -catenin in response to LiCl as measured by western blot for anti-ABC or by TCF/ β -catenin reporter assays (not shown). It is likely that these renal carcinoma cells lack some upstream Wnt component.

VHL is a physiological target of Wnt signaling

At the bottom of intestinal crypts, stem cells give rise to a transient population of undifferentiated cells that vigorously proliferate as they migrate towards the lumen of the intestine (Fig. 2A, right panel). Epithelial cells that reside at the bottom-most position of the crypts, close to the putative Wnt source, accumulate nuclear β -catenin and accordingly show high levels of proteins positively regulated by Wnt (16). To determine whether VHL also demonstrates characteristics of a Wnt-target in physiological circumstances we performed immunohistochemical analysis of VHL staining in normal adult intestine. Consistent with the *in vitro* data and our previous observations (15), VHL expression is limited to cells at the bottom of crypts, near the Wnt source, and tapers off along the crypt-villus axis (Fig. 2A, left). Interestingly, expression of HIF1 α inversely correlates with that of VHL; it is absent near the presumptive Wnt source at the bottom of the crypt, low at the intermediate positions in the crypt and peaks at the surface epithelium. This spatial division of the epithelium into two domains complementarily expressing either VHL or HIF1 α (cartoon, Fig. 2A) suggests that VHL efficiently regulates

HIF1 α levels in the intestine. These findings represent the first positive staining for HIF1 α in normal normoxic tissue and show that HIF1 α expression could have a function in normal homeostasis in the intestine in the absence of hypoxia.

The distribution of VHL and HIF1 α in the gut prompted us to examine the intestines of mice deficient for Tcf4. In the intestinal epithelium, Tcf4 is the most prominently expressed TCF family member (20). In the late fetal small intestine Tcf4 expression is mainly confined to the intervillus pockets, the prospective crypts of Lieberkühn (28). To study whether the expression of VHL in the intestine is dependent on TCF4, we determined the expression pattern of Vhl in the small intestine of E18 Tcf4 mutant embryos (Fig. 2B); older mice could not be examined because these mice die perinatally as a result of tearing of the intestinal epithelial lining and fluid imbalance. These mice have a striking small-intestinal phenotype with a selective loss of cycling intestinal crypt cells (28). In the Tcf4 $^{+/-}$ control mice, VHL expression (Fig. 2B, left) was readily detectable in the pseudostratified intervillous epithelium. In sharp contrast, the intestinal epithelium of Tcf4 $^{-/-}$ mice did not show any VHL staining (Fig. 2B, right). Unfortunately, there are no available antibodies that recognize murine HIF1 α , thus we were unable to examine the expression pattern of HIF1 α in a Tcf4 $^{-/-}$ background.

VHL is upregulated in FAP patient polyps

A large body of data supports a model in which mutational activation of β -catenin/TCF in intestinal epithelial cells leads to polyp formation, the first morphological alteration that ultimately results in colorectal cancer [reviewed in (29)]. These polyps can be viewed as abnormal expansions of the crypts as far as gene expression patterns are concerned (16). To further explore our hypothesis, we studied the expression of VHL in the intestinal mucosa of patients with familial adenomatous polyposis (FAP), an uncommon colorectal cancer syndrome associated with germline mutations of the APC tumor suppressor gene. In all atypical crypt foci and polyps examined from 12 FAP patients, VHL was highly expressed (Fig. 2C, D). Nuclear β -catenin was observed in all polyp and adenoma tissues (not shown). Accordingly, HIF1 α could not be detected in

these early lesions (Fig. 2D). The above data imply that both legitimate and illegitimate activation of Wnt signaling stimulate VHL expression in intestinal mucosa through TCF4/ β -catenin.

Expression of VHL is lost in spontaneous CRCs

In order to further support the notion that β -catenin/TCF signaling acts as a switch that inversely controls VHL and HIF1 α expression, we performed immunohistochemical analyses on 19 spontaneous colorectal tumors of various pathological grades. Interestingly, it was immediately evident that the earliest lesions displayed heterogeneous expression of VHL (not shown and Fig. 3A). Upon closer inspection of early adenomatous lesions, clonal loss of VHL could be observed, suggestive of a selective mechanism (Fig. 3A-B). In some adenomas loss of VHL expression was quite striking, and correlated perfectly with HIF1 α stabilization (Fig. 3A). Although a layer of dysplastic cells expressing VHL surrounded HIF1 α -positive adenoma cells, intermingling of the two cell populations was never seen in normal or neoplastic epithelium. Examining CRCs further along the adenoma-carcinoma sequence, we never detected VHL expression in late adenomas and carcinomas, despite the increased levels of cytoplasmic and nuclear β -catenin in the tumor tissue (Fig. 4A-B, top row). Relatively normal adjacent tissue expressed normal levels of VHL (Fig. 4A-B, middle row). Loss of VHL expression coincided with accumulation of HIF1 α expression (Fig. 4A-B, bottom row). In short, while nuclear β -catenin continues to accumulate during adenoma-carcinoma progression, at some point VHL levels become uncoupled from the Wnt pathway, perhaps through selection for clones downregulating VHL either by promoter methylation, by chromosome loss, or by gene mutation.

Examining the HIF1 α staining in our series of CRCs closely, we were able to identify two distinct patterns: in 9/19 samples, the nuclear HIF1 α staining was prominent in perinecrotic regions (not shown), while in the remaining 10 samples it generally localized to well-vascularized regions (not shown). The presence of stabilized nuclear HIF1 α in areas that should be well-oxygenated (ie adjacent to blood vessels) suggests

a hypoxia-independent mechanism –such as VHL inactivation- for HIF1 α stabilization. It will be interesting to determine whether the pattern of HIF1 α staining in CRCs correlates with patient prognosis, as has been recently established for breast cancer (30).

Discussion

In the past few years, multiple downstream genes of β -catenin/TCF have been identified (reviewed at www.stanford.edu/~rnusse/wntwindow.html), yet the role of such individual genes in gut physiology or tumorigenesis is not completely understood. In this study we provide evidence that the VHL tumor suppressor gene acts as a physiological Wnt target in the intestines of mice and humans. Large-scale analyses of the genetic program driven by β -catenin/TCF in normal and neoplastic intestinal epithelium have demonstrated that measuring RNA or protein levels are at least as biologically relevant as promoter studies in characterizing putative Wnt target genes (16,31). Nevertheless, it is interesting to note that the TCF4 consensus binding site CTTTGA (32) is found –468 nucleotides upstream of the transcriptional start of human VHL (GenBank AF010238), suggestive of direct regulation. Our data demonstrate that the proliferative cells residing in the intestinal crypts express VHL, whereas HIF1 α is expressed in a complementary fashion in adjacent differentiated cells. Furthermore, it was recently shown that VHL/HIF signaling plays an important role in maintaining colonic integrity in a colitis model (33). Another report has suggested that the expression of a HIF1 α target gene –the intestinal trefoil factor- at the intestinal lumen might be essential for barrier formation and injury repair in intestinal mucosa (34).

Secondly, we demonstrate that while both pathways remain intact and coordinated in early neoplastic lesions, they become uncoupled from each other upon downregulation of VHL expression in CRC development. Heterogeneous expression of VHL in early adenomas suggests that clonal selection and subsequent expansion of cells with reduced VHL is already taking place. In human CRC samples a strict compartmentalization of adjacent VHL-expressing relatively normal tissue and HIF1 α -expressing tumor tissue was evident. These findings suggest the presence of selective forces encouraging

VHL inactivation at the adenoma stage of tumor progression. In the light of these observations, the function of VHL proposes an interesting hypothesis. VHL functions as the target recognition moiety of an ubiquitin E3 ligase complex, targeting HIF1 α for ubiquitination and subsequent proteasomal degradation. Biallelic inactivation of *VHL* allows HIF1 α to escape degradation, accumulate and stimulate expression of several genes encoding for growth factors, such as *VEGF*. Clinically, tumors lacking *VHL* secrete high levels of VEGF and other pro-angiogenic factors and manifest as highly vascularized lesions. Furthermore, the presence of nuclear HIF1 α has been extensively associated with the advent of angiogenesis in many tumor settings (22,35,36). Thus, correlative data and biological plausibility support a role for *VHL* down-regulation in the angiogenic switch in CRC progression. This hypothesis is supported by the wealth of data on the regulation of HIF1 α and VEGF by VHL [reviewed by Maynard and Ohh (6)], in addition to our findings that decreased VHL levels in colorectal cells correlated with increased HIF1 α and VEGF.

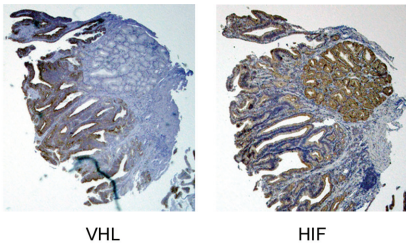
A number of studies support a role for VHL inactivation/HIF1 α stabilization in the progression of colorectal cancer. Firstly, loss or alteration of the VHL locus on chromosome 3p is commonly associated with the progression and poor prognosis of CRC (37-39). Accordingly, while allelic loss of VHL has not been detected in intestinal early adenomas, 64% of carcinomas have been reported to harbor VHL deletions, indicating a role for VHL loss in later stages of tumor progression (40). Another recent study sequenced *VHL* in 88 paraffin-embedded CRC specimens and found 10 (11%) point mutations (41). A relationship between HIF levels, *VEGF* expression, tumor invasion, liver metastasis and microvessel density was recently demonstrated in colorectal cancer patients (36). Almost 60% of archived colorectal cancer samples expressed HIF1 α protein at a high level. These findings support the notion that HIF1 α may play a role in angiogenesis and tumor progression via regulation of VEGF in human colorectal carcinoma. Another study reported nuclear HIF1 α overexpression in 22/22 colon adenocarcinomas examined (42). Lastly, HIF1 α overexpression has been implicated in colon carcinoma cell invasion (43).

It has been previously shown that β -catenin

signaling resulted in an upregulation of *VEGF-A* mRNA and protein levels by 250-300% (44). The authors postulated that the upregulation of VEGF was mediated by a direct binding of TCF/ β -catenin to consensus binding sites within the gene promoter of VEGF. However, our data support the role of HIF1 α in VEGF regulation in CRC cells reported by Semenza and colleagues (45). These two mechanisms of VEGF regulation are not mutually exclusive; our data simply suggest that an alternative pathway exists where Wnt signaling can induce VEGF and angiogenesis through VHL/HIF regulation.

It is tempting to speculate that downregulation of VHL expression might be prevalent in other cancer types exhibiting illegitimate Wnt signaling. For example, selective loss of *VHL* has been described in thyroid tumors (46), where Wnt signaling is thought to play a critical role (47). It would also be interesting to examine *VHL* in other tumors commonly associated with activating mutations of the Wnt pathway, including breast, pancreatic, and liver tumors (1). Interestingly, these tumor types have already been significantly associated with HIF1 α overexpression (42). Lastly, our data demonstrate a role for Wnt signaling in *VHL* regulation; manipulation of this pathway might be instrumental in the future design of therapeutic interventions for tumors associated with loss of *VHL*.

A



B

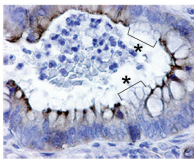


Figure 3: Clonal loss of VHL in early adenomas

(A) Immunohistochemistry of VHL (left) and HIF1 α (right) demonstrate complementary staining in early adenoma. (B) Single crypt from spontaneous adenoma reveals localized loss of VHL staining (marked with *), suggestive of clonal expansion.

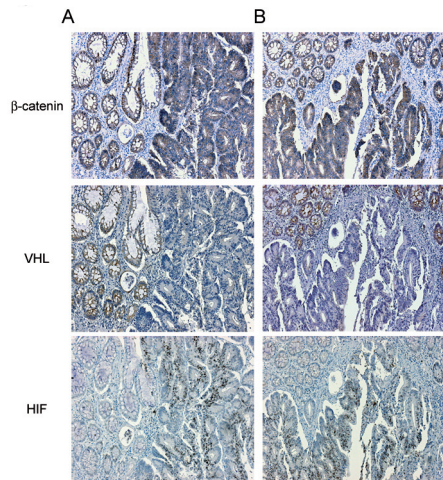


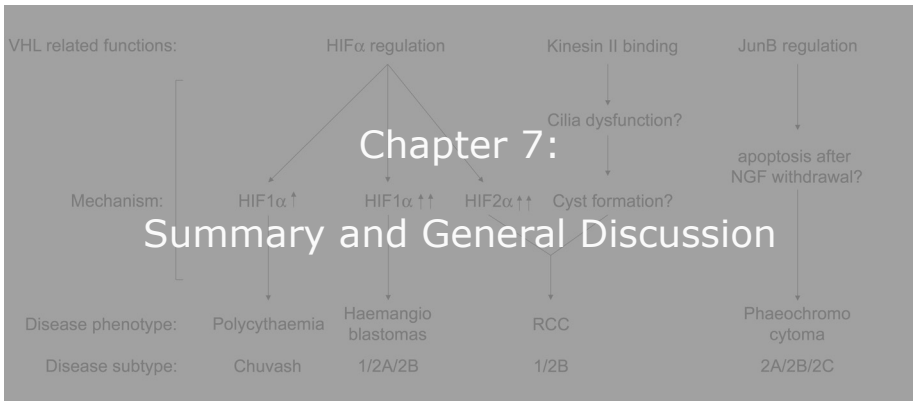
Figure 4. Advanced colorectal carcinomas uncouple VHL regulation from Wnt signaling.

(A and B) Sequential sections of two representative carcinomas (A and B, respectively) stained for β -catenin (upper panels), VHL (middle panels) and HIF1 α (lower panels). Whereas β -catenin nuclear and cytoplasmic staining increases in the carcinoma tissue, VHL stains only the adjacent normal tissue, whereas nuclear HIF1 α stains in a purely complementary fashion to VHL.

References

- Giles, R. H., van Es, J. H., and Clevers, H. (2003) *Biochim Biophys Acta* 1653(1), 1-24
- Folkman, J., Watson, K., Ingber, D., and Hahnen, D. (1989) *Nature* 339(6219), 58-61
- Aotake, T., Lu, C. D., Chiba, Y., Muraoka, R., and Tanigawa, N. (1999) *Clin Cancer Res* 5(1), 135-142
- Dannenberg, A. J., and Subbaramaiah, K. (2003) *Cancer Cell* 4(6), 431-436
- Mayer, R. J. (2004) *N Engl J Med* 350(23), 2406-2408
- Maynard, M. A., and Ohh, M. (2004) *Am J Nephrol* 24(1), 1-13
- Cockman, M. E., Masson, N., Mole, D. R., Jaakkola, P., Chang, G. W., Clifford, S. C., Maher, E. R., Pugh, C. W., Ratcliffe, P. J., and Maxwell, P. H. (2000) *J Biol Chem* 275(33), 25733-25741
- Kamura, T., Koepp, D. M., Conrad, M. N., Skowyra, D., Moreland, R. J., Iliopoulos, O., Lane, W. S., Kaelin, W. G., Jr., Elledge, S. J., Conaway, R. C., Harper, J. W., and Conaway, J. W. (1999) *Science* 284(5414), 657-661
- Ohh, M., Park, C. W., Ivan, M., Hoffman, M. A., Kim, T. Y., Huang, L. E., Pavletich, N., Chau, V., and Kaelin, W. G. (2000) *Nat Cell Biol* 2(7), 423-427
- Ivan, M., Kondo, K., Yang, H., Kim, W., Valianido, J., Ohh, M., Salic, A., Asara, J. M., Lane, W. S., and Kaelin, W. G., Jr. (2001) *Science* 292(5516), 464-468

11. Jaakkola, P., Mole, D. R., Tian, Y. M., Wilson, M. I., Gielbert, J., Gaskell, S. J., Kriegsheim, A., Hebestreit, H. F., Mukherji, M., Schofield, C. J., Maxwell, P. H., Pugh, C. W., and Ratcliffe, P. J. (2001) *Science* 292(5516), 468-472
12. Epstein, A. C., Gleadle, J. M., McNeill, L. A., Hewitson, K. S., O'Rourke, J., Mole, D. R., Mukherji, M., Metzzen, E., Wilson, M. I., Dhanda, A., Tian, Y. M., Masson, N., Hamilton, D. L., Jaakkola, P., Barstead, R., Hodgkin, J., Maxwell, P. H., Pugh, C. W., Schofield, C. J., and Ratcliffe, P. J. (2001) *Cell* 107(1), 43-54
13. Wizigmann-Voos, S., Breier, G., Risau, W., and Plate, K. H. (1995) *Cancer Res* 55(6), 1358-1364
14. Los, M., Aarsman, C. J., Terpstra, L., Wittebol-Post, D., Lips, C. J., Blijham, G. H., and Voest, E. E. (1997) *Ann Oncol* 8(10), 1015-1022
15. Los, M., Jansen, G. H., Kaelin, W. G., Lips, C. J., Blijham, G. H., and Voest, E. E. (1996) *Lab Invest* 75(2), 231-238
16. van de Wetering, M., Sancho, E., Verweij, C., de Lau, W., Oving, I., Hurlstone, A., van der Horn, K., Battle, E., Coudreuse, D., Haramis, A. P., Tjon-Pon-Fong, M., Moerer, P., van den Born, M., Soete, G., Pals, S., Eilers, M., Medema, R., and Clevers, H. (2002) *Cell* 111(2), 241-250
17. Shibamoto, S., Higano, K., Takada, R., Ito, F., Takeichi, M., and Takada, S. (1998) *Genes Cells* 3(10), 659-670
18. Wang, G. L., and Semenza, G. L. (1993) *J Biol Chem* 268(29), 21513-21518
19. Luckow, B., and Schutz, G. (1987) *Nucleic Acids Res* 15(13), 5490
20. Korinek, V., Barker, N., Morin, P. J., van Wichen, D., de Weger, R., Kinzler, K. W., Vogelstein, B., and Clevers, H. (1997) *Science* 275(5307), 1784-1787
21. van Noort, M., Meeldijk, J., van der Zee, R., Destree, O., and Clevers, H. (2002) *J Biol Chem* 277(20), 17901-17905
22. Bos, R., Zhong, H., Hanrahan, C. F., Mommers, E. C., Semenza, G. L., Pinedo, H. M., Abeloff, M. D., Simons, J. W., van Diest, P. J., and van der Wall, E. (2001) *J Natl Cancer Inst* 93(4), 309-314
23. Battle, E., Henderson, J. T., Beghtel, H., van den Born, M. M., Sancho, E., Huls, G., Meeldijk, J., Robertson, J., van de Wetering, M., Pawson, T., and Clevers, H. (2002) *Cell* 111(2), 251-263
24. Bluysen, H. A., Lolkema, M. P., van Beest, M., Boone, M., Snijckers, C. M., Los, M., Gebbink, M. F., Braam, B., Holstege, F. C., Giles, R. H., and Voest, E. E. (2004) *FEBS Lett* 556(1-3), 137-142
25. Zhong, H., and Simons, J. W. (1999) *Biochem Biophys Res Commun* 259(3), 523-526
26. Stambolic, V., Ruel, L., and Woodgett, J. R. (1996) *Curr Biol* 6(12), 1664-1668
27. Staal, F. J., Noort Mv, M., Strous, G. J., and Clevers, H. C. (2002) *EMBO Rep* 3(1), 63-68
28. Korinek, V., Barker, N., Moerer, P., van Donselaar, E., Huls, G., Peters, P. J., and Clevers, H. (1998) *Nat Genet* 19(4), 379-383
29. Fodde, R., Smits, R., and Clevers, H. (2001) *Nat Rev Cancer* 1(1), 55-67
30. Vleugel, M. M., Greijer, A. E., Shvarts, A., van der Groep, P., van Berkel, M., Aarbodem, Y., van Tinteren, H., Harris, A. L., van Diest, P. J., and van der Wall, E. (2005) *J Clin Pathol* 58(2), 172-177
31. Willert, J., Epping, M., Pollack, J. R., Brown, P. O., and Nusse, R. (2002) *BMC Dev Biol* 2(1), 8
32. Oosterwegel, M. A., van de Wetering, M. L., Holstege, F. C., Prosser, H. M., Owen, M. J., and Clevers, H. C. (1991) *Int Immunol* 3(11), 1189-1192
33. Karhausen, J., Furuta, G. T., Tomaszewski, J. E., Johnson, R. S., Colgan, S. P., and Haase, V. H. (2004) *J Clin Invest* 114(8), 1098-1106
34. Furuta, G. T., Turner, J. R., Taylor, C. T., Hershberg, R. M., Comerford, K., Narravula, S., Podolsky, D. K., and Colgan, S. P. (2001) *J Exp Med* 193(9), 1027-1034
35. Carmeliet, P., Dor, Y., Herbert, J. M., Fukumura, D., Brusselmans, K., Dewerchin, M., Neeman, M., Bono, F., Abramovitch, R., Maxwell, P., Koch, C. J., Ratcliffe, P., Moons, L., Jain, R. K., Collen, D., Keshert, E., and Keshet, E. (1998) *Nature* 394(6692), 485-490.
36. Kuwai, T., Kitadai, Y., Tanaka, S., Onogawa, S., Matsutani, N., Kaio, E., Ito, M., and Chayama, K. (2003) *Int J Cancer* 105(2), 176-181
37. Goel, A., Arnold, C. N., Niedzwiecki, D., Chang, D. K., Ricciardiello, L., Carethers, J. M., Dowell, J. M., Wasserman, L., Compton, C., Mayer, R. J., Bertagnolli, M. M., and Boland, C. R. (2003) *Cancer Res* 63(7), 1608-1614
38. Fujii, H., Ajioka, Y., Kazami, S., Takagaki, T., Gong Zhu, X., Hirose, S., Watanabe, H., and Shirai, T. (2002) *J Pathol* 197(3), 298-306
39. Iniesta, P., Massa, M. J., Gonzalez-Quevedo, R., de Juan, C., Moran, A., Sanchez-Pernaute, A., Cerdan, J., Torres, A., Balibrea, J. L., and Benito, M. (2000) *Cancer* 89(6), 1220-1227
40. Zhuang, Z., Emmert-Buck, M. R., Roth, M. J., Gnarr, J., Linehan, W. M., Liotta, L. A., and Lubensky, I. A. (1996) *Hum Pathol* 27(2), 152-156
41. Kuwai, T., Kitadai, Y., Tanaka, S., Hiyama, T., Tanimoto, K., and Chayama, K. (2004) *Cancer Sci* 95(2), 149-153
42. Zhong, H., De Marzo, A. M., Laughner, E., Lim, M., Hilton, D. A., Zagzag, D., Buechler, P., Isaacs, W. B., Semenza, G. L., and Simons, J. W. (1999) *Cancer Res* 59(22), 5830-5835
43. Krishnamachary, B., Berg-Dixon, S., Kelly, B., Agani, F., Feldser, D., Ferreira, G., Iyer, N., LaRusch, J., Pak, B., Taghavi, P., and Semenza, G. L. (2003) *Cancer Res* 63(5), 1138-1143
44. Easwaran, V., Lee, S. H., Inge, L., Guo, L., Goldbeck, C., Garrett, E., Wiesmann, M., Garcia, P. D., Fuller, J. H., Chan, V., Randazzo, F., Gundel, R., Warren, R. S., Escobedo, J., Aukerman, S. L., Taylor, R. N., and Fantl, W. J. (2003) *Cancer Res* 63(12), 3145-3153
45. Fukuda, R., Kelly, B., and Semenza, G. L. (2003) *Cancer Res* 63(9), 2330-2334
46. Hinze, R., Boltze, C., Meyer, A., Holzhausen, H. J., Dralle, H., and Rath, F. W. (2000) *Endocr Pathol* 11(2), 145-155
47. Garcia-Rostan, G., Camp, R. L., Herrero, A., Carcangiu, M. L., Rimm, D. L., and Tallini, G. (2001) *Am J Pathol* 158(3), 987-996



Summary and General Discussion

Lolkema MP

Understanding the function of tumor suppressor genes is an important way to understand how tumors arise from normal tissue. In this thesis we studied the effects of the von Hippel-Lindau tumor suppressor gene (VHL) involved in tumor suppression in the kidney. In the Introduction we argue that there is a function for VHL, which is as yet unknown. HIF regulation is a well established function ascribed to VHL (1-3) however there are at least two very compelling arguments for an additional function for VHL. The first argument is that there are two different isoforms of the VHL protein: p30 and p19, in which p19 lacks the N-terminal acidic domain (4,5). This acidic domain is not necessary for HIF regulation as p19 is fully capable of adequately regulating HIF levels but does contain tumorigenic mutations, implying a functional significance for this domain (6). Furthermore, von Hippel-Lindau disease patients can be classified into different subtypes of disease according to the genetic mutations that are found. Four different subtypes of disease can be classified with different risk for developing the different tumors associated with the VHL syndrome, in which the type 2C mutations are normally able to regulate HIF levels in vitro (7-9). A single function for VHL would not suffice to explain this complex genotype-phenotype correlation.

The data represented in this thesis describe aspects of the biology of the VHL protein and suggest the presence of an alternative function for VHL in addition to the regulation of HIF levels. The concept of HIF-independent functions for VHL has been widely recognized and is represented in the international literature in a wide variety of publications; however the mechanism behind this function remains unknown (1,10-13). The approach of using differential expression profiling with microarray technology has been used in different set-ups and has shown in multiple experiments to reproduce VHL-regulated genes, which seem to be independent of HIF regulation (14-19). The data presented in the second chapter contributes to this knowledge and addresses another well known VHL phenomenon, namely altered fibronectin matrix formation. Ohh et al. described the

binding of VHL to fibronectin and suggested that this binding is essential in the formation of a correct extracellular matrix (13). This binding of VHL to fibronectin seems to be disrupted in all tumorigenic mutants of VHL that have been tested thus far, in contrast to the HIF regulatory function of VHL which has been shown to be intact in the type 2C mutants of VHL (8). The expression of fibronectin however is also regulated by VHL; thereby strengthening the notion that fibronectin might be a major contributor to the tumor suppressor function of VHL. In a *C. elegans* genetic system, cross-breeding HIF-deficient worms with VHL-deficient worms revealed differential regulation of extracellular matrix genes by VHL that were independent of HIF function (12). These studies flesh out the above in vitro studies, confirming in vivo the transcriptional regulation of the extracellular matrix as an important –and HIF-independent–VHL function.

The third, fourth and fifth chapters address what the molecular mechanism of the VHL-mediated HIF-independent function could be. As discussed in the first chapter our “prime suspect” to determine the HIF-independent function for VHL lies within the N-terminal acidic domain, which has not previously been assigned a function. We show that the acidic domain of VHL can be phosphorylated and that this modification is essential for tumor suppression in vivo. The acidic domain is also involved in binding the kinesin-2 complex and this interaction between the kinesin-2 complex and VHL plays a role in promoting microtubule stability in the cell periphery. Furthermore, we show that the kinesin-2 complex and VHL cooperate in the formation of primary cilia. These data represent the first pieces of experimental evidence that the acidic domain has a function. The model that arises from the data presented in this thesis is that the acidic domain plays an important role in determining the HIF-independent role for VHL; however, the exact molecular mechanism needs to be elucidated.

The most important question that these data evoke is: how do the extracellular matrix formation, microtubule stability and ciliogenesis affect the formation of tumors?

From literature we know that the interaction of tumor cells with the extracellular matrix is an important regulator of various signal transduction events leading to more or less proliferation and migration (20), but could this be an explanation for the tumor suppressor effect of VHL? In the various *in vivo* models that have been studied, the major confounder to answering this question has been the presence of two variables: higher levels of HIF expression and the mutation of VHL. However, in studies performed by the groups of Kaelin and Klausner, 786-O human renal cell carcinomas were tested in nude mice that expressed both VHL and a form of HIF that is insensitive to the VHL mediated ubiquitination and subsequent degradation (21,22). These experiments show that HIF2 α can induce tumor formation in the presence of wild-type VHL in the background of the 786-O renal cell carcinoma cell line. The reciprocal experiments where HIF2 α was knocked down using RNAi in the absence of VHL in the same 786-O cell line showed that tumorigenesis in this model is dependent upon the presence of HIF2 α (23,24). So in the background of the 786-O renal cell carcinoma cell line the HIF-mediated tumor growth in nude mice induced by HIF2 α is dominant over any other VHL-mediated effect. However, the *in vivo* experiments that were performed in chapter 4 of this thesis showed that a mutant of VHL, that could not be phosphorylated, allowed tumor formation after 8-10 weeks, a time point after the *in vivo* experiments in other reports were terminated (25). The question remains whether HIF stabilization alone could be responsible for the tumor formation in VHL-deficient cells under more physiologic circumstances. The conditional VHL knock out mice that were bred using the Cre-Lox system could have answered this question but these mice do not develop tumors in the kidney (26). Therefore the role for the VHL-dependent extracellular matrix deposition and the interaction of the tumor cell with its environment *in vivo* cannot be adequately judged from existing data.

The oncogenic potential of HIF-mediated transcription would be another way to show that VHL-dependent carcinogenesis depends on its function in regulating HIF levels. A role for HIF as an oncogene has not been detected in human tumors. Whereas the mutations in well defined oncogenes such as RAS have been detected in a large set of tumors,

for HIF the mutational status has not shown activating mutations in human tumors. However, polymorphisms of HIF detected in renal cell carcinomas, head and neck cancer and prostate cancer may result in more active forms of HIF. These alleles are normally present in the general population and seem to increase the risk of developing these tumors (27,28). This is a completely different pattern of mutation compared to the classical oncogenes that undergo selection for mutations in the tumor that are not germline. Recent analysis of HIF expression in breast cancer has shown that the global expression of HIF inside tumors is associated with less aggressive behavior compared to expression in perinecrotic tumor tissue (29). Therefore, HIF activation alone does not correlate with aggressive tumor behavior; its expression pattern also influences the biological behavior of tumor cells. Experimental models such as transgenic mice bearing activated HIF genes have not been reported to date. The selective inactivation of HIF has been reported in different models and contradicting evidence has been shown using these approaches. Whereas one HIF knock out ES cell line has been shown to enhance teratoma growth, another with a somewhat different knock out allele was shown to be deficient in forming teratomas (30,31). However these models do not address the proper question of HIF-dependent tumorigenesis as the teratoma model is too sensitive for developmental deficiencies. Teratomas may be deficient in their growth simply because of the fact that they are incapable of differentiating into tumors (e.g. APC-deficient teratomas) and could explain the smaller teratomas that developed from VHL deficient ES cells (32,33). So with the current evidence there is no indication that HIF functions as an independent oncogene in humans.

The existence of a HIF-independent function for VHL is a plausible yet not fully proven and elucidated phenomenon. Recent data showed that JunB is up regulated in the presence of VHL and this seems to be independent of HIF as type 2C mutants that are capable of regulating HIF levels show defective JunB regulation (34). This is another link to a molecular mechanism of understanding how VHL influences the cellular behavior besides regulating HIF levels. JunB is known to play a role in promoting cell cycle arrest and apoptosis (35). These

features are mostly due to the antagonistic effect on c-Jun, which is a known oncogene. Could this be the link to the HIF-independent tumor suppressor effect of VHL? The authors of this recent paper suggest that in the development of pheochromocytoma the apoptosis after NGF withdrawal is the general mechanism behind the development of pheochromocytoma in all hereditary pheochromocytoma syndromes (34). These arguments are compelling for the development of pheochromocytoma but the development of these tumors probably has a different etiology within VHL disease. Type 2C mutations, only predisposing for the development of pheochromocytoma, could be seen as a different disease when compared to the other subtypes. The data acquired in this thesis suggests that the HIF-independent function of VHL we describe might have a role in the development of renal cell carcinoma, as the type 2A and type 2B mutations seem to be differentially affected. The cell biological behavior of cells that lack VHL seems to be characterized by the inability to communicate with the exterior of the cell. Defective extracellular matrix deposition in the form of deficiency in producing and depositing fibronectin and the defects in forming fibrillar adhesion increases the mobility of VHL defective cells (13,36,37). These changes will ultimately lead to less attachment to the basal membrane of kidney tubular cells creating a niche for autonomous development. Defective microtubule stability at the cell membrane will disturb the ability of epithelial cells to polarize properly as stable vertical microtubule arrays seem to be essential in directing the polarized distribution of cell surface molecules (38). Finally, defective cilia formation leads to a decreased ability of these cells to understand the stimuli from outside the cell (39). Clues like flow on the surface of the cell will no longer lead to the appropriate signals as could be seen in our experiments looking at flow-induced Ca^{2+} responses. I would like to propose a model in which VHL functions as a master-switch for cells to behave in a "social" fashion. Loss of function of VHL leads to cells incapable of communicating and simultaneously activates a strong survival program with the activation of HIF-dependent transcription. The interaction of VHL with the kinesin-2 motor protein seems to play a central role

in the mechanism behind this behavior of VHL deficient cells. The kinesin-2 motor protein complex has been shown to play an important role in the establishing proper polarization in neuronal cells and kidney epithelial cells (40,41). Illustrative of the function of kinesin-2 motor complex to target molecules to the cell-cell interaction is the effect of targeted deficiency of Kif3a in the kidneys of mice. In these kidneys not only the presence of cysts but also the mislocalization of beta-catenin was shown. The mice with targeted inactivation of Kif3a in the kidney did not develop tumors but cysts (41). It is tempting to speculate on an additive effect of both deregulation of kinesin 2 function and HIF activation in the pathogenesis of renal cell carcinoma with cysts as pre-malignant lesions and therefore the interaction between VHL and the kinesin-2 complex deserves more attention in future research. Especially the functional correlation between VHL-kinesin-2 binding and phosphorylation and the link between kinesin-2 and fibronectin deposition are essential in determining whether indeed the interaction between VHL and kinesin-2 is central in the HIF-independent function for VHL.

The second central question in this thesis and in the research field of VHL is the functional significance of the genotype-phenotype correlation. As discussed in the introduction, VHL disease predisposes to different tumors and the distribution of specific tumor development correlates with specific mutations. The first division is between type 1 and type 2 VHL disease in which patients with type 2 mutations and not type 1 mutations predispose to developing pheochromocytomas. This first and most important division defines pheochromocytoma as a separate entity within VHL disease and therefore one could assume that there should also be a functional dissection between type 1 and type 2 VHL disease. The second argument for distinguishing pheochromocytoma as a functional separate entity is the existence of the type 2C disease in which mutations of *VHL* are included that uniquely predispose for pheochromocytoma. Important for this argument is the existence of different unrelated point mutations in different codons for different amino acid substitutions that lead to type 2C disease. This means that independent mutational events can lead

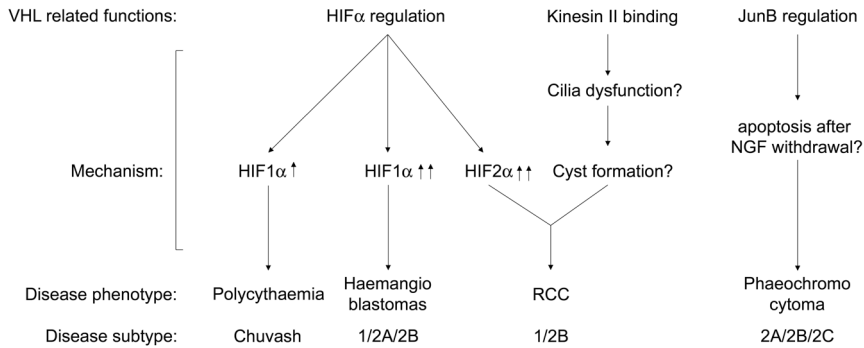


Figure 1: Schematic overview of the VHL related functions.

This figure represents an hypothetical model for the VHL related functions published until now and reported in this thesis. We propose a trichotomy in the VHL related functions as depicted in the upper pane. Through different mechanisms these function cause disease phenotypes as can be observed in patients suffering from mutations in the VHL gene and their corresponding clinical subtype of VHL disease.

to the disruption of a function of *VHL* in preventing development of pheochromocytoma. Moreover, the type 1 mutations comprise most of the large deletions of the VHL most likely to completely inactivate all VHL functionality. Therefore inactivation of all VHL functionality leads to hemangioblastomas and RCC but does not lead to pheochromocytoma development. This could be interpreted as an argument for residual VHL function in the development of pheochromocytoma or a gain-of-function effect of the mutated type 2C VHL allele. So pheochromocytomas are definitely a distinct entity within the clinical presentation of VHL disease.

The second manifestation that could be considered to be a distinct entity within the VHL disease is ccRCC. Type 2A disease patients have a much lower chance of developing ccRCC without losing the chance of developing hemangioblastomas and pheochromocytomas. These patients are distinct from the patients that develop type 2B disease, which are susceptible to all known VHL disease associated manifestations. So now should we consider type 2A mutations a different entity and ccRCC associated with yet another VHL function? Notably, type 2A mutations are extremely rare. The true nature of the type 2A disease phenotype remains puzzling in light of the abundance of known mutations in the VHL gene and the low frequency of this particular type of disease. However, two recent lines of research do assign unique functions to the type 2A mutant alleles: type 2A alleles seem to be deficient in the microtubule

stabilizing function of VHL and the type 2A mutants retain the ability to stabilize JADE-1, a putative tumor suppressor gene in the kidney (43-45). A way of reconciling the available data would be that the loss-of-heterozygosity (LOH) targeting the normal allele would lead to a remaining mutated allele with residual microtubule stabilizing function as would be the case with type 2B mutants, leading to a supposed survival benefit. If the remaining mutated allele lacks all microtubule stabilizing capacity as is the case with type 2A mutants, the hypothesis would be that it does not confer survival benefit in the kidney. This argument functionally separates renal cancer from the hemangioblastomas in the CNS and eyes. I believe that the data we and others have acquired favor a model of three separate VHL-mediated functions: HIF regulation with hemangioblastomas as clinical manifestation, impairing pheochromocytoma development and a function which, in conjunction with HIF activation, leads to the development of ccRCC (Fig. 1). These arguments lead to the proposed model of ccRCC development in VHL disease: the inactivation of VHL due to LOH in the kidney leads to the development of atypical cysts due to the relative insufficiency in sensing and adapting to extracellular signals. This phenomenon could be attributed to deficient cilia formation. These atypical cysts in early stages upregulate HIF levels (personal communication Dr. P. Maxwell). These lesions remain silent or grow very slowly as HIF expression per se does not induce an "oncogenic program" but more likely induces

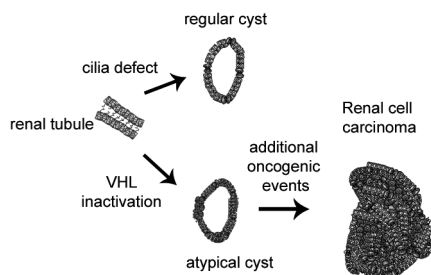


Figure 2: Model for VHL mediated tumorigenesis in the kidney.

This model implies that tumorigenesis in the kidney is a multi-step chain of events in which atypical cyst formation is essential. These atypical cysts arise with the loss-of-function of VHL and differ from regular cysts because they lose cilia function and activate illegitimate HIF function. Additional oncogenic events will give rise to full blown renal cell carcinoma.

a “survival program”. From the moment that these independent cell populations emerge, they will acquire additional mutational events but these will take some time to develop as these lesions have the tendency to grow slowly (Fig. 2). This model could explain a number of observations in patients with VHL disease: the relatively benign nature of the kidney lesions, the “pre-malignant” nature of cysts in VHL disease and the successful local resection of lesions with >3cm (42). Furthermore it explains the relative benign nature of cRCC with *VHL* mutations and the relative large size of the tumors when they are detected in the general population (46).

The sixth chapter deals with a somewhat different aspect of VHL biology being the regulation of *VHL* expression and its role in the physiology of the intestine. We found that the expression of *VHL* was regulated by active wnt-signaling and displays the expression pattern of a typical wnt-signaling target in the intestinal mucosa. Interestingly there was reciprocal expression of HIF under normoxic conditions, which might represent the regulatory mechanism for HIF-mediated enhancement of barrier function in the intestinal villi (47) and the increase in oxygenation through stimulation of angiogenesis. These data show for the first time that regulation of expression of *VHL* has functional consequences and can lead to normoxic activation of HIF.

In colorectal tumor progression, a clear cut-

off point between non-invasive and invasive tumors could be seen with the loss of *VHL*. This suggests that loss of *VHL* could represent the molecular mechanism for the angiogenic switch in normal colonic tissue and colorectal cancer. Whereas the rest of this thesis has dealt with the functionality of the VHL tumor suppressor gene in the manifestations of patients with VHL disease, this chapter shows the relevance for dissecting the functions of VHL. Its role in regulating HIF, the best described and understood function now leads to a better understanding of tumor progression of colorectal cancer. With the novel anti-VEGF strategies that have shown benefit in trials for metastasized colorectal cancer we now show broad significance for VHL expression in tumors. Fully understanding the HIF-independent functions for VHL could also lead to improvement in our thinking about tumorigenesis and lead to better therapies for patients with cancer in the future.

Concluding remarks:

The experimental work in this thesis has generated a number of new insights into the biology of VHL. The role for HIF-independent functions might not have been elucidated fully, I believe its existence has been made probable. The unmasking of the molecular mechanism of this HIF-independent function has been made extremely difficult by evolution through the unconditional coupling of the HIF regulatory pathway to the other VHL functions. However, the genetic evidence for multiple functions for the *VHL* gene product lies within the genotype-phenotype correlations of VHL patients. Future research into this new area of tumor suppressor function will reveal the full functional consequence of VHL loss.

Reference List:

1. Kaelin, W. G., Jr. (2004) Clin Cancer Res 10(18 Pt 2), 6290S-6295S
2. Maynard, M. A., and Ohh, M. (2004) Am J Nephrol 24(1), 1-13
3. Maxwell, P. H., Pugh, C. W., and Ratcliffe, P. J. (2001) Adv Exp Med Biol 502, 365-376
4. Iliopoulos, O., Ohh, M., and Kaelin, W. G., Jr. (1998) Proc Natl Acad Sci U S A 95(20), 11661-11666
5. Schoenfeld, A., Davidowitz, E. J., and Burk, R. D. (1998) Proc Natl Acad Sci U S A 95(15), 8817-8822
6. Giles, R. H., Lolkema, M. P., and Voest, E. E. (2005) submitted

7. Clifford, S. C., Cockman, M. E., Smallwood, A. C., Mole, D. R., Woodward, E. R., Maxwell, P. H., Ratcliffe, P. J., and Maher, E. R. (2001) *Hum Mol Genet* 10(10), 1029-1038
8. Hoffman, M. A., Ohh, M., Yang, H., Klco, J. M., Ivan, M., and Kaelin, W. G., Jr. (2001) *Hum Mol Genet* 10(10), 1019-1027
9. Neumann, H. P., and Bender, B. U. (1998) *J Intern Med* 243(6), 541-545
10. Czyzyk-Krzeska, M. F., and Meller, J. (2004) *Trends Mol Med* 10(4), 146-149
11. Rathmell, W. K., Hickey, M. M., Bezman, N. A., Chmielecki, C. A., Carraway, N. C., and Simon, M. C. (2004) *Cancer Res* 64(23), 8595-8603
12. Bishop, T., Lau, K. W., Epstein, A. C., Kim, S. K., Jiang, M., O'Rourke, D., Pugh, C. W., Gleadle, J. M., Taylor, M. S., Hodgkin, J., and Ratcliffe, P. J. (2002) *PLoS Biol* 2(10), e289
13. Ohh, M., Yauch, R. L., Lonergan, K. M., Whaley, J. M., Stemmer-Rachamimov, A. O., Louis, D. N., Gavin, B. J., Kley, N., Kaelin, W. G., Jr., and Iliopoulos, O. (1998) *Mol Cell* 1(7), 959-968
14. Ivanov, S. V., Kuzmin, I., Wei, M. H., Pack, S., Gell, L., Johnson, B. E., Stanbridge, E. J., and Lerman, M. I. (1998) *Proc Natl Acad Sci U S A* 95(21), 12596-12601
15. Wykoff, C. C., Pugh, C. W., Maxwell, P. H., Harris, A. L., and Ratcliffe, P. J. (2000) *Oncogene* 19(54), 6297-6305
16. Ivanov, S., Liao, S. Y., Ivanova, A., Danilkovitch-Miagkova, A., Tarasova, N., Weirich, G., Merrill, M. J., Proescholdt, M. A., Oldfield, E. H., Lee, J., Zavada, J., Waheed, A., Sly, W., Lerman, M. I., and Stanbridge, E. J. (2001) *Am J Pathol* 158(3), 905-919
17. Karumanchi, S. A., Jiang, L., Knebelmann, B., Stuart-Tilley, A. K., Alper, S. L., and Sukhatme, V. P. (2001) *Physiol Genomics* 5(3), 119-128
18. Zatyka, M., da Silva, N. F., Clifford, S. C., Morris, M. R., Wiesener, M. S., Eckardt, K. U., Houlston, R. S., Richards, F. M., Latif, F., and Maher, E. R. (2002) *Cancer Res* 62(13), 3803-3811
19. Jiang, Y., Zhang, W., Kondo, K., Klco, J. M., St Martin, T. B., Dufault, M. R., Madden, S. L., Kaelin, W. G., Jr., and Nacht, M. (2003) *Mol Cancer Res* 1(6), 453-462
20. Danen, E. H., and Yamada, K. M. (2001) *J Cell Physiol* 189(1), 1-13
21. Kondo, K., Klco, J., Nakamura, E., Lechpammer, M., and Kaelin, W. G., Jr. (2002) *Cancer Cell* 1(3), 237-246
22. Maranchie, J. K., Vasselli, J. R., Riss, J., Bonifacio, J. S., Linehan, W. M., and Klausner, R. D. (2002) *Cancer Cell* 1(3), 247-255
23. Kondo, K., Kim, W. Y., Lechpammer, M., and Kaelin, W. G., Jr. (2003) *PLoS Biol* 1(3), E83
24. Zimmer, M., Doucette, D., Siddiqui, N., and Iliopoulos, O. (2004) *Mol Cancer Res* 2(2), 89-95
25. Lolkema, M. P., Gervais, M. L., Sniijckers, C. M., Hill, R. P., Giles, R. H., Voest, E. E., and Ohh, M. (2005) *J Biol Chem* 280(23), 22205-22211
26. Haase, V. H. (2005) *Semin Cell Dev Biol* 16(4-5), 564-574
27. Ollerenshaw, M., Page, T., Hammonds, J., and Demaine, A. (2004) *Cancer Genet Cytogenet* 153(2), 122-126
28. Fu, X. S., Choi, E., Buble, G. J., and Balk, S. P. (2005) *Prostate* 63(3), 215-221
29. Vleugel, M. M., Greijer, A. E., Shvarts, A., van der Groep, P., van Berkel, M., Aarbodem, Y., van Tinteren, H., Harris, A. L., van Diest, P. J., and van der Wall, E. (2005) *J Clin Pathol* 58(2), 172-177
30. Ryan, H. E., Lo, J., and Johnson, R. S. (1998) *Embo J* 17(11), 3005-3015
31. Carmeliet, P., Dor, Y., Herbert, J. M., Fukumura, D., Brusselmans, K., Dewerchin, M., Neeman, M., Bono, F., Abramovitch, R., Maxwell, P., Koch, C. J., Ratcliffe, P., Moons, L., Jain, R. K., Collen, D., and Keshert, E. (1998) *Nature* 394(6692), 485-490
32. Kielman, M. F., Rindapaa, M., Gaspar, C., van Poppel, N., Breukel, C., van Leeuwen, S., Taketo, M. M., Roberts, S., Smits, R., and Fodde, R. (2002) *Nat Genet* 32(4), 594-605
33. Mack, F. A., Rathmell, W. K., Arsham, A. M., Gnarra, J., Keith, B., and Simon, M. C. (2003) *Cancer Cell* 3(1), 75-88
34. Lee, S., Nakamura, E., Yang, H., Wei, W., Linggi, M. S., Sajan, M. P., Farese, R. V., Freeman, R. S., Carter, B. D., Kaelin, W. G., Jr., and Schlisio, S. (2005) *Cancer Cell* 8(2), 155-167
35. Shaulian, E., and Karin, M. (2002) *Nat Cell Biol* 4(5), E131-136
36. Kamada, M., Suzuki, K., Kato, Y., Okuda, H., and Shuin, T. (2001) *Cancer Res* 61(10), 4184-4189
37. Esteban-Barragan, M. A., Avila, P., Alvarez-Tejedo, M., Gutierrez, M. D., Garcia-Pardo, A., Sanchez-Madrid, F., and Landazuri, M. O. (2002) *Cancer Res* 62(10), 2929-2936
38. Musch, A. (2004) *Traffic* 5(1), 1-9
39. Pan, J., Wang, Q., and Snell, W. J. (2005) *Lab Invest* 85(4), 452-463
40. Nishimura, T., Kato, K., Yamaguchi, T., Fukata, Y., Ohno, S., and Kaibuchi, K. (2004) *Nat Cell Biol* 6(4), 328-334
41. Lin, F., Hiesberger, T., Cordes, K., Sinclair, A. M., Goldstein, L. S., Somlo, S., and Igarashi, P. (2003) *Proc Natl Acad Sci U S A* 100(9), 5286-5291
42. Duffey, B. G., Choyke, P. L., Glenn, G., Grubb, R. L., Venzon, D., Linehan, W. M., and Walther, M. M. (2004) *J Urol* 172(1), 63-65
43. Zhou, M. I., Foy, R. L., Chitalia, V. C., Zhao, J., Panchenko, M. V., Wang, H., and Cohen, H. T. (2005) *Proc Natl Acad Sci U S A* 102(31), 11035-11040
44. Zhou, M. I., Wang, H., Foy, R. L., Ross, J. J., and Cohen, H. T. (2004) *Cancer Res* 64(4), 1278-1286
45. Zhou, M. I., Wang, H., Ross, J. J., Kuzmin, I., Xu, C., and Cohen, H. T. (2002) *J Biol Chem* 277(42), 39887-39898
46. Yao, M., Yoshida, M., Kishida, T., Nakaigawa, N., Baba, M., Kobayashi, K., Miura, T., Moriyama, M., Nagashima, Y., Nakatani, Y., Kubota, Y., and Kondo, K. (2002) *J Natl Cancer Inst* 94(20), 1569-1575
47. Furuta, G. T., Turner, J. R., Taylor, C. T., Hershberg, R. M., Comerford, K., Narravula, S., Podolsky, D. K., and Colgan, S. P. (2001) *J Exp Med* 193(9), 1027-1034

Nederlandse Samenvatting

Nederlandse Samenvatting

Introductie

Dit proefschrift behandelt de vraag hoe de uitschakeling van het von Hippel-Lindau tumor suppressor gen (VHL) kan leiden tot het ontstaan van tumoren. De erfelijke ziekte waarbij dit gen betrokken is, is ontdekt in het begin van de 20ste eeuw door Dr. Eugen von Hippel en later ook beschreven door Dr. Arven Lindau. Men was opgevallen dat in een aantal patiënten tumoren voorkomen in de ogen, het centraal zenuwstelsel en de nieren. De patiënten met deze tumoren bleken allen familie van elkaar te zijn. Deze observatie suggereerde dat het ontstaan van deze tumoren een erfelijke of familiale oorzaak heeft. Deze tumoren bestonden voor een groot deel uit zeer vaatrijke structuren. In de loop van de 20ste eeuw is deze ziekte verder beschreven en de uitingen die ermee geassocieerd zijn, zijn:

- haemangiomen van de retina (bloedvatwoekering in het netvlies)
- haemangiomen van het centraal zenuwstelsel met name in het cerebellum (kleine hersenen) en het ruggemerg
- Grawitz tumoren van de nier (niercel tumoren)
- Pheochromocytoma (bijniertumoren die hormonen produceren)
- Zeldzamere tumoren: pancreastumoren, cystadenoma van de epididymus bij mannen, endolymphatische zak tumoren (bij de oren)

De VHL ziekte kenmerkt zich door het vroege ontstaan van de bovengenoemde aandoeningen op meerdere plaatsen en kan door de gevolgen ernstig invaliderend zijn. Met name vele chirurgische ingrepen in de hersenen en aan de nieren geven functie verlies van de aangedane organen, daarnaast is de dreigende blindheid als gevolg van de oogandoeningen een groot probleem.

Het VHL gen: een tumor suppressor gen

Het VHL gen is een speciaal soort gen wat betrokken is bij de ontwikkeling van tumoren. Een tumor kan ontstaan doordat een bepaald gen zijn functie meer of beter uitvoert, dit is dan een "onco-gen". Voorbeelden hiervan zijn genen die de cel aanzetten tot celdeling.

Hierbij is het vaak zo dat één gemuteerde kopie van dit gen dat "altijd" actief is, leidt tot ongebreidelde proliferatie. Daarmee kan dit het begin zijn van een tumor. VHL is echter een gen dat bij normale functie juist de ontwikkeling van tumoren onderdrukt. Dit zijn zogenaamde "tumor suppressor genen" waarvan wordt aangenomen dat voor de normale functie één goed functionerende kopie van zo'n gen voldoende is om tumoren te voorkomen. Echter, de inactivatie van een tumor suppressor gen leidt in het algemeen tot het actief worden van processen die tot tumoren kunnen leiden. Wanneer mensen een "foute" kopie van zo'n tumor suppressor gen van hun ouders erven, hoeft er nog maar één kopie te worden veranderd om een normale cel tot tumorcel te maken. In alle normale cellen die gedurende het leven celdelingen doormaken worden fouten gemaakt bij het "overschrijven" van de informatie in het DNA. Deze toevallige fouten leiden normaal gesproken niet tot problemen omdat de kans dat de twee kopieën van een tumor suppressor gen tegelijkertijd worden aangedaan uitermate klein is. Als men daarentegen al een verkeerde kopie bij zich draagt wordt de kans op inactivatie van een tumor suppressor gen een stuk groter. Deze "tweede hit" is een hypothese om te verklaren waarom mensen met één verkeerde kopie van tumor suppressor genen een verhoogde kans hebben om tumoren te ontwikkelen. Het VHL gen is geïdentificeerd en de sequentie is bepaald in 1988 en sindsdien is er veel onderzoek gedaan naar de functies van dit gen. Een eerste en zeer opvallende observatie is dat dit gen niet alleen de VHL ziekte veroorzaakt maar ook betrokken is bij de ontwikkeling van andere spontaan ontstane Grawitz tumoren. Ongeveer 50-70% van alle Grawitz tumoren vertonen een afwijking in beide kopieën van het VHL gen. Dit maakt het ontrafelen van de functie van VHL ook belangrijk voor het merendeel van de patiënten met Grawitz tumoren.

De functie van het VHL gen: zuurstof meten in de cel.

Het VHL gen blijkt een rol te spelen in de normale reactie van cellen op een tekort aan zuurstof, zogenaamd hypoxie. Zuurstof is een van de essentiële bestanddelen voor

de stofwisseling van cellen. Met behulp van zuurstof kan de cel voedingsstoffen, met name suikerbestanddelen "verbranden" tot water en koolzuur en daarbij komt dan de energie vrij die nodig is voor het normale functioneren. Onder hypoxische omstandigheden moeten cellen zich aanpassen aan de hoeveelheid zuurstof die beschikbaar is. De respons op hypoxie bestaat onder andere uit het proberen meer zuurstof aanbod te krijgen. Dit kan door de vaatnieuwvorming te stimuleren. Daarnaast zal de cel zijn energie op een andere manier dan met behulp van zuurstof afhankelijke verbranding moeten opwekken om te voorkomen dat de cel dood gaat. Hiervoor is de zogenaamde anaërobe verbranding, zonder het gebruik van zuurstof, noodzakelijk. De enzymen die nodig zijn voor de anaërobe verbranding worden ook tijdens hypoxie aangemaakt. Daarnaast moet de cel alle niet-essentiële activiteiten uitschakelen en voorkomen dat er celdood optreedt. Deze complexe reactie op een verandering in de omgeving wordt gecoördineerd door de activatie van een transcriptie factor: hypoxie geïnduceerde factor (HIF). Transcriptie factoren zijn de "managers" van de cel die belangrijke processen, zoals de reactie op stimuli van buitenaf aansturen. HIF stimuleert de aanmaak van tal van eiwitten die nodig zijn voor de cellulaire reactie op hypoxie. Onder normale zuurstof spanningen is HIF een instabiel eiwit dat zeer snel wordt afgebroken. Dit gebeurt in de proteasoom: een gespecialiseerde structuur die eiwitten snel kan afbreken. VHL speelt een belangrijke rol in de respons op hypoxie. VHL stimuleert de afbraak van HIF door zgn. ubiquitine moleculen aan HIF te binden. Dit leidt tot afbraak van HIF door de proteasoom. Onder hypoxie bindt VHL niet meer aan HIF en daardoor kan het ook niet meer afgebroken worden. De ophoping van HIF geeft cellen een betere kans op overleving onder hypoxische omstandigheden. Als cellen zonder hypoxie HIF activeren, zoals bij de inactivatie van VHL, dan kan dat leiden tot gedragsveranderingen van de cel. Deze vaatnieuwvormingen kunnen goed verklaard worden door de aanmaak van groeifactoren, zoals de vaatgroeifactor VEGF. Echter het ontstaan van kwaadaardige Grawitz tumoren kan niet alleen door de activatie van HIF worden verklaard.

Is zuurstof meten de enige functie van VHL?

In de introductie van dit proefschrift beschrijven we een aantal redenen waarom wij denken dat VHL meerdere functies heeft. De eerste reden is dat het VHL gen uiteindelijk 2 verschillende eiwitten maakt: een lange vorm: p30 en een korte vorm: p19. Het verschil tussen de twee eiwitten is een stukje van slechts 54 bouwstenen (aminozuren) zonder dat hiervoor een functie is beschreven. Beide vormen p30 en p19 zijn in staat om HIF te markeren voor afbraak maar in dat 54 aminozuren grootte stukje van het eiwit kunnen wel fouten ontstaan die leiden tot tumoren. Deze fouten (mutaties van het gen) hebben geen invloed op de functie van p19 dus moet dat stukje haast wel een functie hebben. Het andere argument voor meerdere functies voor het VHL gen komt uit de kliniek. De patiënten met mutaties in het VHL gen kunnen worden geclassificeerd aan de hand van hun specifieke mutaties en hebben dan meer of minder kans op verschillende tumoren. Heel typisch zijn de zogenaamde type 2C mutaties die eigenlijk alleen een verhoogde kans geven op pheochromocytomen zonder een verhoogde kans op de andere tumoren. Er moeten dus minstens twee functies zijn voor het VHL gen.

Samenvatting van de conclusies uit dit proefschrift:

Het tweede hoofdstuk beschrijft een zogenaamde microarray studie waarbij in één experiment tot duizenden genen tegelijkertijd onderzocht kunnen worden op de hoeveelheid gen-product in een cel populatie. Met deze methode hebben we cellen met en zonder VHL vergeleken en gevonden dat VHL ook genen reguleert onafhankelijk van hypoxie. Dit was wederom een aanwijzing dat VHL ook een functie heeft die niet aan hypoxie is gerelateerd.

Het derde hoofdstuk gaat over het mechanisme van een HIF onafhankelijke functie van VHL. Hierin beschrijven we een nieuwe bewerking van VHL: fosforylatie. Fosforylatie is het proces waarbij zgn. fosfaat groepen aan een eiwit worden gekoppeld en dit beïnvloedt de activiteit van het eiwit. Fosforylatie van VHL leidt tot een betere export van fibronectine, een eiwit dat een

deel van de ondergrond vormt waarop cellen groeien. Deze fosforylatie van VHL vindt plaats in het eerder genoemde 54 aminozuren deel van VHL waarvoor nog geen functie was beschreven. Verandering van het VHL eiwit zodat het niet meer gefosforyleerd kan worden leidt tot een VHL eiwit dat normaal HIF kan afbreken maar toch niet kan voorkomen dat er tumoren gevormd worden. Dit is de eerste aanwijzing in de literatuur dat dit eerste deel van VHL daadwerkelijk een functie heeft.

Het vierde en vijfde hoofdstuk beschrijft de invloed die VHL heeft op de stabiliteit van microtubuli. Deze buisvormige structuren zijn als het ware het "skelet" van de cel wat moet zorgen voor de vorm, beweeglijkheid en stevigheid. Belangrijke processen zoals celdeling en de juiste communicatie van cellen met elkaar en met de ondergrond waarop ze groeien zijn afhankelijk van de juiste balans tussen stevigheid en dynamiek van microtubuli. In vele tumoren is die balans verstoord en nu blijkt dat ook voor VHL afhankelijke tumoren het geval te zijn. Daarnaast laten we zien dat bij deze functie wederom het 54 aminozuren grote domein van VHL belangrijk is. VHL bindt met behulp van dit domein aan een complex van eiwitten genaamd het kinesin-2 complex. Dit complex functioneert in de cel als "motor" eiwit en is in staat om andere eiwitten langs microtubuli te vervoeren. De interactie tussen VHL en het kinesin-2 complex is ook belangrijk voor de juiste aanmaak van zogenaamde cilia. Dit zijn een soort voel-spieten die voornamelijk bestaan uit microtubuli die op de cellen groeien en belangrijk zijn voor het "voelen" van stroming buiten de cel. In de nieren is dit erg belangrijk omdat de cellen waaruit de VHL gerelateerde tumoren ontstaan tubulaire cellen zijn. Deze cellen vormen de bekleding van de buizen waardoor de urine stroomt en bewerkt wordt. Defecte cilia en dus onvoldoende signalering van cilia leidt in het algemeen tot het ontstaan van holtevormige afwijkingen ook wel cysten genoemd. Onze hypothese is dat het veelvuldig voorkomen van cysten bij VHL patiënten samenhangt met deze functie van het VHL eiwit. Normale cysten in de nier hebben slechts een hele kleine kans om een kwaadaardige tumor te worden. Bij VHL patiënten gebeurt dit wel. Dit verschil

kan mogelijk verklaard worden doordat in de cysten die bij VHL patiënten ontstaan ook HIF geactiveerd wordt. Beide factoren samen: het activeren van HIF en de formatie van cysten zou wel eens tot tumoren kunnen leiden.

Het zesde hoofdstuk is een uitstap naar een functie van VHL in de darm. In dit hoofdstuk tonen we aan dat VHL ook in tumoren van de darm wordt uitgeschakeld. In tegenstelling tot de goedaardige voorlopers van deze tumoren waarin juist veel VHL eiwit aanwezig is. Het uitschakelen van de functie van VHL en daarmee het versterken van de functie van HIF geeft darmtumoren een groeivoordeel. Dit gaat gepaard met een toename van vaatnieuwvorming die de bloedtoevoer verhoogt. Dit hoofdstuk toont aan dat ook voor patiënten met andere tumoren dan Grawitz tumoren de functie van VHL belangrijk is.

Conclusie:

In dit proefschrift is de functie van een belangrijk tumor suppressor gen beter beschreven. VHL speelt niet alleen een rol bij het meten van zuurstof maar ook bij de vorming van cilia. De uiteindelijke betekenis van deze nieuw beschreven functie en de precieze achterliggende mechanismen zijn een belangrijk onderwerp van onderzoek. De rol van VHL en HIF in vaatnieuwvorming heeft geleid tot de ontwikkeling van geneesmiddelen. Deze geneesmiddelen kunnen de tumorgroei vertragen door de vaatnieuwvorming af te remmen. Door inzicht in de HIF-onafhankelijke functie van VHL te verkrijgen, kan in de toekomst de behandeling van Grawitz tumoren ook gericht worden op de andere functies van het VHL gen. Om dit soort gerichte therapie te kunnen ontwikkelen is het noodzakelijk om precies de achterliggende mechanismen te ontdekken die van belang zijn voor de ontwikkeling en de groei van tumoren. In het geval van VHL is er hoogst waarschijnlijk meer dan alleen een rol in de regulatie van HIF en is er dus ruimte voor verdere ontwikkeling van therapieën voor Grawitz tumoren.

Dankwoord

Dankwoord

Zoals velen voor mij hebben ervaren, is het schrijven van een proefschrift niet alleen afhankelijk van de inzet van de promovendus maar ook van de steun die hij uit zijn omgeving krijgt. Een aantal mensen zijn van essentieel belang geweest voor het afronden van dit werken die wil ik graag in deze sectie bedanken.

Lieve Nicole, zonder jou was niet alleen het schrijven van dit proefschrift onmogelijk geweest. Jij bent degene die mijn leven altijd een groot feest maakt, ongeacht de alledaagse beslommeringen. En natuurlijk vergeet ik Bob niet: onze rode kater die het slapen en spinnen tot kunst heeft verheven. Soms zou ik willen dat ik een kat ben, maar meestal niet.

Beste Emile, geachte promotor, jij hebt mij de afgelopen jaren naar dit moment toe begeleid en ik denk dat we samen trots kunnen zijn op de uitkomst van dit werk. Het combineren van onderzoek met klinische werkzaamheden is geen gemakkelijke combinatie maar jij weet als geen ander op beide vlakken te excelleren. Daarmee inspireer je jonge mensen zoals mijzelf om deze belangrijke combinatie uit te proberen. Je hebt me een bijna onvoorwaardelijke vertrouwen en de kans om mezelf te ontplooiën gegeven. Daarnaast heb je op cruciale momenten de juiste richting gegeven aan ons onderzoek. Je bent onmisbaar geweest in het tot stand komen van dit proefschrift en voor het ontwikkelen van mijn verdere carrière.

Beste Rachel, geachte co-promotor, je kwam, je zag, nu moet je nog overwinnen. De frisse wind die uit Clevers lab kwam waaien: zo kwam je halverwege mijn promotie traject het laboratorium medische oncologie binnen. Met jou samen heb ik mijn gedachten over de inhoud van dit proefschrift kunnen vormen. Je stelde de juiste vragen en wist me te boeien met een intellectuele discussie. Je hebt me laten zien dat wetenschap meer is dan uitkomsten van proeven maar ook een stukje creativiteit vereist.

In mijn carrière heb ik nog twee sterke vrouwen ontmoet die aan mijn wetenschappelijke vorming een onuitwisbare bijdrage hebben

geleverd: Claire Boog en Polly Matzinger.

Claire, bij jou mocht ik mijn eerste stapjes in het lab zetten en daarbij heb je ontzettend veel geduld gehad. Samen met Benito heb je me de basisvaardigheden bijgebracht: ik was traag en onhandig. Desalniettemin heb ik met ontzettend veel plezier bij jou gewerkt. Je hebt nooit onder banken of stoelen gestoken dat je graag je bijdrage wilde leveren aan de wetenschappelijke ontwikkeling van artsen. Die gedachte en de uitvoering ervan waren mijn eerste echte aansporing om te gaan doen wat ik nu doe: wetenschap en geneeskunde combineren.

Dear Polly, as I have finished my thesis I would like to thank you for the contribution you made to my personal and scientific development. My 11-month stay in your lab has been a roller coaster ride: together with Steffi we performed experiments and talked about theories until late at night. You two showed me the energy that gifted and ambitious scientists can project on others. You also taught me to think as an independent person and gave me the confidence I could do so. Thanks to your supervision and the cooperation with Steffi I learned to appreciate the challenges of basic research.

Het laboratorium medische oncologie en de mensen die er werk(t)en ben ik veel dank verschuldigd. Martijn Gebbink en Moniek van Beest: jullie waren de moleculaire biologen die mij hebben voorzien van alle moleculaire biologische kennis die ik nu bezit. Dat moet voor jullie een hele opgave zijn geweest: de zoveelste arts die probeert wetenschap te doen! Gelukkig hebben jullie het nooit opgegeven. Er moeten momenten zijn geweest die jullie tot wanhoop hebben gedreven maar ook dan waren jullie er. Onno: ook jij hebt een bijzondere positie gehad. Als een van de weinigen ben je over van de mensen die in het lab werkten toen ik er begon. Je bent voor mij altijd de criticus geweest, de man die om controles vroeg. Daarmee ben je cruciaal geweest voor de kwaliteit van het werk dat hier wordt gepresenteerd, ook al sta je niet in de auteurslijsten. Dan zijn er de analisten die gedurende het tweede en derde jaar van mijn promotie ontzettend hard hebben gewerkt om een aantal artikelen

af te maken: Cristel en Anita. Ik heb het voorrecht gehad om als promovendus jullie hulp te krijgen. Van mijn mede promovendi verdient Niven een aparte vermelding jij hebt een belangrijke bijdrage geleverd aan het werk dat in dit boekje staat. Dan waren er nog de studenten: Michelle, Thomas en Mirjam. Jullie hebben een deel van jullie studie onder mijn begeleiding in het lab gewerkt. Dankzij jullie is het opleiden van mensen in het lab een ontzettend leerzame en inspirerende bezigheid voor mij geweest.

Verder wil ik alle andere werknemers van het laboratorium medische oncologie waarmee ik heb gewerkt bedanken: we hebben de jaren die ik er nu werk tot een gedenkwaardige mix van gezelligheid, inhoudelijke discussies en mooie uitgaansmomenten gemaakt.

Dan wil ik nog mijn paranimfen bedanken. Beste Dorus, de laatste jaren van mijn promotie traject en zeker de tijd die ik al weer met klinische werkzaamheden heb gevuld, ben jij ontzettend belangrijk geweest voor het afmaken van de artikelen die nog af moesten. Jij hebt een belangrijk aandeel in dit boekje gehad. Harald Jan, wij kennen elkaar vanaf onze studie geneeskunde en ik ben er trots op dat je nu op dit moment naast me staat. Je bent nu weliswaar chirurg in opleiding maar toch: ik waardeer je vriendschap.

Tenslotte wil ik twee mensen die erg belangrijk voor mij zijn noemen: papa en mama. Dankzij jullie heb ik dit bereikt en daarvoor ben ik jullie ontzettend dankbaar. Jullie hebben iets gedaan dat niet veel mensen jullie nadoen: mij en mijn broer uit Korea geadopteerd om ons hier in Nederland een warme en liefdevolle jeugd te geven. Daarnaast hebben jullie ook nog 4 pleegkinderen langdurig opgevangen en verzorgd. Hiervoor verdienen jullie alle lof van de wereld!

Curriculum Vitae

De auteur van dit proefschrift is op 11 juni 1974 geboren in Woolju, Korea. Op 13 maart 1975 werd hij geadopteerd door Gerrit en Mia Lolkema en is opgegroeid in Breda en Seedorf, Duitsland. Hij heeft het VWO doorlopen op het Newman College te Breda en is in 1992 geneeskunde gaan studeren aan de Universiteit van Amsterdam. Deze studie werd onderbroken door een eerste onderzoeksstage van één jaar op het Centraal Laboratorium voor de Bloedtransfusie dienst (CLB) te Amsterdam onder begeleiding van dr. Claire Boog en daarna een jaar stage aan het National Institutes of Health (NIH) te Bethesda, USA onder begeleiding van dr. Polly Matzinger. Beide stages heeft hij gewerkt aan de stimuli voor dendritische cellen die leiden tot activatie van het specifieke immuunsysteem. December 1999 werd de studie geneeskunde succesvol afgerond met het artsexamen.

De eerste klinische ervaring deed hij op in het Anthonius Ziekenhuis te Nieuwegein op de afdeling cardiologie. Mei 2000 begon de opleiding interne geneeskunde in het Eemland Ziekenhuis te Amersfoort (opleider: dr. Albert van der Wiel) waar hij anderhalf jaar heeft gewerkt. De opleiding werd september 2001 onderbroken door het verrichten van promotie onderzoek in het kader van een AGIKO constructie. Gedurende drie jaar heeft hij onderzoek verricht op het laboratorium medische oncologie op het Universitair Medisch Centrum te Utrecht onder begeleiding van prof. Emile Voest. Daarna heeft hij zijn opleiding hervat aan het Universitair Medisch Centrum Utrecht (opleider: prof. Elsken van der Wal) waar hij nu werkzaam is als assistent in opleiding tot internist-oncoloog.

List of Publications

Natural adjuvants: endogenous activators of dendritic cells. Gallucci S, **Lolkema M**, Matzinger P. *Nat Med*. 1999 Nov;5(11):1249-55.

Epithelial cell-specific laminin 5 is required for survival of early thymocytes. Kim MG, Lee G, Lee SK, **Lolkema M**, Yim J, Hong SH, Schwartz RH. *J Immunol*. 2000 Jul 1;165(1):192-201.

Fibronectin is a hypoxia-independent target of the tumor suppressor VHL. Bluysen HA*, **Lolkema MP***, van Beest M, Boone M, Snijckers CM, Los M, Gebbink MF, Braam B, Holstege FC, Giles RH, Voest EE. *FEBS Lett*. 2004. Jan 2;556(1-3):137-42.

The von Hippel-Lindau tumor suppressor protein influences microtubule dynamics at the cell periphery. **Lolkema MP**, Mehra N, Jorna AS, van Beest M, Giles RH, Voest EE. *Exp Cell Res*. 2004 Dec 10;301(2):139-46.

Tumor suppression by the von Hippel-Lindau protein requires phosphorylation of the acidic domain. **Lolkema MP***, Gervais ML*, Snijckers CM, Hill RP, Giles RH, Voest EE, Ohh M. *J Biol Chem*. 2005 Jun 10;280(23):22205-11.

Interplay between VHL/ HIF1 α and Wnt/ β -catenin pathways during colorectal tumorigenesis. Giles RH, **Lolkema MP**, Snijckers CM, Jorna AS, van der Groep P, van Beest M, van Noort M, Goldschmeding R, van Diest PJ, Clevers H, Voest EE. *Oncogene in press*